2026

Renske van der Peet

Engineered Living Textiles:
Integrating Microalgae into Multilayer Woven Architectures

Master thesis

MSc. Integrated Product Design

7 May, 2026

Delft University of Technology

Faculty of Industrial Design Engineering

Landbergstraat 15, Delft, The Netherlands

Author:

Renske van der Peet

5797394

Supervisory team:

Chair: Dr. J. Joana Soares de Oliveira Martins (Delft University of Technology)

Mentor: Dr. H.L. (Holly) McQuillan (Delft University of Technology)

Preface

This thesis presents the exploration and evaluation of microalgae-textile biocomposites, with the aim of supporting microalgal viability within a textile matrix, while exploring its potential for CO_2 sequestration. The research was conducted as a graduation project within the master's programme Integrated Product Design at the TU Delft.

My interest in biodesign developed during earlier courses in the master's programme, where I was introduced to the potential of combining living systems with product design. This motivated me to pursue this field for my graduation thesis and explore how biological processes can be embedded within material systems to address environmental challenges.

During this project, I worked in a laboratory-driven design context, which required learning to operate across both experimental and design methodologies. This combination introduced challenges, especially in working with biological systems that require strict environmental control, consistent measurement conditions and strict protocol planning. At the same time, it provided valuable insight into the constraints and the sensitivity of living materials.

In addition, I had no prior experience in textile weaving at the start of this thesis. Through iterative experimentation, I gradually developed an understanding of textile-based fabrication processes and their potential as carriers for biological systems.

This thesis reflects both the outcomes of the research and the learning process behind working at the intersection of design, material science, and biology. It marks the completion of my studies and reflects both the outcomes of the research and my learning process behind it.

Abstract

This thesis explores the development and optimisation of engineered living textiles by integrating microalgae into multilayer woven cotton-hydrogel architectures. The research evaluates the potential of microalgae-textile biocomposites as a novel approach to carbon capture, aiming to support microalgal viability within a textile matrix and to evaluate their capacity for CO_2 sequestration.

The study builds upon prior work demonstrating the feasibility of immobilising *Scenedesmus* sp. within textile-hydrogel systems. However, key challenges remained regarding long-term viability, structural stability, and quantitative CO_2 uptake. To address these gaps, a research-through-design methodology was employed, combining iterative material development with controlled laboratory experimentation. Multiple variables were systematically investigated, including textile architecture, hydrogel cross-linking methods, cryopreservation conditions, inoculation strategies, and environmental parameters.

Initial pilot studies evaluated baseline immobilisation methods and highlighted moisture retention as a critical factor for sustaining microalgal viability. Plain cotton textiles supported initial microalgae attachment but exhibited rapid drying and reduced long-term viability. The introduction of a multilayer cotton-hydrogel matrix improved hydration but revealed additional challenges, including structural inconsistencies, contamination, and reduced viability following freeze-thaw processing.

The technical characterisation of the study focused on optimising the hydrogel matrix, microalgae viability and preservation methods. Freeze-thaw and freeze-drying techniques were compared for cross-linking performance, showing that both methods produced structurally stable composites, though with limited long-term moisture retention. Cryoprocessing experiments demonstrated that freezing at −80 °C best preserved microalgal viability, while the use of glycerol as a cryoprotectant negatively affected photosynthetic performance. Additionally, subsequent experiments demonstrated that microalgae can be successfully introduced into the textile matrix after hydrogel cross-linking, providing an alternative immobilisation strategy that avoids exposing cells to damaging processing conditions.

These findings emphasise the sensitivity of microalgae to processing conditions and the importance of balancing material stability with biological functionality.

CO_2 measurement experiments were conducted using a custom-built sensor system. However, consistent photosynthetic CO_2 uptake was not achieved across experiments. Instead, increases in CO_2 concentration were frequently observed, indicating respiration or loss of metabolic activity, particularly after freezing treatments. Furthermore, the results indicate that the microalgae-textile biocomposite does not yet demonstrate higher CO_2 uptake compared to conventional suspension cultures. This highlights the difficulty of maintaining active photosynthesis within the engineered textile system under the tested conditions.

Overall, the research demonstrates that microalgae can be successfully immobilised within multilayer woven textile matrices, and that material design significantly influences cell attachment and distribution. However, maintaining long-term viability and achieving reliable CO_2 sequestration remain unresolved challenges. The study identifies key factors affecting system performance, including moisture retention, textile structure, preservation conditions, and environmental control.

This work contributes to the emerging field of engineered living materials by providing insights into the integration of biological systems within textile architectures. While the current system does not yet achieve consistent functional performance or outperform conventional cultivation methods, it establishes a foundation for future research aimed at developing scalable, stable, and effective living materials for carbon capture applications.

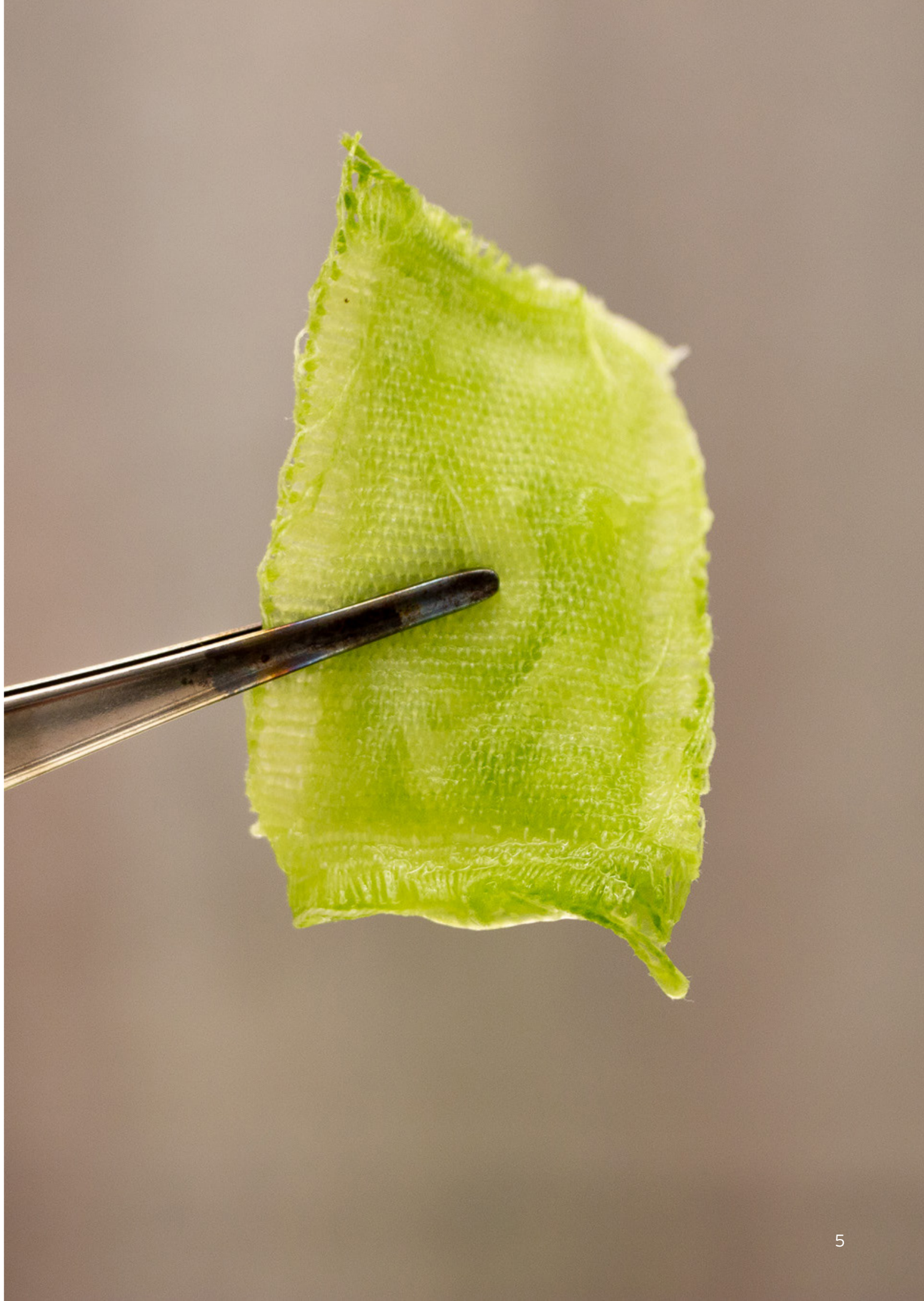

Glossary

AdaCAD: An open-source design software used for creating and simulating woven textile structures and patterns.

BG11 medium: A medium containing all the essential nutrients required for the microalgae cultivation [1].

Biocomposite: A material that consists of two or more distinct materials (one being naturally derived) to produce a new material with enhanced performance compared to the individual components [2].

Biological replicate: independent, biologically distinct samples, such as organisms of the same type maintained under identical conditions, that capture biological variation [3].

Biomass: The total amount of organic material produced by living organisms in a particular area

Biotechnology: The application of living organisms, or their components, as cellular factories to produce valuable products from renewable feedstocks [4].

Carbon sequestration: The process of capturing and long-term storing atmospheric carbon dioxide, serving as a strategy to lower atmospheric CO_2 concentrations and mitigate global climate change [5].

Centripetal effects: The inward acceleration that keeps an object moving in a circular path. It is produced by a net force, called the centripetal force, that acts toward the centre of the circle [6].

Compound twill: A twill is a weaving pattern where the threads interlace in a repeating diagonal step (creating a visible diagonal rib). A compound twill is when multiple twill patterns are combined or layered within the same fabric to form more complex structures.

Cryoprotectant: A solute that enables the preservation of cells at very low cryogenic temperatures while maintaining high functionality, despite possible metabolic and biophysical effects [7].

Cross-linking: The process of forming covalent or ionic bonds between a polymer and a cross-linking agent, creating a reinforced network structure that improves the polymer's mechanical strength and water stability [8].

Engineered living materials (ELM): Materials that are inspired by nature and incorporate living cells to produce dynamic, responsive materials with programmable biological functions [9].

Fluorescence Spectrometer (Plate reader): An analytical instrument that excites a sample with a specific wavelength of light and measures the intensity and spectral distribution of the emitted fluorescence to study its properties [10].

Fluorescence quantum yield: The ratio of the number of photons emitted as fluorescence to the number of photons absorbed during excitation; for microalgae, this indicates how efficiently the absorbed light energy is re-emitted as fluorescence and provides insight into their photosynthetic performance [11].

Freeze-thawing (F-T): The process of creating polymer structures by repeatedly freezing and thawing a solution. When frozen, the solvent forms ice crystals that push the polymer chains together, allowing them to form physical bonds that remain after thawing [12]. Freeze-thawing generally happens between -4 °C and -80 °C. Lower freezing temperatures lead to smaller pore sizes and result in greater total intrusion volume and overall porosity [13]. With each cycle, the gel-like network becomes more stable because additional crystalline structures form during the freezing phase [14].

Freeze-drying (F-D): Also called lyophilisation, is a process where frozen water is removed from a material under low pressure by turning the ice directly into vapour (sublimation) [15].

Glycerol: A widely used penetrating cryoprotective agent (CPA) that protects cells from freezing damage by reducing ice crystal formation, stabilising membranes, and enabling vitrification at low temperatures [16].

Greenhouse gases (GHGs): Gases in the atmosphere that trap heat and cause global warming [17].

Hydrogel: Three-dimensional polymeric networks capable of absorbing large volumes of water relative to their mass. Both natural and synthetic hydrogels exist [18].

Immobilisation: The physical attachment of microalgal cells within a supporting matrix or scaffold, such that the cells remain spatially fixed while retaining metabolic activity. Within the context of this study, immobilisation refers specifically to the containment of cells within the textile structure. However, the exact localisation and mechanism of this retention are not resolved. It remains unclear whether cells are embedded within the cotton or hydrogel yarns, adhered to individual fibres, or retained within the spaces between the yarns of the woven structure.

Material degradation: The deterioration of a material's properties caused by processes such as changes in composition, material loss, embrittlement, phase changes, or cracking, often resulting in reduced strength and increased friction [19].

Microalgae: Photosynthetic organisms, including both prokaryotes and eukaryotes, that can grow rapidly in many different environments under photoautotrophic conditions [20].

Microalgae-textile biocomposite: A material made by combining microalgae with a textile structure to create a single functional material. In this type of biocomposite, the textile acts as a structural support, while the microalgae are embedded in, coated on, or grown within the textile matrix [21].

Multilayer woven textile: A textile made of two or more woven layers that are connected during the weaving process to form one integrated structure. The layers are interlinked by specific yarns, which give the textile greater thickness, strength, and structural complexity compared to single-layer fabrics.

Nature-based solutions (NBS): Solutions to sequestrate carbon with the aim to enhance carbon storage capacity in ecosystems such as biomass reservoirs, soils and oceanic sinks [22].

Optical density (OD): The logarithmic ratio between the intensity of incoming light and the light transmitted through a material, showing the loss of light due to absorption, reflection, and scattering, and indicating the amount of biomass present [23].

Photosynthesis: A metabolic process in which plants and other photosynthetic organisms use light energy to convert carbon dioxide (CO_2) and water into sugars with the release of oxygen (O_2) [24].

Plain weave: The simplest weaving structure, where each weft thread alternately passes over and under each warp thread, creating a tight, balanced checkerboard-like pattern.

Polyvinyl Alcohol (PVA): A versatile, water-soluble synthetic polymer known for its ability to form films and hydrogels, non-toxicity, chemical stability, mechanical strength, and excellent barrier properties, making it suitable for applications ranging from biomedical and pharmaceutical uses to packaging, sensing devices, and wastewater treatment [26].

Pulse-Amplitude-Modulation (PAM): A non-invasive technique that measures chlorophyll fluorescence to assess the photosynthetic activity and efficiency of photosynthetic organisms such as microalgae [25].

Scenedesmus: A genus of green microalgae recognised for its potential in bioremediation, especially for removing antibiotic pollutants from wastewater, with rapid acclimation and adaptability to diverse environmental conditions [27].

TC2: A computer-controlled digital weaving loom that allows direct programming of individual warp and weft thread movements to create complex woven structures.

Technical replicate: Repeated measurements of the same sample reflect variability originating from measurement instruments and experimental procedures. [3].

Warp: The set of lengthwise threads held under tension on a loom through which the weft is woven.

Weft: The crosswise threads that are woven over and under the warp threads to form a textile.

Table of Contents

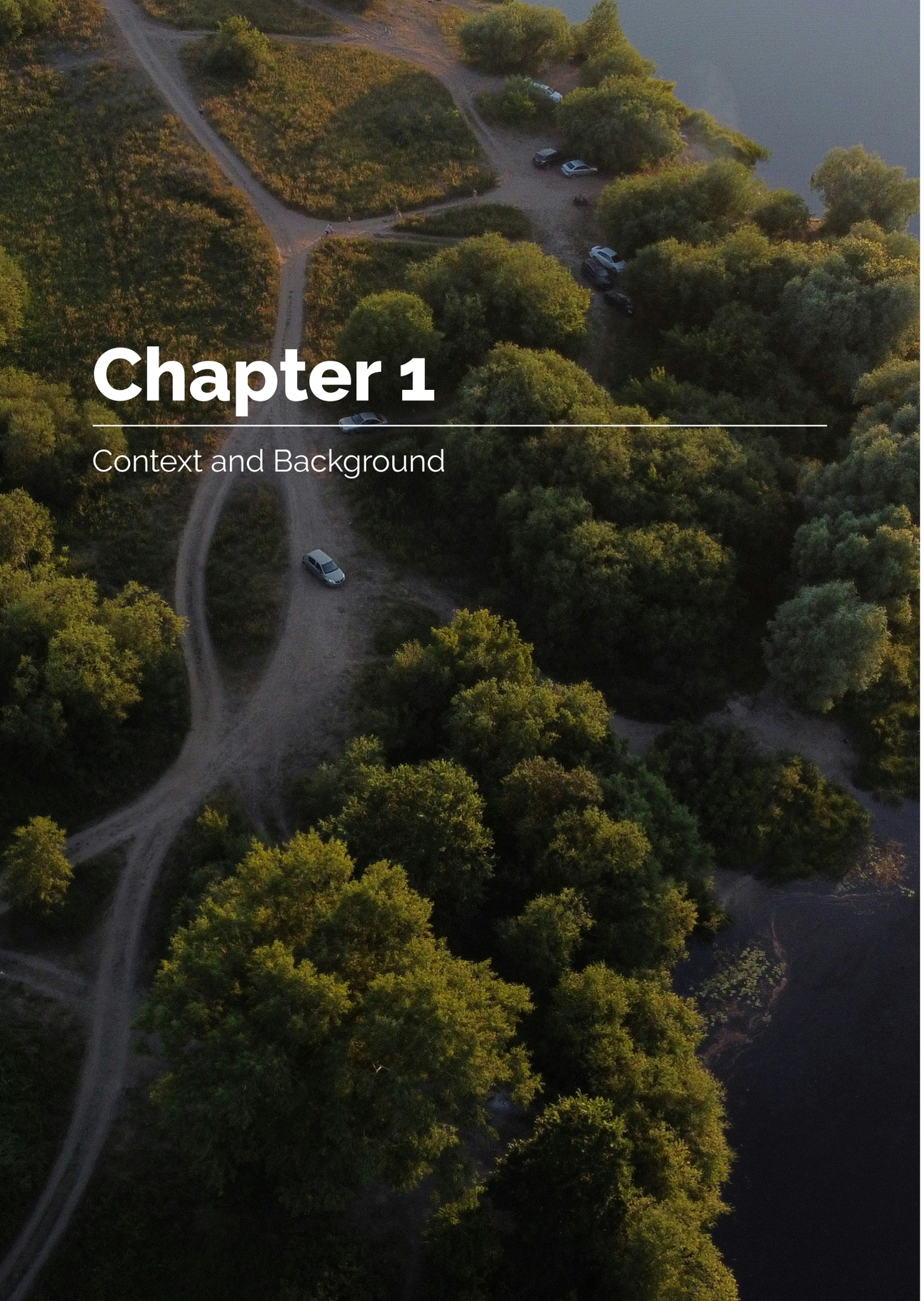

Chapter 1

Context and Background

1.1 Climate Change and Greenhouse Gases

Recent years have been characterised by unprecedented global warming, highlighting the increasing urgency of climate mitigation efforts. Global average temperatures continue to rise [28], with the National Oceanic and Atmospheric Administration (NOAA) reporting that 2024 was the warmest year recorded since the beginning of global temperature measurements [29].

Human-generated greenhouse gases (GHGs) are the primary driver of rising global temperatures. The largest contributor to global GHG emissions is carbon dioxide (CO_2), accounting for 79.7% of total emissions in 2022 [30]. The rapid rise in atmospheric CO_2 concentrations is largely attributable to the widespread combustion of fossil fuels since the Industrial Revolution [28]. Rising atmospheric CO_2 concentrations contribute to climate change and associated environmental impacts, including ocean acidification, extreme weather events, sea-level rise, and biodiversity loss [31], [32]. Current annual CO_2 emissions exceed the carbon uptake capacity of natural sinks, highlighting the urgency for effective mitigation strategies [33]. Despite international agreements, such as the Paris Agreement, aiming to achieve net-zero emissions, global fossil CO_2 emissions continue to rise [34].

Although emission reduction remains essential, it is no longer sufficient on its own [35]. Consequently, carbon capture and sequestration technologies are increasingly recognised as necessary strategies to mitigate climate change. Carbon sequestration refers to the capture and long-term storage of carbon dioxide (CO_2) [36]. Among carbon sequestration strategies, nature-based solutions (NBS) are increasingly explored due to their low energy requirements and ecological co-benefits. These approaches enhance the carbon storage capacity of ecosystems such as biomass reservoirs, soils, and oceanic sinks [22]. Within nature-based solutions, photosynthetic microorganisms such as microalgae and cyanobacteria are particularly promising due to their potential for scalability and cost-effective carbon sequestration [22], [37].

1.2 Microalgae and Carbon Sequestration

Microalgae are particularly promising organisms for nature-based carbon capture due to their high photosynthetic efficiency and ability to fix carbon dioxide. As eukaryotic organisms, they contain chlorophyll, a pigment that enables the absorption of light energy and its conversion into chemical energy [41]. During photosynthesis, carbon dioxide (CO_2) and water are converted into organic compounds, such as sugars, and oxygen (O_2) is released (Figure 1). The produced sugars serve as both an energy source and structural building material, resulting in biomass formation as microalgae assimilate CO_2. Consequently, high microalgal viability is often associated with increased biomass production, which is reflected in a higher intensity of green pigmentation.

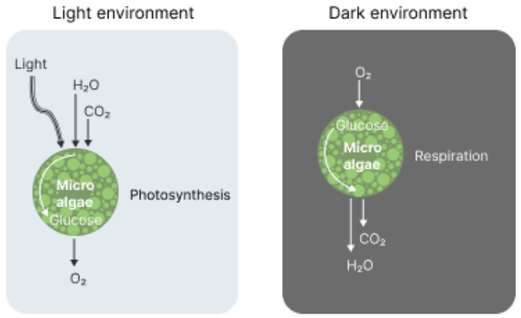

Figure 1: Processes of photosynthesis (left) and respiration (right) of microalgae as a simplified illustration.

Microalgae are an essential contributor to Earth's total photosynthetic activity, accounting for approximately 50% of total photosynthetic activity on Earth and playing a major role in oxygen production and carbon dioxide fixation [42]. Their photosynthetic efficiency is generally higher than that of terrestrial plants due to their high chlorophyll content [42]. Microalgae can therefore absorb CO2 at rates up to 50 times higher than terrestrial plants [43].

Beyond their role in carbon sequestration, microalgae have also gained attention because of their wide range of biotechnological applications. These include wastewater treatment, biofuel production, bioplastics, food and nutritional supplements, agricultural inputs, and the production of natural pigments and dyes, highlighting their broad relevance for sustainable environmental and industrial solutions.

Currently, microalgae cultivation happens in two major cultivation systems, open ponds and closed photobioreactors (PBRs) (Figure 2). Open pond cultivation systems are vulnerable to contamination, suffer significant water loss through evaporation, and provide limited control over environmental conditions. In addition, they require large land areas, which restricts their scalability [44]. In contrast, photobioreactors provide greater process control and higher cultivation efficiency but are associated with high construction, operation, and maintenance costs, as well as significant energy demands for light and temperature regulation. Making large-scale implementation challenging [44]. These limitations have motivated the exploration of alternative approaches, including the integration of microalgae into engineered systems.

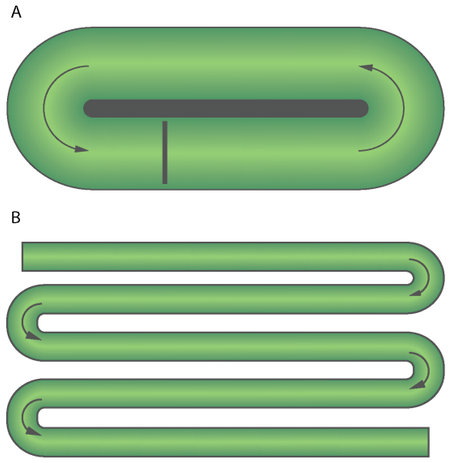

Figure 2: Schematic representations of microalgae cultivation systems: (A) top-view illustration of an open raceway pond, and (B) simplified depiction of a tubular photobioreactor system.

1.2.1 *Scenedesmus*

In addition to improving cultivation systems, selecting suitable microalgal species is critical for achieving efficient carbon capture and system stability. Among the wide diversity of microalgal genera, certain genera are particularly suitable for integration into engineered systems due to their robustness and high biomass productivity. One such genus is *Scenedesmus*, which has been widely studied due to its robustness, high biomass yield, and adaptability to diverse growth conditions, making it a suitable candidate for engineered living systems [45], [46]. These characteristics enable stable cultivation and efficient carbon assimilation under varying environmental conditions. Accordingly, *Scenedesmus* sp. and *bacillaris* are selected as the microalgal genus for this study.

1.3 Biodesign and Engineered Living Materials

Recent developments in biotechnology and biodesign have expanded opportunities to integrate biological systems into technological and material applications. Biotechnology refers to the application of biological systems, living organisms, or their components to develop products and services across sectors such as agriculture, medicine, and environmental management [38]. Biodesign, in contrast, focuses on the integration of biological processes and organisms into the design of systems, materials, and environments in order to address sustainability challenges [39].

Within this context, engineered living materials (ELMs) have emerged as a promising approach to biodesign. ELMs are materials inspired by nature and incorporate living cells to produce dynamic, responsive materials with programmable biological functions [40]. These materials can exhibit properties such as self-growth, self-healing, and responsiveness to environmental conditions.

The living component, often referred to as the chassis cell, can consist of microorganisms such as bacteria, yeast, algae, or fungi [40]. Microalgae are particularly promising chassis organisms for ELMs due to their ability to perform photosynthesis and fix atmospheric CO_2. This enables the development of living materials capable of active carbon sequestration while simultaneously exploring an alternative cultivation approach.

1.4 Microalgae Biocomposites and Engineered Living Materials

Recent research has explored the immobilisation of microalgae within material matrices or scaffold structures composed of natural and synthetic materials to create microalgae-based biocomposites. In these systems, living cells are immobilised within structured materials while maintaining metabolic activity, thereby enabling engineered living materials (ELMs) with functional biological properties [47].

1.4.1 Hydrogel

Hydrogels are widely used as matrix materials in microalgae ELMs due to their ability to retain water and nutrients while supporting cell growth [18]. Hydrogels are three-dimensional polymeric networks capable of absorbing large volumes of water relative to their mass. Hydrogels require cross-linking to effectively absorb and retain water.

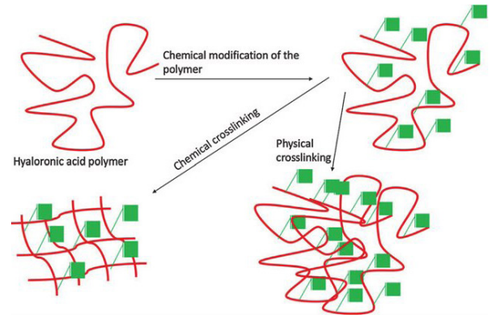

Figure 3: Schematic representation of chemical and physical cross-linking mechanisms, illustrating the formation of intermolecular bonds [63].

This can be achieved through physical or chemical cross-linking [18] (Figure 3). Physical cross-linking, as used in this study, relies on non-covalent interactions such as hydrogen bonding, ionic interactions, or freeze-thaw cycles, producing reversible structures that allow nutrient and gas exchange [18].

1.4.2 Matrix-Based Microalgae Biocomposites

Within this context, microalgae have been immobilised into three-dimensional biocomposite matrices composed of natural materials such as loofah-derived scaffolds. The intrinsic porosity and interconnected structure of the loofah provide a high surface area for microalgal attachment while facilitating light penetration and transport of nutrients and gases. This structural configuration supports microalgal viability and sustained metabolic activity, enabling stable immobilisation within the matrix. Such systems demonstrate the potential of matrix-based microalgae biocomposites to enhance biological CO_2 capture [48].

1.4.3 Microalgae-textile Biocomposites

Building on matrix-based approaches, microalgae-textile biocomposites have been developed in which microalgae cells are immobilised into textile matrices to create photosynthetically active materials for carbon capture. In these systems, the microalgae attach to fibrous substrates such as cotton or polyester, with some configurations incorporating hydrogel coatings to enhance cell retention. The fibrous architecture of the textile provides a high surface area for cell attachment while allowing light penetration and facilitating the transport of nutrients and gases.

The resulting living biocomposites demonstrated significantly higher CO_2 absorption rates compared to suspended microalgae cultures [47]. These findings demonstrate strong potential for supporting microalgal growth and enhancing biological CO_2 capture, while reducing water and land requirements relative to conventional cultivation systems.

A particularly relevant development within this field is the work of Mancini, which serves as the foundation for this study. Martina Mancini developed an immobilisation approach in which *Scenedesmus* sp. was inoculated within a multilayer woven textile composite composed of cotton and polyvinyl alcohol (PVA) hydrogel [49] (Figure 4). During the fabrication of the microalgae-textile biocomposite, the textile was first immersed in a *Scenedesmus* sp. suspension, followed by a single freeze-thaw cycle to induce physical cross-linking of the hydrogel.

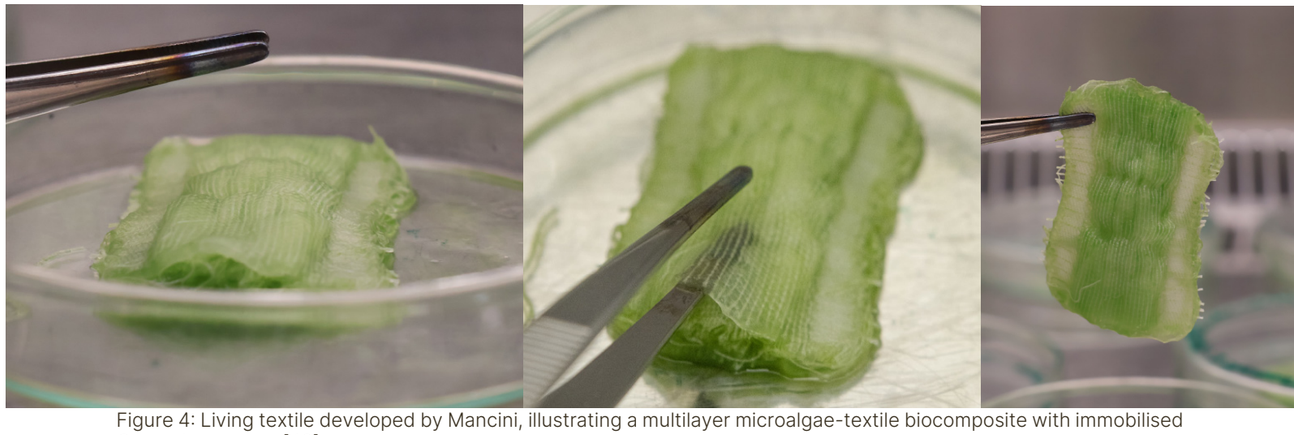

Figure 4: Living textile developed by Mancini, illustrating a multilayer microalgae-textile biocomposite with immobilised *Scenedesmus* sp. [49].

This process enabled microalgal encapsulation while allowing nutrient transport due to the hydrogel's high hydrofluid absorption capacity [18]. Building on this approach, the primary aim of this study is to optimise the textile-hydrogel environment to improve microalgal immobilisation and viability. The secondary aim is to quantify the CO_2 uptake of the resulting living textile system in order to evaluate its functional performance.

1.4.4 Limitations

Despite these advances, the long-term stability and performance of textile-based microalgal systems remain insufficiently understood. It remains untested to what extent multilayer textile configurations contribute to enhanced CO_2 capture compared to conventional microalgae suspension cultures.

Key challenges also persist in maintaining biomass retention over time, as suboptimal ratios of microalgal cells to hydrogel can lead to biomass loss. This may occur through degradation of the hydrogel structure or through uncontrolled cellular overgrowth, resulting in microalgal escape from the matrix [47]. Furthermore, commonly used cross-linking methods, such as freeze-thaw cycles for physical hydrogel formation, may impose stress on the embedded microalgae, potentially reducing cell viability and overall system performance.

These limitations emphasise the need to optimise matrix design, immobilisation strategies, and cross-linking methods, while systematically evaluating their impact on CO_2 capture performance to ensure sustained cell viability, structural integrity, and effective carbon sequestration.

This page is intentionally left blank

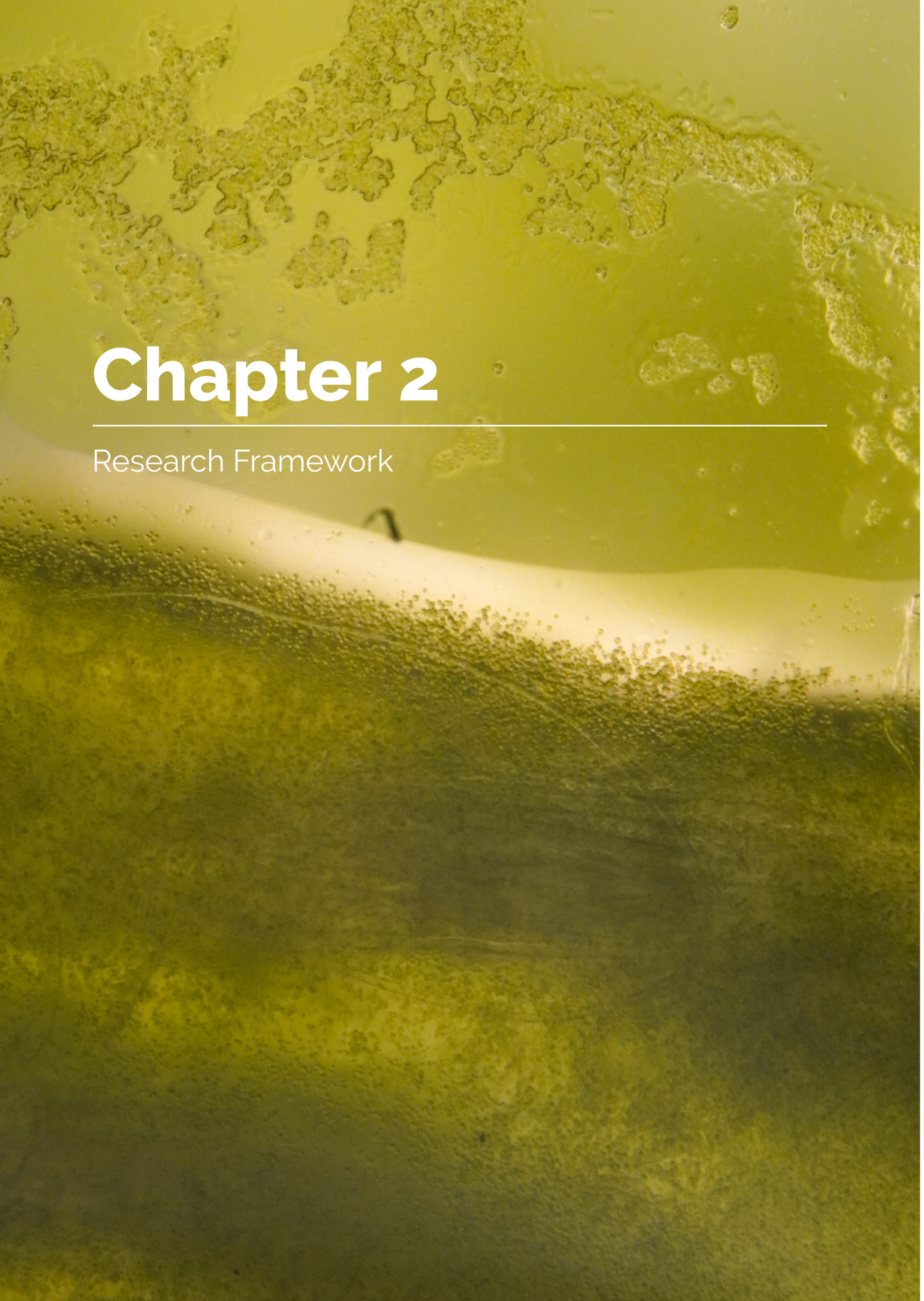

Chapter 2

Research Framework

2.1 Context and Research Gap

Recent research into microalgae-textile biocomposites has demonstrated their potential to achieve higher CO_2 uptake than conventional suspension cultures [47]. Within this field, Mancini demonstrated that *Scenedesmus* sp. can be immobilised within a multilayer woven textile composed of cotton and PVA, supporting microalgal growth and photosynthetic activity [49]. This system represents the first microalgae-textile biocomposite in which a hydrogel is integrated directly into the woven structure, forming a multilayer matrix designed for microalgae immobilisation. The resulting material enables effective microalgal immobilisation while maintaining nutrient transport through the hydrogel network [18].

Despite these promising results, several uncertainties remain. Quantitative data on CO_2 uptake in textile-based microalgal systems are unknown, and the influence of three-dimensional woven architectures on carbon sequestration efficiency is not well understood. In addition, the long-term viability, stability, and functional lifespan of microalgae-textile biocomposites remain largely unexplored.

As a result, it remains unclear whether microalgae-textile biocomposites can function as efficient and reliable platforms for microalgae cultivation and carbon capture.

2.2 Research Aim

To address the research gap, the primary aim of this study is to optimise the textile-hydrogel system to enhance stable microalgal immobilisation and viability by refining the textile matrix design, immobilisation strategies, and cross-linking methods. The secondary aim is to evaluate the functional performance of the resulting microalgae-textile biocomposite through quantitative assessment of CO_2 uptake.

1. To investigate how material design and biocomposite protocol variations influence the immobilisation of *Scenedesmus* sp. within textile-based materials.
2. To evaluate microalgal immobilisation efficiency, viability, and stability within the developed textile systems.

2.4 Research Questions

Textile design

1. How do textile architecture and material composition influence microalgal attachment and spatial distribution within the textile matrix?

Hydrogel Cross-linking

2. How do hydrogel cross-linking methods and preservation conditions affect the structural integrity of the composite and the viability of *Scenedesmus* sp.?

Microalgal Viability

3. To what extent can the textile-hydrogel system support stable microalgal viability and long-term biomass retention?

Functional Performance and CO_2 Uptake

4. How does the microalgae-textile biocomposite perform in terms of CO_2 uptake compared to conventional suspension cultures?

2.5 Methodology

This study investigates the optimisation of a textile-based living matrix that supports stable immobilisation and long-term viability of microalgae, while evaluating the CO_2 uptake performance of the resulting microalgae-textile biocomposite. The research is conducted in the research-through-design framework, in which material development and experimental testing are used to generate knowledge about the system [52].

Rather than applying a strictly goal-oriented engineering approach, this study combines the Material-Driven Design (MDD) method with the Parallel Prototyping Method (PPM) [50], [51]. This combined approach allows for an iterative and exploratory development process, in which multiple material configurations and experimental conditions are tested and compared. Within this framework, prototyping serves not only as a tool for solution development but also as a method to investigate the behaviour and performance of the microalgae-textile system. Figure 5 shows an overview of the full method.

Importantly, the research questions are not addressed through isolated experimental protocols but are instead interwoven throughout the experimental phases. Each protocol is designed to simultaneously generate insights relevant to multiple research questions, rather than assigning one protocol per research question.

The research is structured as a lab-based research-through-design process [52], where controlled experimental conditions are used to examine the relationship between material properties and biological performance. The first phase of the study focuses on the evaluation of the immobilisation method developed by Mancini [49], using three pilot protocols. These initial protocols establish a baseline for microalgal immobilisation within the multilayer cotton-hydrogel textile matrix.

Subsequently, the study progresses into a systematic exploration of key variables within Mancini's method [49]. This phase addresses the research gap identified in Section 2.2 and focuses on optimising the matrix design, immobilisation strategies, and hydrogel cross-linking. Key aspects investigated include microalgal attachment within the textile matrix, cell viability over time, and the interactions between biological and material components. Conducting these experiments simultaneously enables direct comparison between variables and prevents early fixation on a single development pathway, thereby facilitating the identification of key parameters influencing microalgal viability and overall system performance.

In parallel, the CO_2 uptake capacity of the microalgae-textile biocomposite is evaluated under controlled conditions. Both quantitative measurements and qualitative observations are used to assess system performance.

Finally, the findings from these experimental phases are used to define the material potential of the microalgae-textile biocomposite. This step translates technical insight into design-relevant knowledge, highlighting opportunities for future applications, while also identifying limitations, challenges, and directions for further research.

2.5.1 Lab Setting and Test Set-up

The protocols for the study were conducted in a small laboratory environment specialised in biodesign, which provided access to essential microbiological and analytical equipment. This included a laminar flow cabinet for sterile handling, incubators for controlled cultivation conditions, and standard measuring equipment for monitoring microalgal growth and system performance. In addition, access to a material laboratory enabled the fabrication of textile samples using a TC2 digital handloom. This setup allowed for the controlled design and production of custom woven textile structures, which were directly integrated into the experimental protocols.

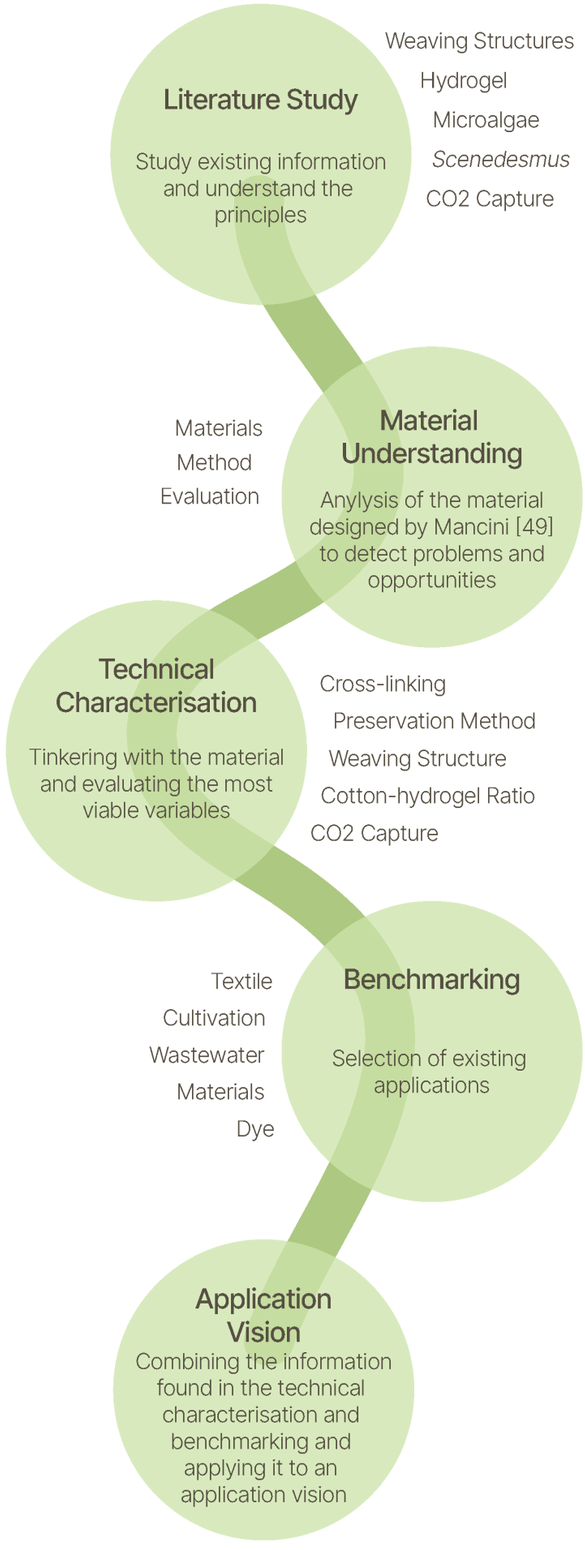

Figure 5: Overview study methodology

2.5.1.1 CO_2 Measuring Setup

To enable quantitative assessment of CO_2 uptake under controlled laboratory conditions, a dedicated measurement system was developed and iteratively refined as part of the experimental framework. This setup is a critical component of the evaluation phase, enabling comparison between microalgae-textile biocomposites and conventional suspension cultures. The final validated configuration, described below, was subsequently used in the experimental protocols presented in Chapters 3 and 4.

2.5.1.1.1 CO_2 Measurement Setup Development and Validation

The system design was based on established approaches for gas exchange measurement in closed environments, in which a CO_2 sensor is integrated into an airtight chamber to monitor temporal changes in concentration. The initial setup was adapted from the methodology described by Jeong-Joo Oh [56] and further modified to suit the requirements of a textile-based biological system.

An autoclave-compatible laboratory bottle was selected as the measurement chamber to ensure sterility (Figure 6). To maintain sterile conditions, all components were designed for disassembly, and the CO_2 sensor was made detachable for cleaning and disinfection with ethanol prior to each measurement cycle (Figure 7). In addition, ultraviolet-C (UVC) exposure was applied to the sensor housing and cap as an additional sterilisation step.

CO_2 concentrations were recorded using a non-dispersive infrared (NDIR) sensor, which operates by measuring the absorption of infrared radiation by CO_2 molecules at a characteristic wavelength. This enables the quantification of the CO_2 concentration based on the amount of absorbed radiation [57]. The SCD41 was selected after evaluation of multiple sensors, due to its measurement stability, size, and integration compatibility (Appendix 2.1).

A Xiao RP2040 microcontroller was selected to log the data generated by the sensor, due to its compact size and ability to store data internally. During initial testing, power instability was observed, which was resolved by integrating a 1000 µF, 10V capacitor into the circuit to stabilise voltage fluctuations. The complete circuit design is shown in Appendix 2.2.

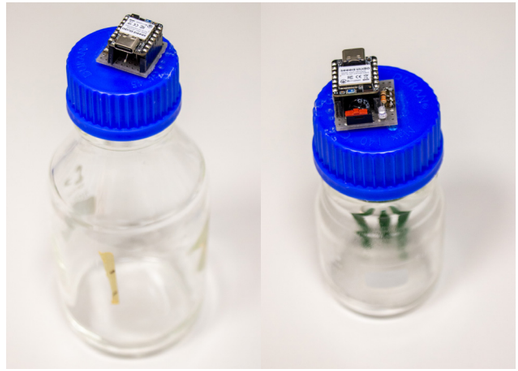

Figure 6: CO_2 measurement setup showing two laboratory bottle sizes, illustrating the adaptability of the measurement chamber volume.

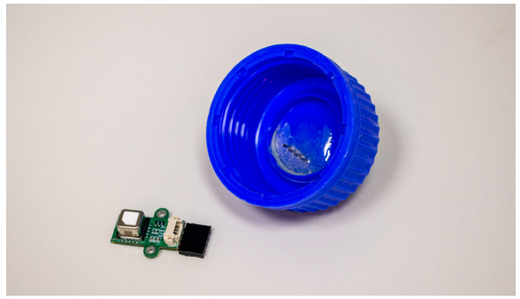

Figure 7: Cap of the CO_2 measurement setup featuring a detachable CO_2 sensor to enable sterilisation.

A key consideration was the positioning of the CO_2 sensor within the chamber. As CO_2 is denser than air and tends to accumulate in lower regions, the sensor was placed at the lowest point of the measurement chamber to improve detection accuracy. Different configurations were applied for suspension cultures and textile samples. For suspension cultures, the sensor was suspended near the liquid culture. While for textile-based samples, the measurement chamber was inverted, positioning the sensor in the cap to optimise gas detection (Figure 8).

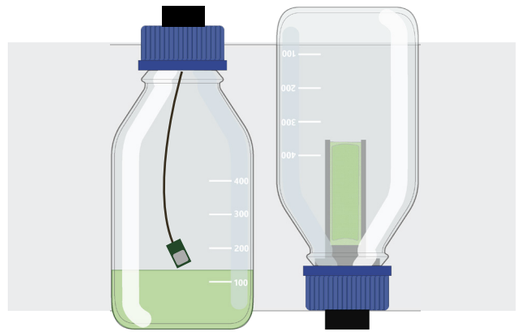

Figure 8: Schematic of CO_2 sensor placement for different sample types: in suspension culture (left), the sensor is positioned above the liquid, whereas for the textile sample (right), the sensor is integrated into the bottle cap.

A 3D-printed sample holder was developed to secure textile samples above the sensor. (Figure 9). Early iterations revealed leakage from the textile samples, which caused corrosion and sensor damage. This was addressed through a redesign of the textile holder that isolated the sensor and electronic components from liquid contact (Figure 10). However, the sensor repeatedly came into contact with liquid dripping from the textile. Therefore, it was subsequently repositioned and suspended at the bottom of the flask (Figure 11, 12).

To ensure airtight conditions, all threaded connections were sealed using PTFE (Teflon) tape, and bottles with integrated sealing rings were used (Figure 13). Initial system validation without biological material revealed fluctuations in CO_2 readings, indicating instability in the measurement environment. These inconsistencies were resolved by disabling automatic self-calibration (ASC), applying external calibration using a reference device, and correcting for temperature effects within the chamber.

Figure 9: Evolution of textile holders from old (left) to new (right)

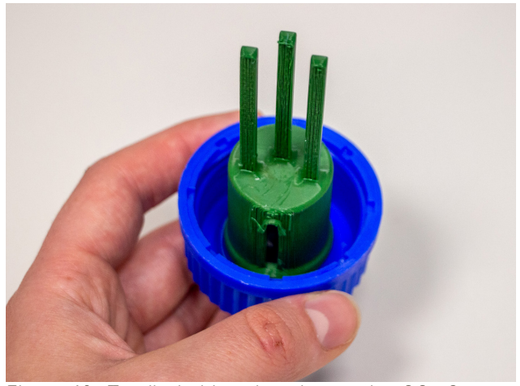

Figure 10: Textile holder placed over the CO_2 Sensor, protecting it from leakage from the textile

Figure 11: Optimised CO_2 measurement setup with sensors positioned near the bottom of the flask to prevent microalgae contact with electronic components.

Following these adjustments, the system demonstrated stable and reproducible CO_2 measurements over time. The final configuration enables continuous recording of CO_2 concentration, temperature, and relative humidity, with timestamped data logging directly on the microcontroller (Appendix 2.3)

This validated measurement system as subsequently applied in the experimental protocols described in Chapters 3 and 4 to quantify CO_2 uptake of microalgae-textile biocomposites under controlled conditions.

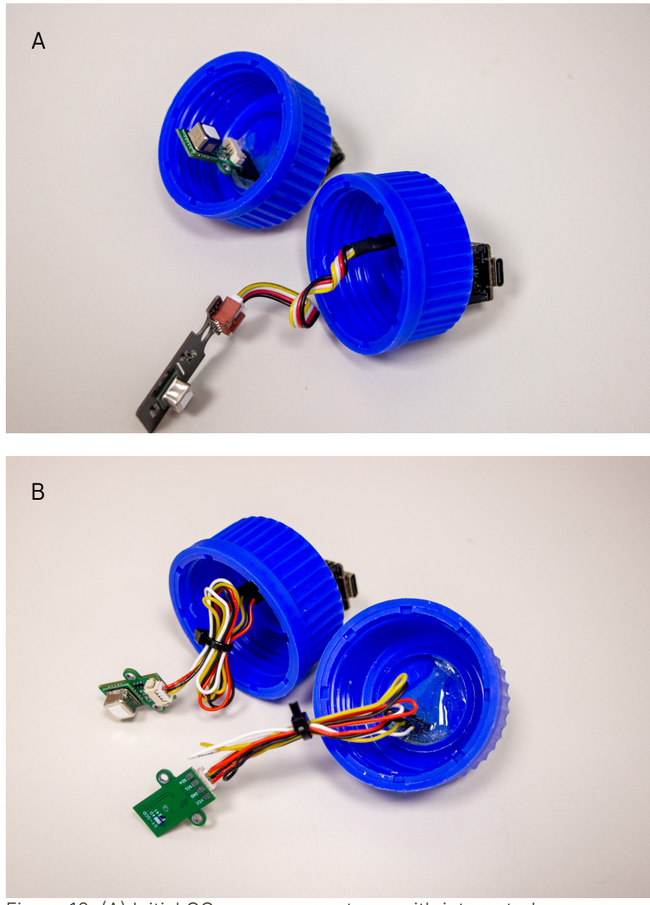

Figure 12: (A) Initial CO_2 measurement cap with integrated sensor; (B) final design with suspended sensors for both textile samples and suspension cultures.

Figure 13: Measurement bottle sealed with PTFE tape and an integrated sealing ring to ensure a gas-tight CO_2 measurement environment.

Chapter 3

Method Evaluation for an Existing Microalgae-Textile Woven Multilayer Bio-Composite

3.1 Pilot 1

Assessment of *Scenedesmus* sp. Viability in Plain Cotton Textiles after Freezing Conditions

Overview Pilot 1

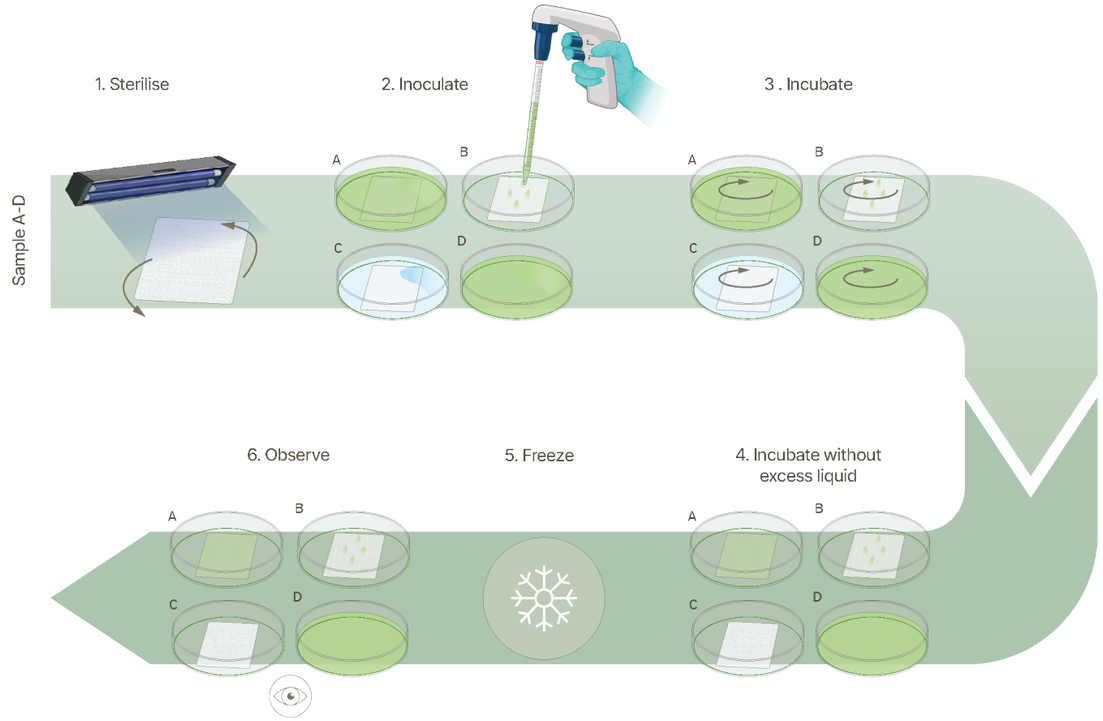

Figure 14: Overview methodology Pilot 1

Table 1: Timeline Pilot 1

Nr.	Action	Protocol day
1	Sterilise with UV-C light for 20 minutes on both sides	1
2	Inoculate sample groups with *Scenedesmus* sp.	1
3	Incubate samples on a rotating platform at 25°C	1-4
4	Remove the excess liquid and incubate at 25°C	4
5	Freeze at -20°C	4-5
6	Observe the samples	6-20

For sample groups see Table 2

3.1.1 Introduction

This study starts with three pilot protocols based on the immobilisation method developed by Mancini [49]. Mancini's protocol demonstrated that the *Scenedesmus* sp. could effectively be incorporated into a cotton-hydrogel textile matrix. In this method (Protocol 6, Timeline 3 [49]), a multilayer textile matrix, consisting of cotton and polyvinyl alcohol (PVA) hydrogel, was first inoculated with a microalgal suspension. Allowing initial attachment and growth within the textile structure. Subsequently, excess medium was removed, and the system was subjected to a single freeze-thaw cycle to physically cross-link the hydrogel, thereby immobilising the microalgae within a hydrated environment that supports microalgae viability.

While this approach provides a functional baseline for microalgae-textile immobilisation, Chapter 2 identified several key uncertainties that remain unresolved, particularly regarding dependency on hydrogel-moisture retention, the influence of a multilayer textile architecture on microalgal attachment, and the viability of *Scenedesmus* sp. after freeze-thawing.

To address this, Pilot 1 aims to establish a baseline by evaluating the growth and survival of *Scenedesmus* sp. on a single-layer cotton-textile matrix without hydrogel-based moisture retention. By simplifying the protocol developed by Mancini [49], the drying behaviour of the textile can be assessed in the absence of a hydrogel that normally retains the growth medium for a longer period. Additionally, samples were incubated on a rotational platform to evaluate whether dynamic conditions influence the rate of microalgal attachment to the cotton-textile matrix.

Based on this rationale, Pilot 1 addresses research questions 1 - 3, and the following sub-questions (SRQs) were defined:

1. How effectively does *Scenedesmus* sp. attach to and grow within a single-layer cotton-textile matrix?
2. How does moisture retention differ between a single-layer cotton textile and the multilayer cotton-hydrogel matrix developed by Mancini [49]?
3. How does rotational incubation affect the growth of *Scenedesmus* sp. within textile-based matrices?
4. To what extent can *Scenedesmus* sp. recover metabolic activity following one freeze-thaw cycle?

Scenedesmus sp. cultures were cultivated according to the Standard Cultivation protocol using an 16 h day and 8 h dark cycle at a temperature of 25 °C (Appendix 1.1). Cultures were initiated at an optical density of 0.540 measured at a wavelength of 680 nm.

Four experimental groups were prepared, as outlined in Table 2. The textile samples consisted of a two-dimensional material composed of 100% cotton. Prior to inoculation, the textile samples were sterilised using UV-C light in a laminar flow cabinet. All sample groups were frozen at −20 °C. Detailed procedural steps are provided in Appendix 3.1.

Each sample was monitored over a two-week period through visual documentation, with pigment intensity used as a proxy for growth and viability.

Table 2: Sample overview Pilot 1

Sample group	Description
A (n=2)	Single-layer textile immersed in *Scenedesmus* sp. suspension
B (n=2)	Centrifuged *Scenedesmus* sp. pipetted onto the single-layer textile surface
C (n=1)	Single-layer textile-only control group immersed in BG11 medium
D (n=2)	*Scenedesmus* sp. suspension culture control group

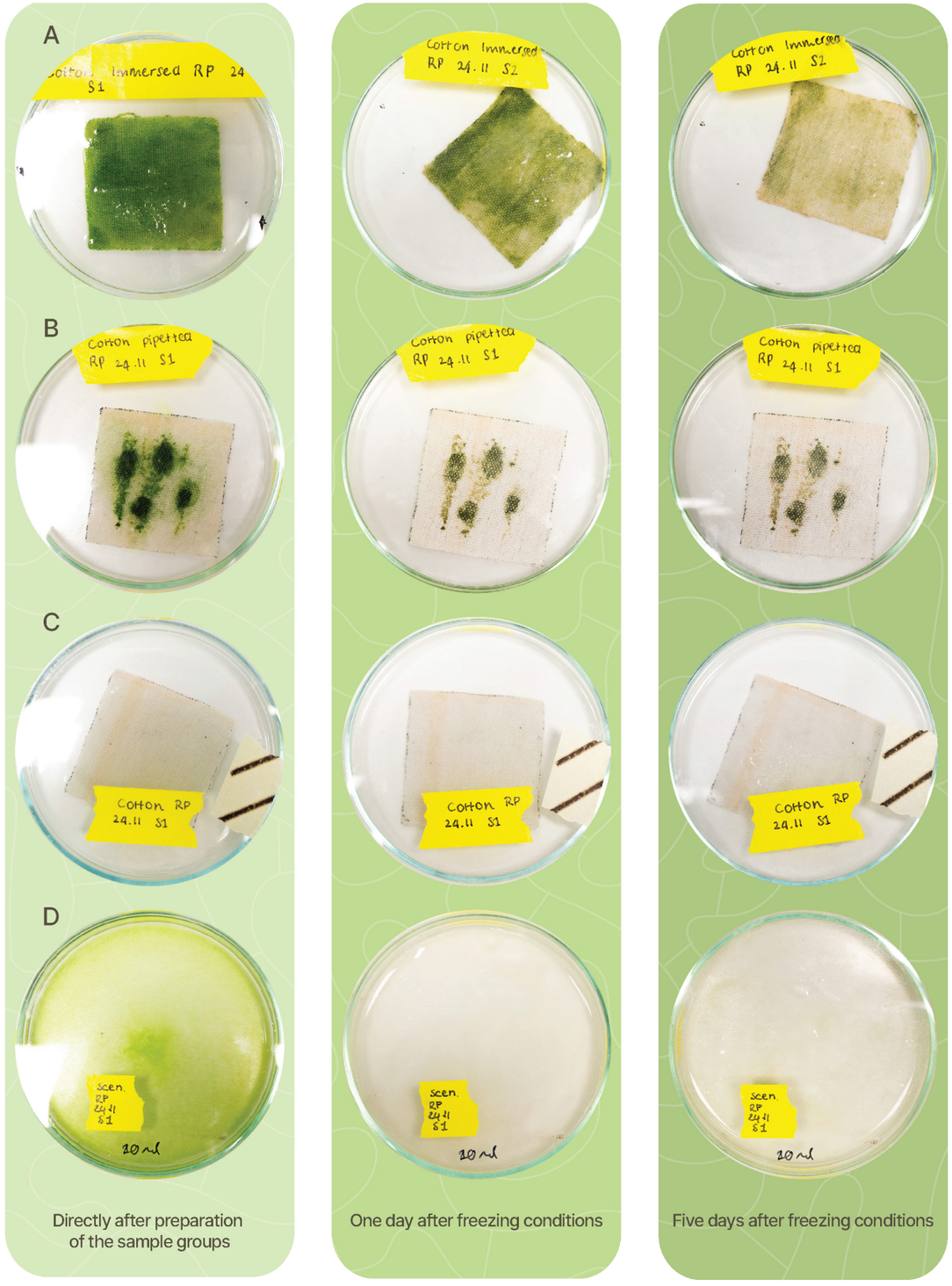

Figure 15: A single representative biological replicate was selected from each sample group for imaging. (A) Textile immersed in *Scenedesmus* sp., showing a significant decrease in pigmentation after freezing; (B) centrifuged *Scenedesmus* sp. pipetted onto textile, showing gradual drying and reduced pigmentation after freezing; (C) cotton-only sample, showing no observable change over the observation period; (D) *Scenedesmus* sp. suspension culture, showing no viability after freezing, indicated by absence of pigmentation.

3.1.2 Results

The textile samples showed cotton surface coating that temporarily reduced hydrophilicity, which limited the initial penetration of *Scenedesmus* sp. into the textile structure. However, following prolonged soaking, the *Scenedesmus* sp. gradually infiltrated the textile.

During incubation, rotational movement of the *Petri* dishes caused the microalgal cells to accumulate toward the centre of the *Petri* dish due to centripetal forces. This increased contact between the microalgae and the textile, resulting in rapid microalgal attachment and a corresponding reduction of cells in the surrounding growth medium (Figure 15).

Textile samples immersed in *Scenedesmus* sp. exhibited a visible increase in green pigment over time, indicating microalgal growth (Figure 15 A). Whereas the pipetted textile samples exhibited no noticeable colour change over time (Figure 15 B). The suspension cultures displayed variable behaviour, with one culture remaining homogeneous while the other developed visible cell clumping (Figure 16 A).

Following a single freeze-thaw cycle, large ice crystals were observed in suspension cultures, whereas textile samples exhibited smaller ice crystal formation (Figure 16 C). After three days of thawing, the suspension cultures had largely lost their green pigmentation, while the textile samples retained partially pigmented areas (Figure 15).

After 14 days of incubation, all textile samples exhibited substantial drying. The immersed samples remained slightly humid and retained green pigmentation, indicating partial viability. In contrast, the pipetted samples were fully dried. Although these samples exhibited dark green colouration, they were presumed to be non-viable due to complete dehydration, which likely caused irreversible cellular damage despite the apparent retention of pigment.

Figure 16: (A) *Scenedesmus* sp. suspension culture showing cell clumping; (B) frozen *Scenedesmus* sp. suspension culture showing large crystal formation; (C) frozen *Scenedesmus* sp. within the textile matrix showing smaller crystallisation.

3.1.3 Discussion and Conclusion

Direct comparison between immersed and pipetted textile samples was limited, as the approaches differed in several key experimental variables. This includes microalgal concentration and growth medium volume. In contrast to Mancini's original protocol [49], which contained samples that had hydrogel woven into the multilayer matrix, microalgal viability in the present study declined more rapidly, with pigment loss occurring within one day following freezing. This reduced viability is attributed to the evaporation of the growth medium, as the microalgae were not immobilised within a cotton-hydrogel matrix, which resulted in insufficient moisture retention and limited long-term survival of *Scenedesmus* sp. Additionally, the centrifugation step applied to the pipetted samples may have resulted in an excessively high cell density relative to the available growth medium, creating nutrient-limited conditions that negatively affected sustained viability.

Rotational movement during incubation appeared to increase microalgal attachment, compared to stationary conditions, as the cells tend to sink to the bottom and stay in place. The rotation caused cells to move toward the centre of the *Petri* dish, increasing contact between *Scenedesmus* sp. and the textile, and promoting more rapid initial immobilisation. Overall, *Scenedesmus* sp. was successfully immobilised within plain cotton-textile matrices, but the absence of a hydrogel component resulted in rapid drying and moisture loss, reducing long-term viability.

Recovery following a single freeze-thaw cycle was limited, as indicated by rapid pigment loss in suspension cultures and decreased pigment intensity over time, suggesting reduced viability. The cotton-textile matrix provided some stability by maintaining viability longer than suspension cultures.

In conclusion, the findings of this Pilot 1 provide partial answers to the sub-research questions outlined above. *Scenedesmus* sp. can be successfully immobilised within a plain cotton-textile matrix, and attachment is enhanced by rotational movement, because of increased contact between cells and textile (SRQ1, SRQ3). However, the absence of a hydrogel component results in limited moisture retention, leading to faster drying and reduced long-term viability compared to the multilayer cotton-hydrogel system developed by Mancini (SRQ2). Recovery following a single freeze-thaw cycle was limited, as shown by reduced pigment intensity over time, indicating decreased metabolic activity (SRQ4). Overall, these results highlight moisture retention as a key factor for viable microalgae-textile biocomposite, which informs Pilot 2 of this study, focusing on hydrogel integration to improve system stability and viability. In addition, rotational incubation will be applied in all subsequent protocols to enhance microalgal attachment.

3.2 Pilot 2

Assessment of *Scenedesmus* sp. Viability and CO_2 Monitoring in Multilayer Textile Matrices

Overview Pilot 2

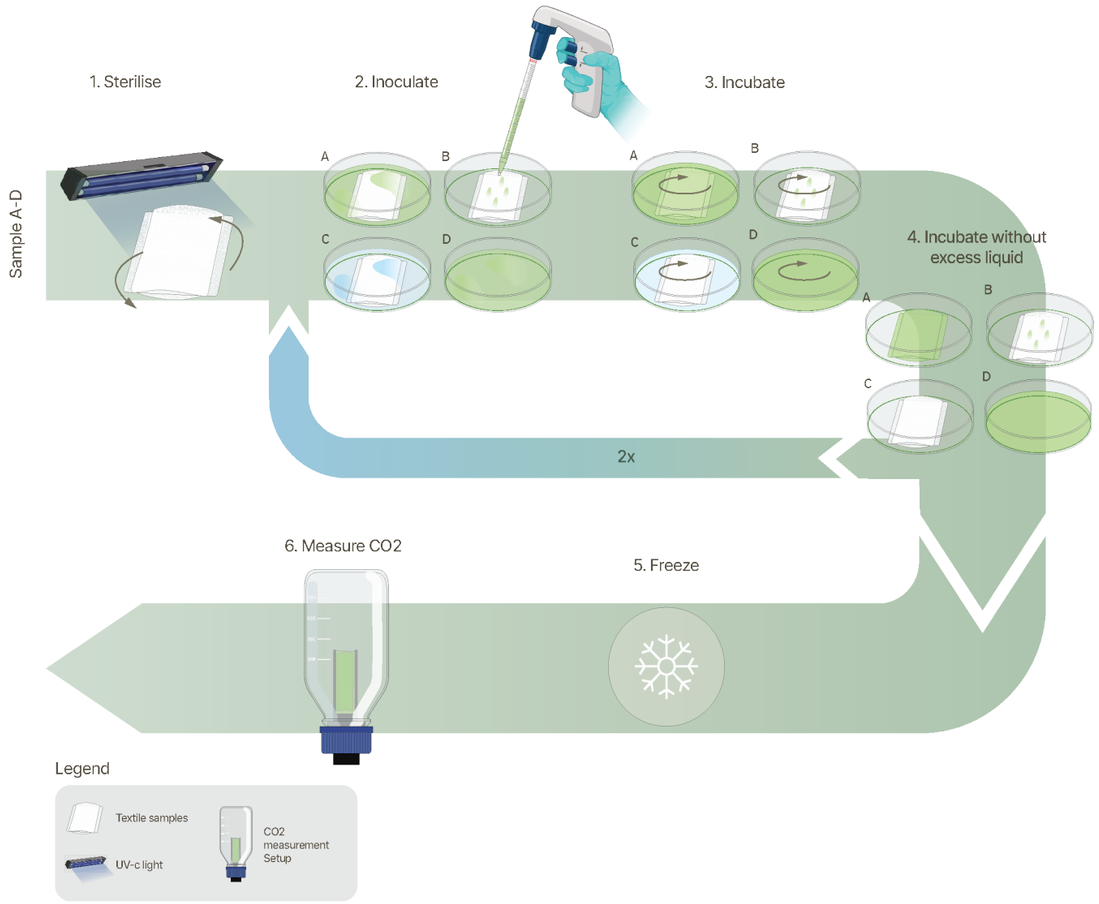

Figure 17: Overview methodology Pilot 2

Table 3: Timeline Pilot 2

Nr.	Action	Protocol day
1	Sterilise with UV-C light for 30 minutes on both sides	1
2	Inoculate sample groups with *Scenedesmus* sp.	1, 7
3	Incubate samples on a rotating platform (25°C, 120 rpm)	1-4, 7-11
4	Remove the excess liquid and incubate at 25°C	4-7, 11-14
5	Freeze at -20°C	14-76
6	Measure CO2	76-79da

For sample groups see Table 4

3.2.1 Introduction

Pilot 2 investigates the viability of *Scenedesmus* sp. in a multilayer woven textile matrix following a single freeze-thaw cycle and evaluates its capacity for CO_2 uptake. Building on the findings of Pilot 1 (3.1), which identified moisture retention as a key limiting factor for sustained microalgal viability, Pilot 2 reintroduces a multilayer cotton-hydrogel textile matrix to provide a hydrated environment that supports long-term stability. The adapted methodology is based on Timeline 3, Protocol 6 developed by Martina Mancini [49], with modifications including repeated microalgal application, rotational incubation, an extended freezing period, and the incorporation of CO_2 measurements.

The use of rotational incubation was informed by findings from Pilot 1 (3.1), where it was shown to enhance microalgal attachment to textile substrates. Repeated inoculation of *Scenedesmus* sp. was implemented to compensate for the anticipated reduction in viable biomass following freeze-thawing, as reported by Prieto-Guevara et al. [53]. The extended freezing period was introduced due to delays in the completion of the CO_2 measurement setup.

Previous work by Mancini demonstrated that *Scenedesmus* sp. can be effectively immobilised within a cotton-hydrogel textile [49], maintaining a hydrated environment that supports microalgal viability. Pilot 2 therefore, aims to determine whether hydrogel integration improves microalgal stability following freeze-thawing and allows for the quantitative assessment of CO_2 uptake. In particular, Pilot 2 compares the CO_2 uptake of the textile-based system to conventional suspension cultures under controlled conditions.

Based on this rationale, Pilot 2 addresses research questions 1 - 4, and the following sub-questions (SRQs) were defined:

1. How effectively does *Scenedesmus* sp. attach to and grow within a multilayer cotton-textile matrix?
2. How does moisture retention within the multilayer cotton-hydrogel textile matrix support sustained microalgal viability?
3. To what extent can *Scenedesmus* sp. recover metabolic activity following one freeze-thaw cycle?
4. How does the CO_2 uptake performance of the microalgae-textile biocomposite compare to conventional suspension cultures?

Scenedesmus sp. cultures were cultivated according to the Standard Cultivation protocol (Appendix 1.1), with initial and subsequent optical densities of 0.050 and 0.102 measured at a wavelength of 680 nm, respectively.

Four experimental groups were prepared, as outlined in Table 4. The textile samples consisted of a multilayer weave (outer layers: 60% cotton, 40% PVA; inner layer: 100% cotton) held together with a compound twill on two sides (Figure 18, Appendix 4.2). Details on the weaving structure are provided in Appendix 4.2. Prior to inoculation, the textile samples were sterilised using UV light in a laminar flow cabinet. All samples were frozen at −20 °C for approximately 2 months. Detailed procedural steps are provided in Appendix 3.2.

Each sample was monitored over a two-week period through visual documentation, with pigment intensity used as a proxy for microalgal growth and viability. In addition, textile samples immersed in *Scenedesmus* sp. and a suspension culture control group were used for CO_2 measurements conducted over a period of two days, with samples maintained under a 16-hour light and 8-hour dark photoperiod.

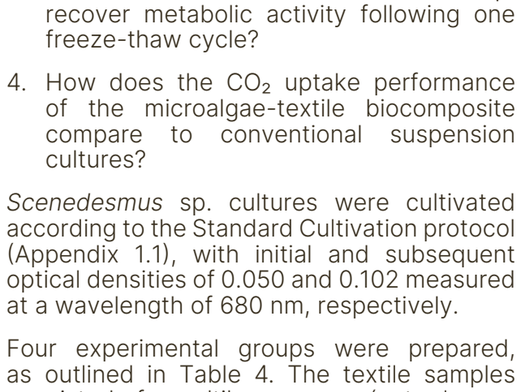

Figure 18: Texile sample, multilayer inner part held together by a compound twill on two sides

Table 4: Sample overview Pilot 2

Sample group	Description
A (n=2)	Multilayer textile immersed in *Scenedesmus* sp. suspension
B (n=2)	*Scenedesmus* sp. pipetted onto the multilayer textile surface
C (n=1)	Multilayer textile-only control group immersed in BG11 medium
D (n=2)	*Scenedesmus* sp. suspension culture control group

3.2.2 Results

During textile fabrication, the weaving pattern provided by Mancini [49] did not fully reproduce the intended multilayer structure. The layers were partially connected, instead of being three separate layers. As well as that, the top and bottom layers exhibited differences in weave structures, although they were designed to be identical. Additionally, the textile samples were prone to fraying.

Upon contact with the culture medium, the hydrogel-textile samples exhibited noticeable curling, particularly in areas directly exposed to the liquid (Figure 19 B).

When *Scenedesmus* sp. was pipetted between the textile layers, the suspension seeped through the spacing within the weave structure. Effectively resulting in immersion rather than localised inoculation.

During incubation, the placement of the *Petri* dishes on a rotating platform resulted in accelerated microalgal attachment to the textile matrix, consistent with observations from Pilot 1 (3.1). A reduction of cells in the surrounding growth medium was observed, while higher cell densities developed within the textile, particularly along the edges, as indicated by increased pigment intensity (Figure 19 A).

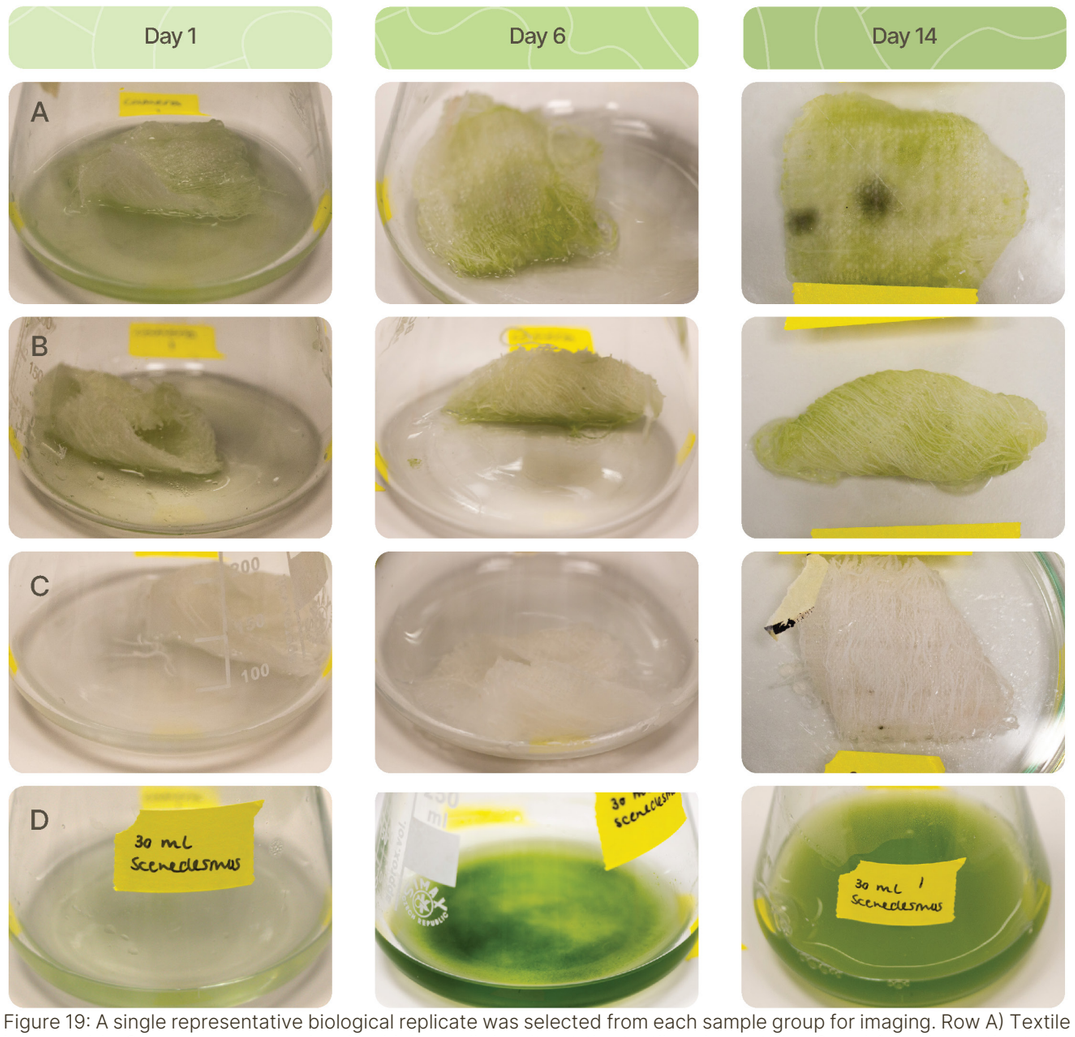

Figure 19: A single representative biological replicate was selected from each sample group for imaging. Row A) Textile immersed in *Scenedesmus* sp., showing higher cell density at the textile edges at day 6 and fungal growth at day 14; Row B) textile with *Scenedesmus* sp. pipetted onto the surface, showing significant curling of the textile; Row C) textile-only control (BG11 medium); Row D) *Scenedesmus* sp. suspension culture control. Time points represent days from the start of the protocol.

Prior to the addition of *Scenedesmus* sp. with a higher optical density, no clear increase in green pigmentation was observed in the textile samples (Figure 19 A, B day 3). In contrast, suspension culture samples showed a visible increase in microalgae growth over time (Figure 19 D). After additional inoculation of *Scenedesmus* sp. with a higher optical density, a slight increase in green pigmentation was observed in the textile samples (Figure Figure 19 A, B day 14).

Despite UV-C sterilisation of the textiles, fungal growth was observed during incubation (Figure 19 A, day 14). After approximately two months of storage at −20 °C, all samples appeared fully crystallised and lower viability after preservation was expected. However, green pigmentation remained visible within the textile samples at this stage (Figure 19 A, B day 14).

After two months of storage, the samples were removed from the freezer and allowed to thaw for one day before being transferred to the CO_2 measurement setup (Figure 20). Following thawing, the textile samples exhibited a significant decrease in pigment intensity. Measurements from the CO_2 setup showed an increase in CO_2 concentration rather than the expected decrease (Figure 21).

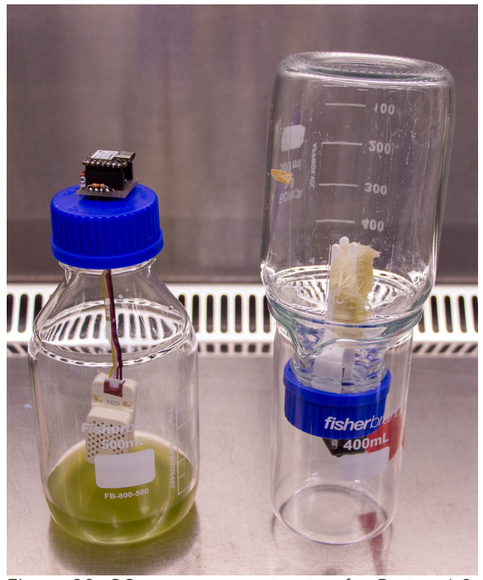

Figure 20: CO_2 measurement setup for Protocol 2. The samples exhibit low viability. The left sample shows a suspension culture (sample Group D), while the right sample shows a microalgae-textile biocomposite sample (sample Group A).

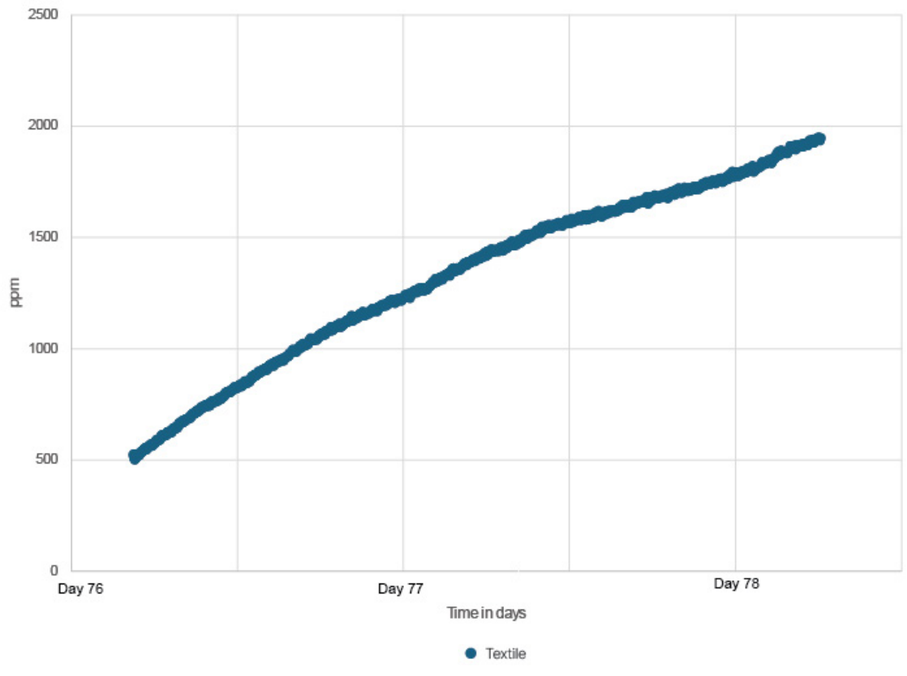

Figure 21: Graph showing CO_2 measurements of the microalgae-textile biocomposite sample (A1), indicating an increase in CO_2 concentration (ppm) over time. Time points represent days from the start of the protocol.

3.2.3 Discussion and Conclusion

The incomplete reproduction of the multilayer structure and fraying along the edges suggest that further optimisation of the textile design is required. Curling of the textile is likely caused by uneven hydrogel swelling, due to partial rather than complete immersion in the *Scenedesmus* sp. culture. Complete immersion of the textile samples is therefore recommended to ensure uniform hydrogel response.

Pipetting *Scenedesmus* sp. between textile layers did not provide localised inoculation, as the open weave structure allowed the suspension to spread throughout the matrix. Moreover, pipetting is labour-intensive and impractical for upscaling. One of the aims of this study is to develop a cultivation method that is superior to the scalability of conventional open pond and photobioreactor systems. Immersion is therefore identified as the most suitable immobilisation method. The elimination of pipetting as an inoculation method enables further optimisation of the textile design, including the implementation of a compound twill along all edges to create a more durable and enclosed matrix.

The limited increase in pigmentation during initial incubation suggests that the starting optical density was insufficient to ensure survival through the freeze-thaw cycle. Future experiments should therefore begin with a higher optical density to increase the proportion of cells capable of recovery after freezing. Observations also indicate that removing excess liquid and conducting a secondary incubation may be unnecessary, as most microalgal cells were already retained within the textile matrix.

The occurrence of fungal contamination highlights the difficulty of fully sterilising multi-layer textile structures using UV-C light due to limited penetration. Increasing UV-C intensity or sterilising within a UV-C light box may improve contamination control in future studies.

CO_2 measurements showed an increase in CO_2 concentration over time rather than the expected decrease. Indicating that photosynthetic activity was not sustained after freezing. This suggests that respiration or decomposition processes dominated, and that the microalgae were no longer metabolically active in a photosynthetic capacity. Post-thaw pigment loss further supports the conclusion that cellular damage occurred during freezing, leading to reduced viability.

In conclusion, this pilot 2 demonstrates that *Scenedesmus* sp. can be immobilised within a multilayer cotton-hydrogel textile matrix, and that rotational incubation enhances microalgal attachment by increasing contact between cells and the textile (SRQ1). However, structural limitations of the textile, insufficient initial optical density, fungal contamination, and prolonged freezing conditions negatively affected microalgal viability and system stability (SRQ2, SRQ3). As a result, no photosynthetic CO_2 uptake was observed, and CO_2 production increased instead, indicating loss of metabolic function (SRQ4). These findings highlight the need for improvements in textile structure, controlled immersion strategies, higher initial cell density, and enhanced sterilisation methods to enable viable microalgae-textile biocomposites. Building on these results, Pilot 3 will apply the same experimental framework with key optimisations, including an improved weaving structure, larger textile samples to increase CO_2 uptake capacity, exclusion of the post-drain incubation step, and a higher initial optical density to enhance post-freeze recovery and overall system performance.

3.3 Pilot 3

Assessment of *Scenedesmus* sp. Viability in Plain Cotton Textiles after Freezing Conditions

Overview Pilot 3

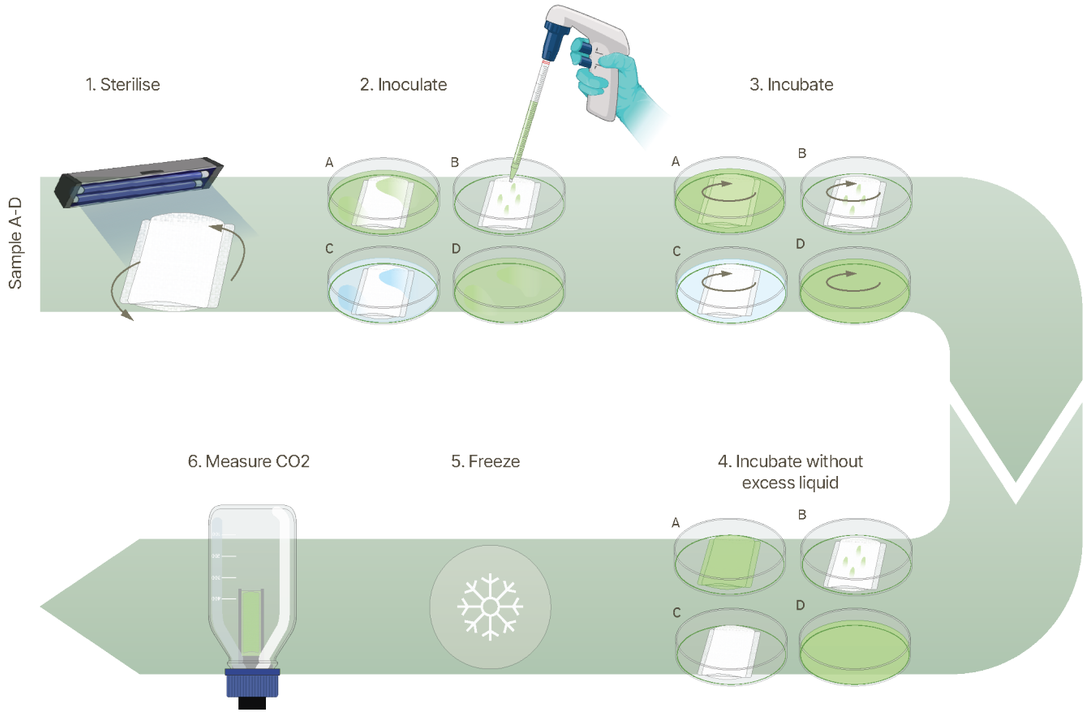

Figure 22: Overview methodology Pilot 3

Table 5: Timeline Pilot 3

Nr.	Action	Protocol day
1	Sterilise with UV-C light for 30 minutes on both sides	1
2	Inoculate sample groups with *Scenedesmus* sp.	1
3	Incubate samples on a rotating platform (25°C, 120 rpm)	1-4
4	Remove the excess liquid and incubate at 25°C	4-7
5	Freeze at -80°C	8-7
6	Measure CO2	8-11

For sample groups see Table 6

3.3.1 Introduction

Pilot 3 builds upon the findings of Pilot 2 (3.2), further investigating the viability of *Scenedesmus* sp. within a multilayer woven textile matrix and evaluating the CO_2 uptake of the resulting microalgae-textile biocomposite. The adapted methodology is based on timeline 3, protocol 6 developed by Mancini [49], with modifications including an improved weaving structure, larger textile sample size, rotational incubation, a higher initial optical density, the incorporation of CO_2 measurements, and the exclusion of the post-drain incubation.

The weaving structure was improved by incorporating a compound twill weave along all edges of the sample, addressing the structural limitations observed in Pilot 2. As Pilot 2 showed that immersion is the preferred inoculation method over pipetting. Therefore, the open spaces in the weave were no longer required. Closing these openings also improves the structural integrity of the textile matrix, resulting in a more robust and stable textile matrix. Increasing the textile size was implemented to enhance CO_2 capture and improve the responsiveness of the biocomposite under measurement conditions. The higher initial optical density was applied to improve post-freeze recovery and increase the likelihood of maintaining viable biomass following freeze-thaw treatment, as reduced viability was identified as a key limitation in Pilot 2. The exclusion of the additional incubation step after liquid removal was based on findings from Pilot 2, which indicated that sufficient microalgal biomass was already retained within the textile matrix, making further incubation unnecessary.

Rotational incubation and CO_2 measurements were maintained to ensure consistency with the experimental framework established in previous Pilots and to allow direct comparison of functional performance across iterations. Overall, Pilot 3 aims to build on the limitations identified in Pilot 2, in order to enable a more stable and functional assessment of microalgae-textile biocomposites and their CO_2 uptake performance following freeze-thaw treatment.

Based on this rationale, Pilot 3 addresses research questions 1 - 4, and the following sub-questions (SRQs) were defined:

1. How effectively does *Scenedesmus* sp. attach to and grow within a multilayer cotton-textile matrix?
2. How does moisture retention within the multilayer cotton-hydrogel textile matrix support sustained microalgal viability?
3. To what extent can *Scenedesmus* sp. recover metabolic activity following one freeze-thaw cycle?
4. How does the CO_2 uptake performance of the microalgae-textile biocomposite compare to conventional suspension cultures?

Scenedesmus sp. cultures were cultivated according to the standard cultivation protocol (Appendix 1.1), with an initial optical density of 0.660 measured at a wavelength 430 nm.

Two experimental groups were prepared, as outlined in Table 6. The sample groups consisting of *Scenedesmus* sp. pipetted onto the multilayer textile surface and the multilayer textile-only control immersed in BG11 medium were excluded in Pilot 3, as previous protocols showed that these conditions did not provide additional experimental value. The textile samples consisted of a multilayer weave (outer layers: 60% cotton, 40% PVA; inner layer: 100% cotton) held together with a compound twill on all sides (Figure 23, Appendix 4.1.1). The samples used in this protocol were four times larger than those used in the previous pilots. Prior to inoculation, the textile samples were sterilised using a UV-C sterilisation box (Appendix 1.2). All samples were frozen at −20 °C for 24 h. Detailed procedural steps are provided in Appendix 3.3.

Each sample was monitored over a two-week period through visual documentation, with pigment intensity used as a proxy for microalgal growth and viability. In addition, textile samples immersed in *Scenedesmus* sp. and a suspension culture control group were used for CO_2 measurements conducted over a period of three days, with samples maintained under a 16-hour light and 8-hour dark photoperiod.

Table 6: Sample overview Pilot 3

Sample group	Description
A (n=2)	Multilayer textile immersed in *Scenedesmus* sp. suspension
B (n=2)	*Scenedesmus* sp. suspension culture control group

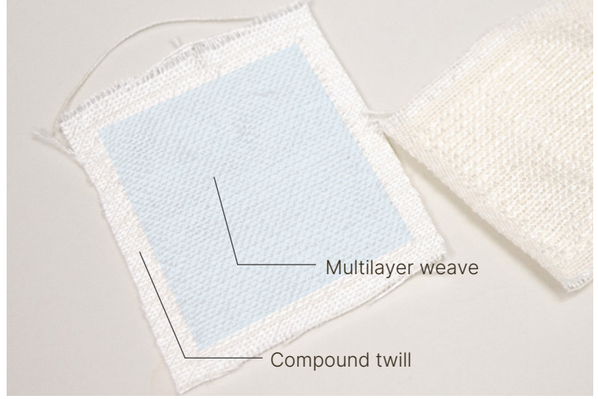

Figure 23: Texile sample, containing a multilayer inner part held together by a compound twill on all sides

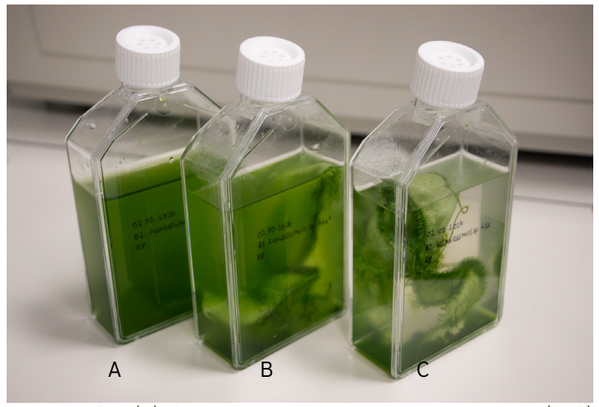

Figure 24: (A) *Scenedesmus* sp. suspension culture ; (B-C) Textile samples immersed in *Scenedesmus* sp.

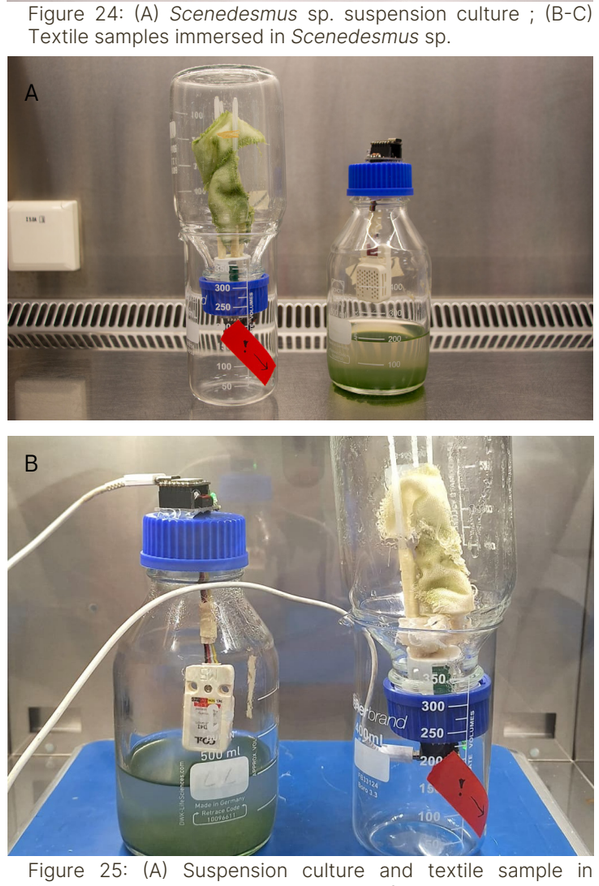

Figure 25: (A) Suspension culture and textile sample in CO_2 measuring setup at the start of the measurement ; (B) Suspension culture and textile sample in CO_2 measuring setup in incubator showing reduced viability

3.3.2 Results

Due to the increased size of the multilayer woven textile matrix, immersion in a *Petri* dish was no longer feasible. The samples were therefore immersed in a cultivation flask containing a larger volume of *Scenedesmus* sp. suspension compared to previous pilots. The vertical positioning of the flask during incubation prevented placement on a rotational platform, resulting in an altered distribution of the microalgal cells within the matrix.

As shown in Figure 24, the distribution of *Scenedesmus* sp. within the textile matrix was non-homogeneous, in contrast to the more uniform distribution observed in Pilots 1 and 2 (3.1, 3.2). Higher pigment intensity was observed in the compound twill regions of the textile, while the multilayer inner structure exhibited lower pigment intensity (Figure 24).

During the initial CO_2 measurement, an increase in CO_2 concentration was recorded for both the textile sample and the suspension culture (Figure 26 A). Following this measurement, the experimental setup was modified. The CO_2 measurement system was placed in an incubator with increased light intensity, additional BG11 medium was added to the samples after freezing, and sterilisation procedures were intensified.

During subsequent CO_2 measurements, the temperature inside the incubator increased to 33 °C due to the heated electronics of the applied light conditions. Following this temperature increase, the textile samples exhibited a substantial decrease in pigment intensity. The suspension culture appeared visibly hazy compared to its initial clear state (Figure 25).

During the CO_2 measurement, liquid dripping from the textile samples contacted the CO_2 sensor, resulting in oxidation of the copper components and loss of signal. Consequently, only the CO_2 data obtained from the suspension culture control are presented (Figure 26 B). The recorded CO_2 concentration in the suspension culture showed an initial decrease, followed by an increase and a subsequent decrease over time.

A

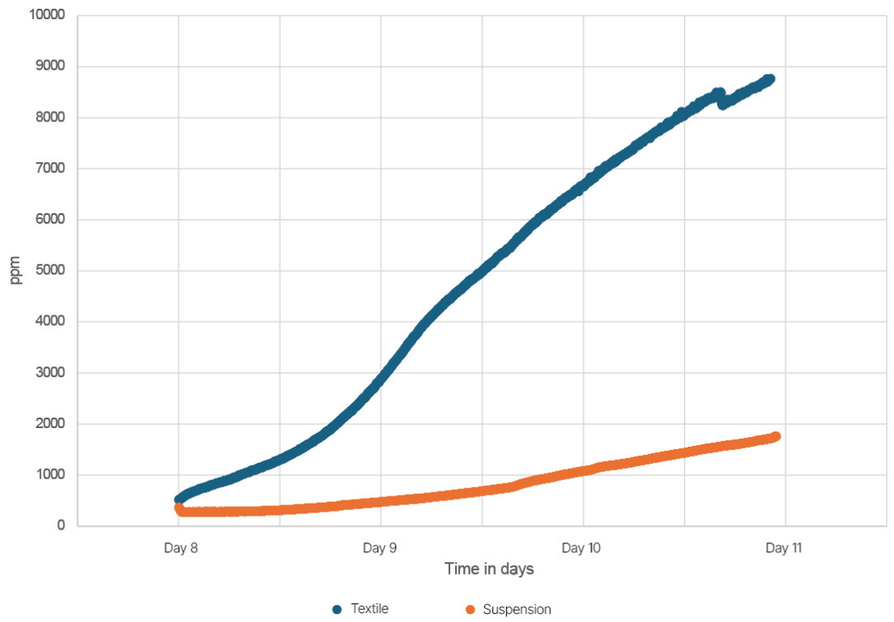

B

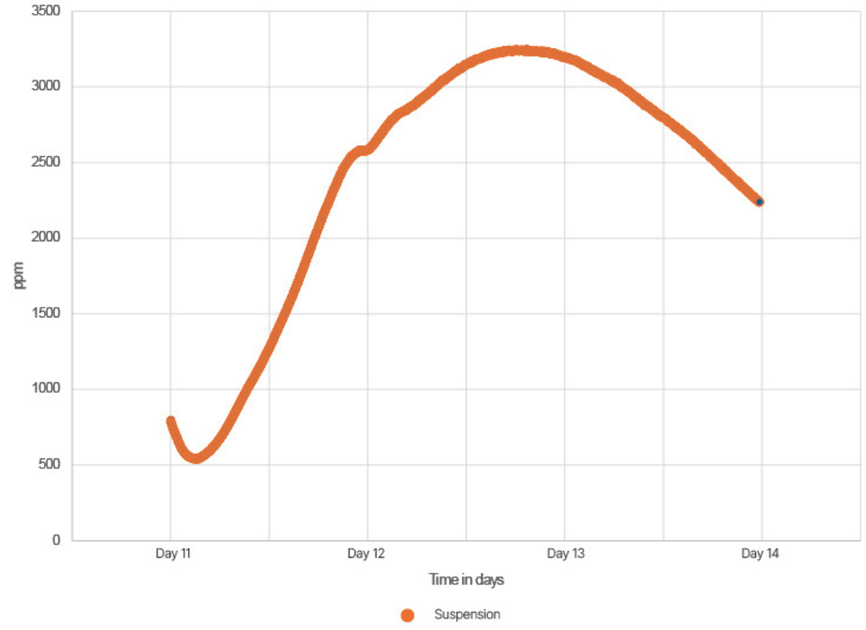

Figure 26: (A) CO_2 measurements for sample groups A and B, showing an increase in CO_2 concentration (ppm); (B) CO_2 measurements for sample group B, showing a slight initial decrease followed by a subsequent increase in CO_2 concentration (ppm). Time points represent days from the start of the protocol.

3.3.3 Discussion and Conclusion

The non-homogeneous distribution of *Scenedesmus* sp. within the multilayer woven textile matrix is likely due to the absence of effective rotational incubation, which limited uniform contact between microalgal cells and the textile surface. Consequently, cell immobilisation occurred in localised regions rather than being evenly distributed throughout the matrix. Higher pigment intensity in the compound twill regions suggests that these areas provided more favourable attachment conditions, likely due to increased cotton content. In contrast, the multilayer structure exhibited lower pigment intensity, indicating limited microalgal attachment.

With respect to moisture-related stability, no direct moisture loss was observed during the short-term measurement phase; however, structural deformation and non-uniform distribution indicate that the current multilayer configuration does not fully ensure stable environmental conditions across the matrix. Recovery following a single freeze-thaw cycle was partially observed through limited pigment retention in textile regions. However, overall viability appeared reduced under elevated incubation temperatures, indicating that the viability is strongly dependent on environmental stability.

Initial CO_2 measurements indicated an increase in CO_2 concentration, suggesting suboptimal photosynthetic conditions in both the microalgae-textile biocomposite and the suspension culture. This may have resulted from insufficient light intensity, limited nutrient availability, or contamination, which could contribute to increased CO_2 via respiration or decomposition. During subsequent measurements, elevated incubator temperatures likely induced physiological stress in *Scenedesmus* sp., as reflected by decreased pigment intensity in textile samples and the hazy appearance of the suspension culture. The observed CO_2 fluctuations likely reflect unstable metabolic activity, with limited or absent CO_2 uptake under the applied conditions. Due to system failure during measurement, a direct and reliable comparison between the microalgae-textile biocomposite and the suspension culture could not be fully established.

In conclusion, this pilot demonstrates that *Scenedesmus* sp. can be immobilised within a multilayer cotton-hydrogel textile matrix, and that textile composition strongly influences spatial distribution, with compound twill regions supporting higher microalgal attachment compared to multilayer sections (SRQ1). However, the absence of rotational incubation and environmental instability prevented homogeneous growth throughout the matrix (SRQ2, SRQ3). The CO_2 uptake could not be reliably quantified due to sensor failure and unstable metabolic activity, with observed CO_2 fluctuations indicating a lack of consistent photosynthetic function compared to suspension cultures (SRQ4). These findings highlight the need for improved control over incubation conditions and more stable measurement conditions to enable reliable evaluation of microalgae-textile biocomposites. Building on the results from Pilots 1-3 (3.1-3.3), the next phase of this study will reintroduce and systematically vary elements of the original protocol developed by Mancini [49], focusing on optimisation of matrix design, immobilisation strategies, hydrogel cross-linking, incubation conditions, and overall process stability, to further refine system performance and enable a more reliable evaluation of CO_2 capture.

Chapter 4

Technical Characterisation for the Optimisation of a Multilayer Microalgae-Textile Biocomposite

4.1 Textile Cross-linking

Effect of Freeze-Thaw and Freeze-Drying Techniques on Hydrogel Cross-linking in Multilayer Cotton-PVA Textiles

Overview Textile Cross-linking

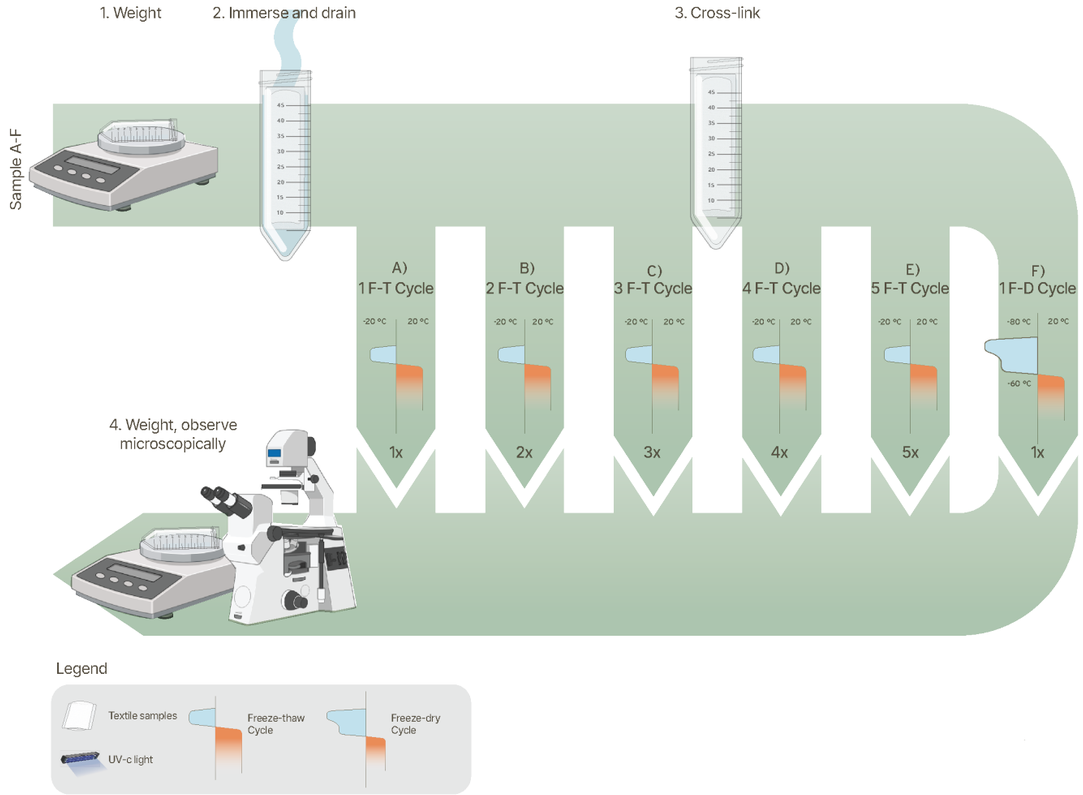

Figure 27: Overview methodology Protocol Hydrogel Cross-linking

Table 7: Timeline Protocol Textile Cross-linking

Nr.	Action	Sample group	Protocol day
1	Weight textile samples	A-F	1
2	Immerse the textile samples for 24 hours in 50 mL demi water, remove the excess liquid after the 24 hours	A-F	1
3	Cross-link the textile samples (24 hours freezing, 24 hours thawing)	A	1-2
		B	1-4
		C	1-6
		D	1-8
		E	1-10
		F	1-3
4	Weight the textiles and observe microscopically	A	2
		B	4
		C	6
		D	8
		E	10
		F	3

For sample groups see Table 8

4.1.1 Introduction

Building on the findings from Pilot 1 and 2 (3.1, 3.2), it was observed that *Scenedesmus* sp. shows reduced viability following a single freeze-thaw cycle, indicating that repeated freezing is not favourable for the biological component of the biocomposite. This protocol focuses specifically on evaluating the structural performance of the textile matrix in the absence of microalgae. The aim is to assess the cross-linking bonds in the hydrogel-textile matrix after freeze-thawing and freeze-drying, ensuring that the material maintains structural integrity and does not decompose over time. The protocol is based on relevant literature [54], which suggests that hydrogels cross-linked by freeze-drying form stronger cross-linking bonds, and that increasing the number of freeze-thaw cycles can enhance cross-linking strength.

By comparing different cross-linking techniques, this study aims to determine which approach optimises the mechanical stability of the cotton-hydrogel matrix, providing a stable foundation for subsequent microalgal immobilisation and growth.

Based on this rationale, this protocol addresses research question 2, and the following sub-questions (SRQs) were defined:

1. How do different hydrogel cross-linking methods (freeze-thawing vs. freeze-drying) influence the structural integrity of the cotton-hydrogel composite?
2. How does the number of freeze-thaw cycles affect the strength and stability of the hydrogel cross-linking within the textile matrix?

The textile samples consisted of a multilayer woven matrix (outer layers: 60% cotton, 40% PVA; inner layer: 100% cotton) secured on all sides with a compound twill (Figure 23, Appendix 4.1.1). Based on the conclusions of Pilot 2 (3.2), the multilayered structure is fully enclosed by a compound twill surrounding the entire perimeter.

Samples were subjected to either one to five freeze-thaw cycles or a single freeze-drying cycle (Table 8). Detailed procedural steps are provided in Appendix 3.4.

Sample evaluation was conducted through mass measurements, tensile strength testing, assessment of surface degradation, and microscopic examination at critical stages. Mass measurements were used to monitor water loss, with higher water retention indicating a stronger cross-linking bond.

4.1.2 Results

No significant difference in mass was observed between samples before and after freeze-thaw cross-linking. When exposed to 30°C in an open Falcon tube, all samples dried within 2 days, regardless of the applied cross-linking method.

Clear differences were observed between freeze-thawed and freeze-dried samples. Freeze-thawed samples exhibited greater shrinkage and slight darkening in colour following cross-linking (Figure 28 C). In contrast, freeze-dried samples were fully dehydrated, displayed a lighter appearance, and exhibited a paper-like texture (Figure 28 B).

Microscopic analysis revealed distinct structural differences between the two treatments. Freeze-dried samples retained a clearly defined structure, whereas freeze-thawed samples appeared less structurally distinct. Additionally, PVA within the freeze-dried samples showed visible darkening, while it remained transparent in the freeze-thawed samples. In both freeze-dried and freeze-thawed samples, the weaving structure appeared denser compared to non-cross-linked samples (Figure 29 A-F).

Table 8: Sample overview Protocol Textile Cross-linking

Sample group	Description
A (n=3)	1 Freeze-thaw cycle
B (n=3)	2 Freeze-thaw cycles
C (n=3)	3 Freeze-thaw cycles
D (n=3)	4 Freeze-thaw cycles
E (n=3)	5 Freeze-thaw cycles
F (n=3)	1 Freeze-drying cycle

No clear structural differences were observed between samples subjected to different numbers of freeze-thaw cycles, either under microscopic examination or by visual inspection (Figure 28 A-E). However, samples exposed to fewer freeze-thaw cycles exhibited a slightly greater degree of surface degradation. Despite this, all samples remained mechanically robust when applying tensile forces.

After complete drying, all samples demonstrated the ability to reabsorb water upon re-immersion, indicating preservation of their water uptake capacity. The post-absorption masses were comparable across all samples (Figure 30).

When exposed to 30 °C and weighed at 15-minute intervals, the samples showed no clear correlation between water retention and the number of cross-linking cycles (Figure 30).

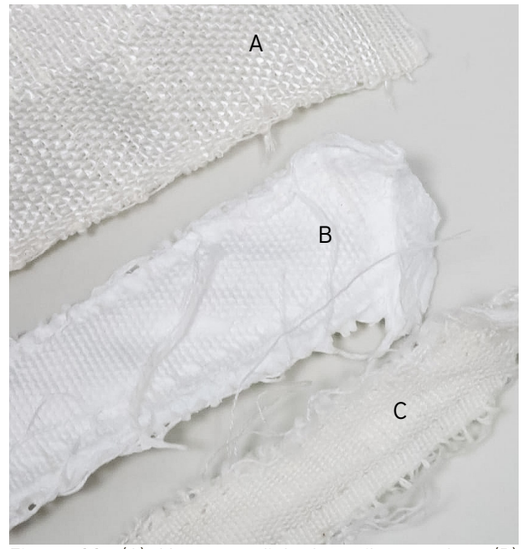

Figure 28: (A) Non-cross-linked textile sample ; (B) Freeze-dried textile sample ; (C) Freeze-thawed textile sample

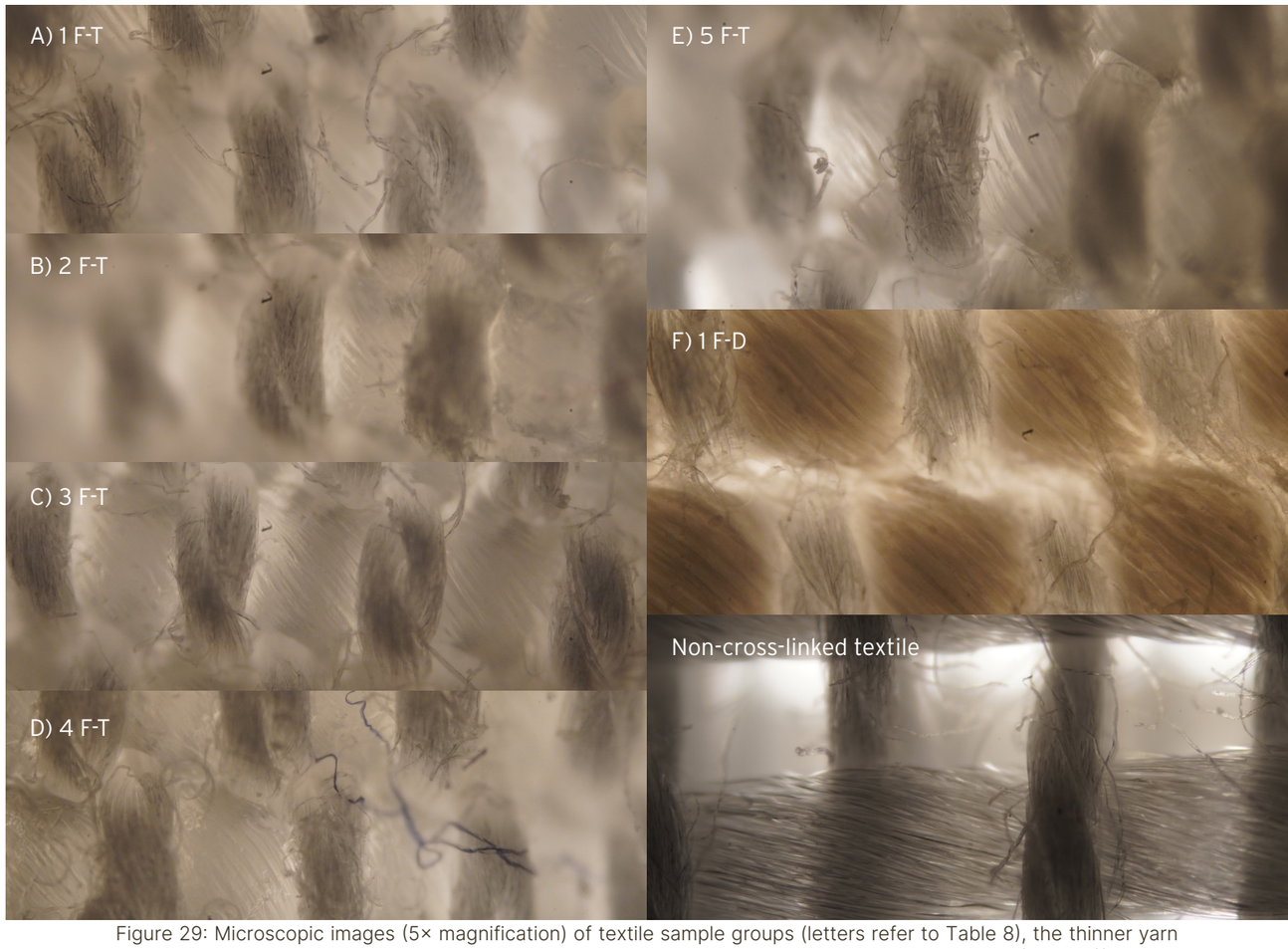

Figure 29: Microscopic images (5× magnification) of textile sample groups (letters refer to Table 8), the thinner yarn showing cotton and the thicker yarn PVA. Swelling is observed in the cross-linked samples. No significant differences are found among the freeze-thaw samples (A-E), while the freeze-dried samples show darkening of the hydrogel yarn.

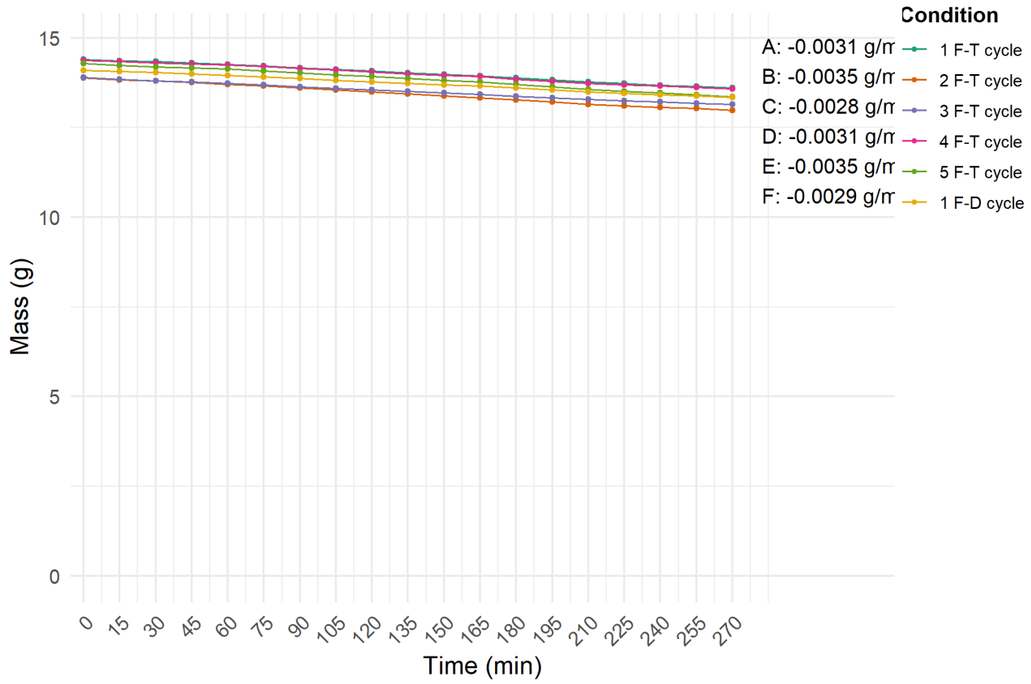

Figure 30: Evaporation of sample groups A-F measured at 15-minute intervals, showing a gradual decrease in mass with no significant differences between sample groups.

4.1.3 Discussion and Conclusion

Across all experimental conditions, textile samples dried completely within two days when exposed to 30 °C in an open environment, indicating that neither freeze-thaw nor freeze-drying techniques substantially enhanced long-term water retention. To further assess evaporation under more controlled conditions, samples were rehydrated and monitored in a closed environment at lower temperatures. This additional rehydration step may have altered the hydrogel structure compared to its state immediately after cross-linking and therefore may have influenced the observed evaporation behaviour.

No clear structural differences were observed between samples subjected to different numbers of freeze-thaw cycles, based on both visual inspection and microscopic analysis. Additionally, similar evaporation behaviour was observed across all samples, suggesting that within the tested range, increasing the number of freeze-thaw cycles did not significantly affect the strength or stability of the hydrogel network. However, samples exposed to fewer cycles showed slightly increased surface degradation, indicating a minor effect on surface stability.

The analytical methods used in this study, including mass measurements, visual inspection, and basic microscopy, provided qualitative insight but were not sufficiently sensitive to detect subtle differences in cross-linking density or network strength. More advanced characterisation techniques, such as mechanical testing or Fourier-Transform Infrared (FTIR) spectroscopy, may be required for more precise evaluation.

In conclusion, both freeze-thaw and freeze-drying methods successfully produced structurally stable cotton-hydrogel textile matrices, with freeze-drying resulting in more distinct structural characteristics (SRQ1). However, increasing the number of freeze-thaw cycles did not lead to clear improvements in cross-linking strength or stability under the tested conditions (SRQ2). These findings indicate that while cross-linking methods influence the material structure, their functional impact remains uncertain and requires further investigation. In addition, as this study applied multiple freeze-thaw cycles, the effect of these conditions on *Scenedesmus* sp. viability remains unclear. The next protocol will therefore focus on evaluating the tolerance of *Scenedesmus* sp. to repeated freeze-thaw cycles in isolation, before reintroducing the biological component into the textile system.

This page is intentionally left blank

4.2 Cryoprocessing *Scenedesmus* sp. 1

Effect of Freeze-Thawing and Freeze-Drying with Cryoprotectant on *Scenedesmus* sp. Viability

Overview Cryoprocessing *Scenedesmus* sp. 1

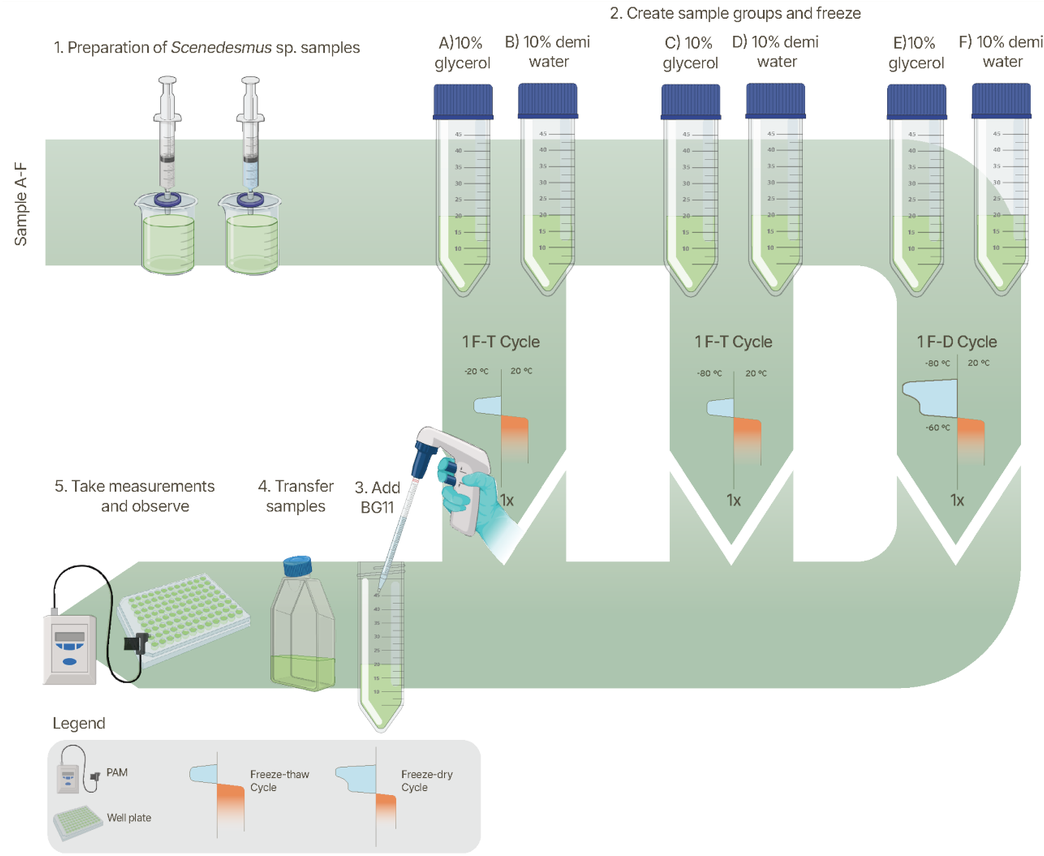

Figure 31: Overview methodology Protocol Cryoprocessing *Scenedesmus* sp. 1

Table 9: Timeline Protocol Cryoprocessing *Scenedesmus* sp. 1

Nr.	Action	Sample group	Protocol day
1	Preparation of *Scenedesmus* sp. samples with either10% glycerol and 10% demi water	A-F	1
2	Prepare six sample groups in Falcon tubes, each containing 20 mL of mixture and freezing them	A-D	1-2
		E-F	1-3
3	Add BG11	A-D	2
		E-F	3
4	Transfer samples into cell cultivation flasks	A-D	2
		E-F	3
5	Take measurements with Fluorescence Spectrometer	A-F	1, 3, 11, 18
	Take measurements with Monitoring Pulse-Amplitude-Modulation	A-F	8, 11, 14, 18
	Observe	A-F	3-18

For sample groups see Table 10

4.2.1 Introduction

Building on the findings of the previous protocol, Textile Cross-linking (4.1), it was shown that both freeze-thawing and freeze-drying can be applied to cross-link the cotton-hydrogel textile matrix. However, the effect of these processes on *Scenedesmus* sp. viability remains uncertain, particularly as earlier pilots demonstrated reduced metabolic activity following freeze-thaw exposure. This highlights the need to further investigate the tolerance of the microalgae to these conditions before reintegration into the textile system.

Protocol Cryoprocessing *Scenedesmus* sp. 1 therefore investigates the effect of cryoprotectant addition on the viability of *Scenedesmus* sp. following freeze-thawing and freeze-drying conditions. The methodology is based on established cryopreservation approaches, incorporating glycerol as a cryoprotectant due to its reported ability to improve post-freezing viability [55]. In addition, different preservation conditions are compared, including freezing at −20 °C and −80 °C, as well as freeze-drying.

This protocol aims to identify conditions that support microalgal viability during freezing-based processing steps, providing a basis for the development of stable microalgae-textile biocomposites in subsequent protocols.

Based on this rationale, this protocol addresses research question 3, and the following sub-questions (SRQs) were defined:

1. How do preservation conditions (freeze-thaw temperature and number of cycles) affect the viability of *Scenedesmus* sp.?
2. To what extent can *Scenedesmus* sp. recover metabolic activity following different preservation methods (freeze-thawing vs. freeze-drying)?
3. How does the addition of a cryoprotectant (glycerol) influence the survival and post-treatment recovery of *Scenedesmus* sp. under these conditions?

Scenedesmus sp. cultures were cultivated according to the standard cultivation protocol (Appendix 1.1), with an initial optical density of 0.333 measured at a wavelength of 430 nm.

Samples were subjected to one of three preservation conditions, either 10% (v/v) glycerol or 10% (v/v) demineralised water used as a control, as outlined in Table 10. Detailed procedural steps are provided in Appendix 3.5.

Each sample was monitored over a two-week period through visual documentation, with pigment intensity used as a proxy for microalgal growth and viability. Additionally, measurements were conducted using a fluorescence spectrometer and pulse-amplitude modulation (PAM) fluorometry to assess biomass growth and the viability of *Scenedesmus* sp.

4.2.2 Results

Incomplete freeze-drying was observed across Groups E and F, as the duration in the freeze dryer was insufficient and residual liquid remained present after processing.

Visual inspection revealed that all samples containing glycerol lost their green pigmentation over the course of the protocol (Figure 32 B, D), whereas samples containing demineralised water retained their pigmentation (Figure 32 A, C, E).

Samples containing glycerol showed a rapid and significant initial increase in biomass. However, this increase was temporal, and optical density values declined again after several days. In contrast, samples containing demineralised water exhibited a gradual but continuous increase in biomass over time (Figure 33).

Table 10: Sample overview Protocol Cryoprocessing *Scenedesmus* sp. 1

Sample group	Preservation method	Additive
A (n=3)	*Scenedesmus* sp. frozen at -20°C	10% glycerol
B (n=3)	*Scenedesmus* sp. frozen at -20°C	10% demineralized water
C (n=3)	*Scenedesmus* sp. frozen at -80°C	10% glycerol
D (n=3)	*Scenedesmus* sp. frozen at -80°C	10% demineralized water
E (n=3)	Freeze-dried *Scenedesmus* sp.	10% glycerol
F (n=3)	Freeze-dried *Scenedesmus* sp.	10% demineralized water

Comparison of preservation method groups indicated that freeze-dried samples consistently exhibited reduced biomass growth compared to frozen samples with the same composition. Among Groups A-D, samples stored at −80 °C exhibited the highest biomass growth and overall performance. Among glycerol-containing samples, Group E exhibited the lowest biomass growth, with a similar trend observed in freeze-dried samples containing demineralised water (Figure 33).

Photosynthetic performance, measured using pulse-amplitude modulated (PAM) fluorometry to determine fluorescence quantum yield, showed reduced photosynthetic efficiency in glycerol-containing samples compared to those containing demineralised water. Group F showed no detectable fluorescence quantum yield after the first measurement and was therefore considered non-viable. Samples containing demineralised water displayed an initial rapid increase in fluorescence quantum yield, followed by a cessation of further increase over time (Figure 34).

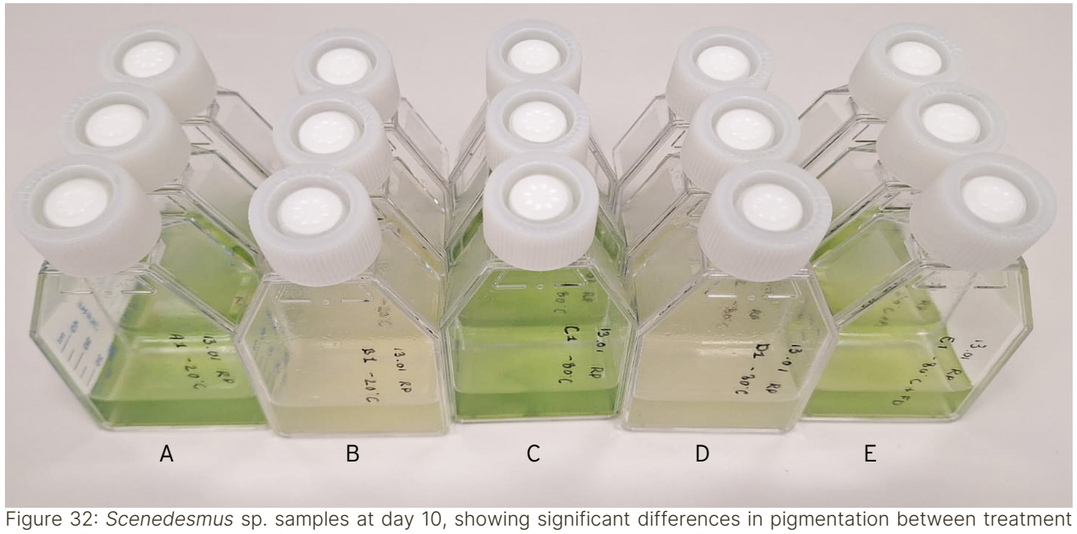

Figure 32: *Scenedesmus* sp. samples at day 10, showing significant differences in pigmentation between treatment groups. Sample groups B and D contain 10% glycerol, while sample groups A, C, and E contain 10% demineralised water. A single representative biological replicate was selected from each sample group for imaging.

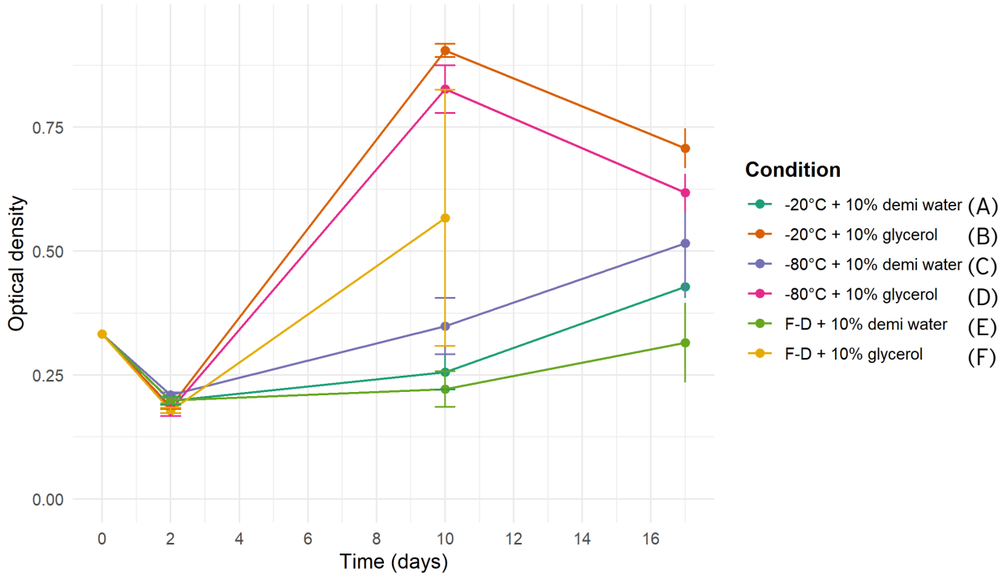

Figure 33: Optical density of the *Scenedesmus* sp. over time measured at wavelength 430nm. The samples containing 10% demi water have an overall lower optical density than sample containing 10% glycerol. The optical desity of the samples containing 10% glycerol is decreasing over time. For the samples with 10% the samples that were perserved in −80 °C show a higher optical density.

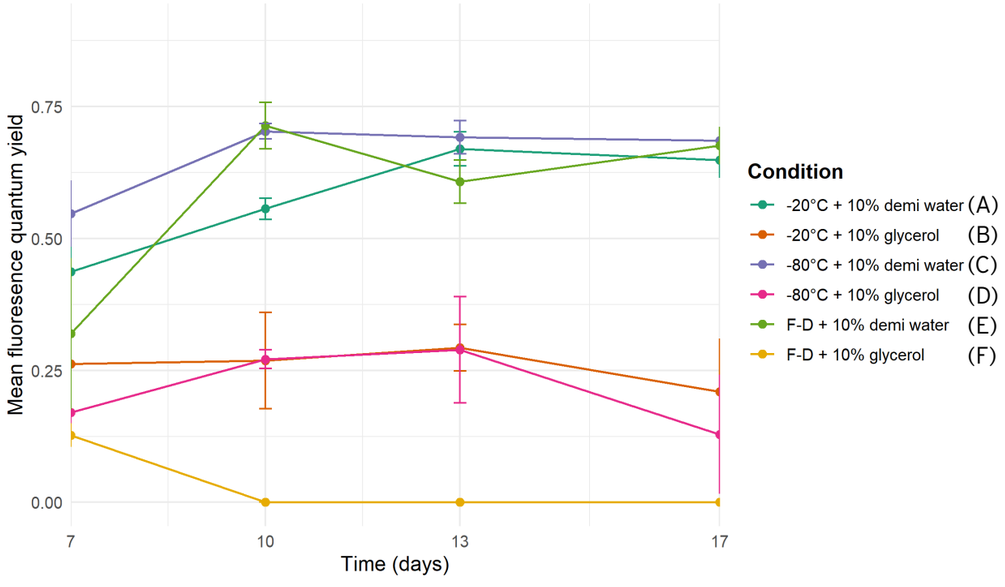

Figure 34: Fluorescence quantum yield of *Scenedesmus* sp. over time. Samples containing 10% glycerol show lower fluorescence quantum yield, indicating reduced metabolic efficiency. Among the glycerol-treated samples, the group preserved at −80 °C exhibits the highest performance. Time points represent days from the start of the protocol.

4.2.3 Discussion and Conclusion

The freeze-drying process was incomplete due to insufficient drying time, which limited the reliability and comparability of the resulting data. Future experiments should apply optimised freeze-drying parameters to ensure full dehydration and enable a valid assessment of this preservation method.

The results indicate that glycerol negatively affected the viability and performance of *Scenedesmus* sp. across all measured groups. Samples containing glycerol showed a decline in biomass and reduced photosynthetic quantum yield, suggesting delayed cytotoxic effects or prolonged metabolic stress. In contrast, samples containing demineralised water exhibited a gradual but continuous increase in biomass, indicating partial recovery and restoration of metabolic activity over time. These findings suggest that glycerol is not suitable as a cryoprotectant for this microalgal system under the tested conditions.

Comparison between preservation methods showed that freezing at −80 °C resulted in the highest biomass growth and photosynthetic performance, highlighting that freezing *Scenedesmus* sp. is less damaging than freeze-drying. Freeze-dried samples consistently exhibited lower biomass growth, suggesting additional stress from the drying process and incomplete recovery.

The findings indicate that both the choice of preservation method and the presence of cryoprotectants strongly influence the viability and recovery of *Scenedesmus* sp. Freeze-dried samples consistently showed reduced biomass growth and lower photosynthetic efficiency, suggesting additional stress induced by the drying process and incomplete cellular recovery.

In conclusion, *Scenedesmus* sp. viability is strongly dependent on preservation conditions used for hydrogel cross-linking. Freezing at −80 °C without glycerol best supported microalgae survival and recovery, while freeze-drying and glycerol addition led to reduced or no metabolic recovery, indicating increased cellular damage (SRQ1-SRQ3). Overall, only limited recovery of photosynthetic activity was observed, with demineralised water samples showing gradual biomass increase, whereas glycerol-containing and freeze-dried samples performed poorly (SRQ2, SRQ3). The next protocol will repeat the experiment under optimised freeze-drying parameters, to confirm the findings of this protocol and establish reliable preservation conditions for *Scenedesmus* sp. before reintroducing the system into the textile-based workflow.

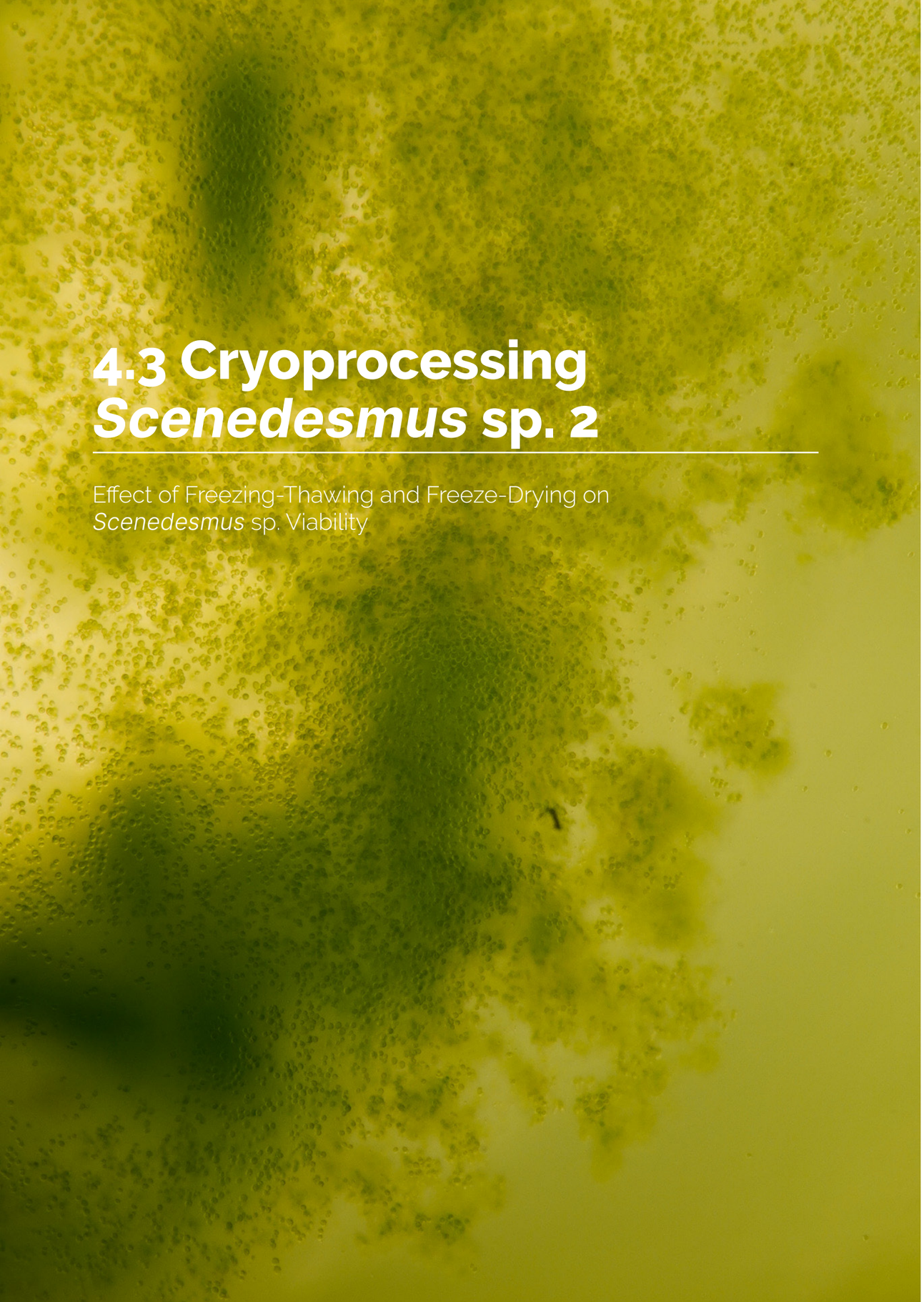

4.3 Cryoprocessing *Scenedesmus* sp. 2

Effect of Freezing-Thawing and Freeze-Drying on *Scenedesmus* sp. Viability

Overview Cryoprocessing *Scenedesmus* sp. 2

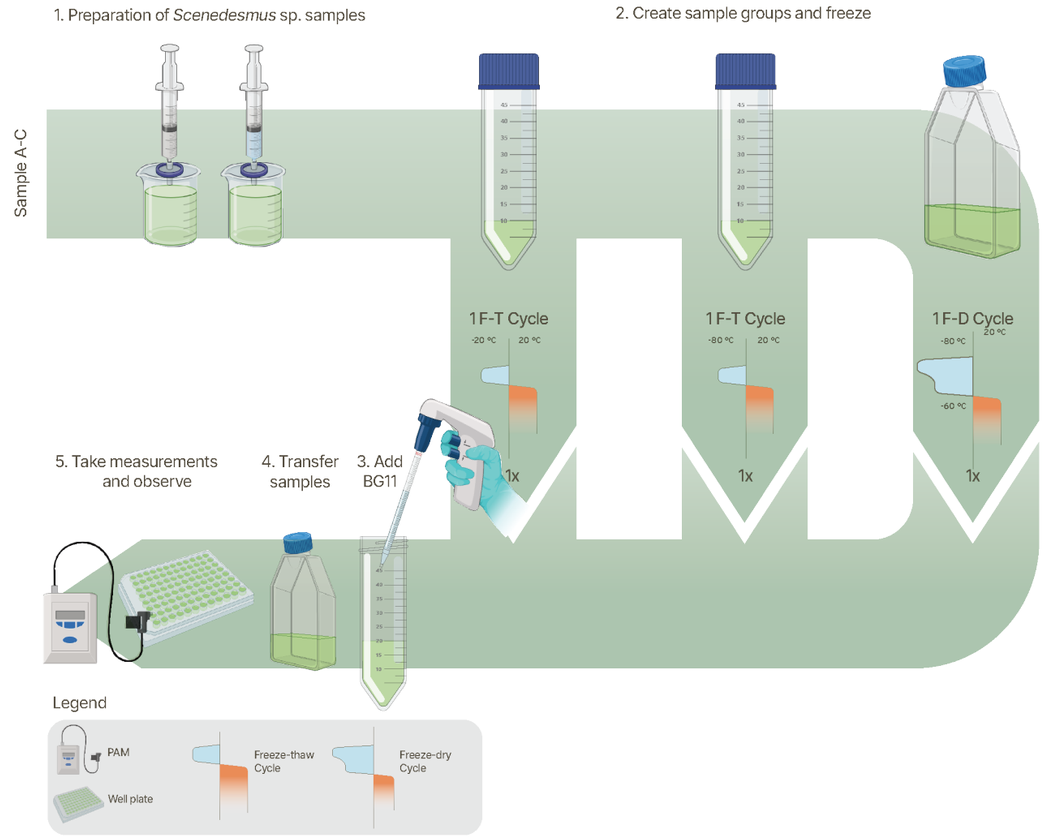

Figure 35: Overview methodology Protocol Cryoprocessing *Scenedesmus* sp. 2

Table 11: Timeline Protocol Cryoprocessing *Scenedesmus* sp. 2

Nr.	Action	Sample group	Protocol day
1	Preparation of *Scenedesmus* sp. samples with 10% demi water	A-C	1
2	Prepare three sample groups in Falcon tubes, each containing 20 mL of mixture and freezing them	A-B	1-2
		C	1-3
3	Add BG11	A-B	2
		C	3
4	Transfer samples into cell cultivation flasks	A-B	2
5	Take measurements with Fluorescence Spectrometer	A-C	1, 7, 9, 12, 29
	Take measurements with Monitoring Pulse-Amplitude-Modulation	A-C	7, 9, 12
	Observe	A-C	3-14

For sample groups see Table 12

4.3.1 Introduction

This protocol builds upon the findings of Protocol Cryoprocessing *Scenedesmus* sp. 1 (4.2), further investigating the effects of freeze-thawing and freeze-drying on *Scenedesmus* sp. cultures using the same experimental framework. Key modifications include extended freeze-drying time to ensure complete dehydration and the exclusion of glycerol as a cryoprotectant.

Protocol Cryoprocessing *Scenedesmus* sp. 2 was conducted to address the limitations identified in Cryoprocessing *Scenedesmus* sp. 1 (4.2), where incomplete freeze-drying reduced data reliability and glycerol negatively affected microalgal viability, likely due to metabolic and cytotoxic stress. These adjustments aim to improve preservation consistency and enable a more reliable assessment of *Scenedesmus* sp. recovery after freeze-thawing and freeze-drying.

Based on this rationale, this protocol addresses research question 3, and the following sub-questions (SRQs) were defined:

1. How do preservation conditions (freeze-thaw temperature and number of cycles) affect the viability of *Scenedesmus* sp.?
2. To what extent can *Scenedesmus* sp. recover metabolic activity following different preservation methods (freeze-thawing vs. freeze-drying)?

Scenedesmus sp. cultures were cultivated according to the standard cultivation protocol (Appendix 1.1), with an initial optical density of 0.413 measured at a wavelength of 430 nm.

Three experimental groups were prepared, as outlined in Table 12. All samples contained 10% (v/v) demineralised water to ensure consistency with the conditions used in Cryoprocessing *Scenedesmus* sp. 1. Detailed procedural steps are provided in Appendix 3.6.

Sample evaluation was performed through optical density measurements, pulse-amplitude modulation (PAM) fluorescence, and visual inspection using light microscopy and colour comparison. These measurements allowed assessment of microalgal viability after different freezing and freeze-drying treatments.

4.3.2 Results

After the extended freeze-drying period, the *Scenedesmus* sp. samples were fully dehydrated. Microscopic examination revealed that cell structures were still visible (Figure 36), although a substantial amount of brown material was observed, which could not be conclusively identified as either degraded microalgal cells or other residues (Figure 36 A, D). Upon rehydration with BG11 growth medium, the medium rapidly turned green, indicating possible resumption of metabolic activity (Figure 37 B). This was supported by PAM measurements, which indicated that some photosynthetic activity was still present immediately after rehydration (Figure 38).

Comparison of biomass growth across preservation conditions (−20 °C, −80 °C, and freeze-drying) showed similar initial optical density values (Figure 39). Over time, samples stored at −80 °C showed faster biomass recovery than those stored at −20 °C or subjected to freeze-drying (Figure 39).

PAM fluorescence measurements further confirmed differences in photosynthetic performance, with −80 °C samples showing the highest quantum yield, while freeze-dried samples consistently showed the lowest (Figure 38).

Table 12: Samples overview Protocol Cryoprocessing *Scenedesmus* sp. 2

Sample groups	Preservation method	Additive
A (n=3)	*Scenedesmus* sp. frozen at -20°C	10% demineralized water
B (n=3)	*Scenedesmus* sp. frozen at -80°C	10% demineralized water
C (n=3)	Freeze-dried *Scenedesmus* sp.	10% demineralized water

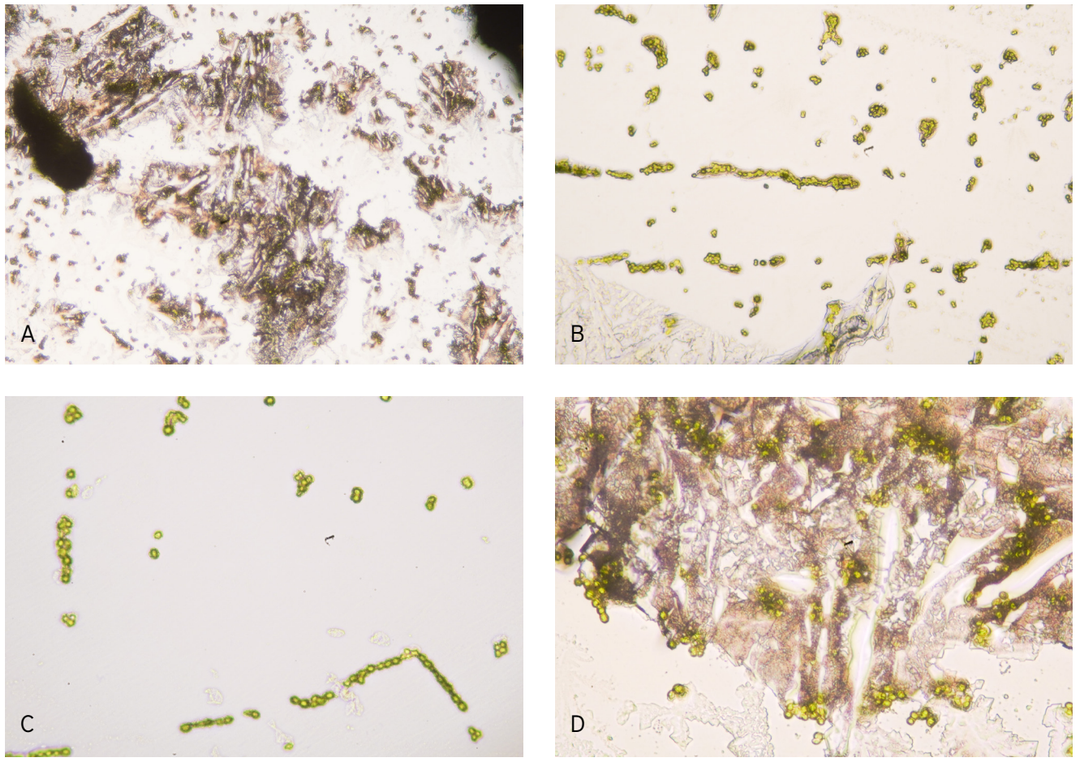

Figure 36: Microscopic images (40× magnification) of freeze-dried *Scenedesmus* sp., with images A and C showing the presence of unidentified brown material.

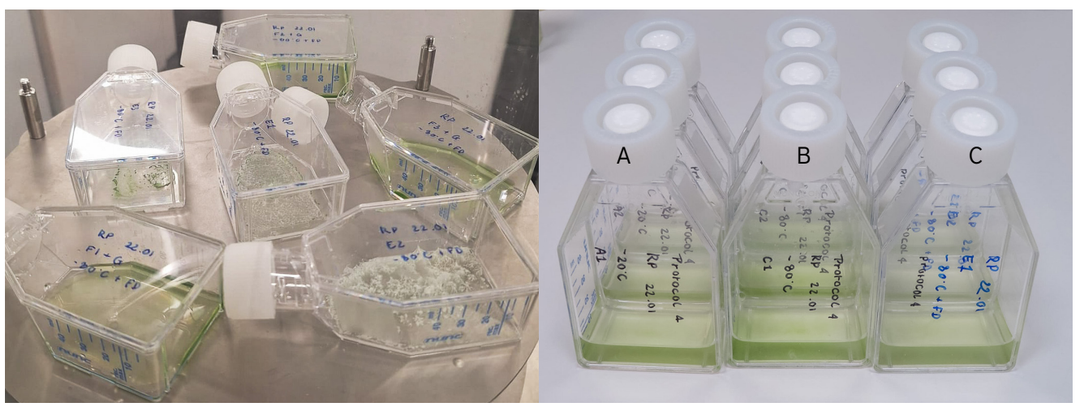

Figure 37: (A) Freeze-dried *Scenedesmus* sp. (sample Group C); (B) restored samples six days after preservation (sample Groups A-C). A single representative biological replicate was selected from each sample group for imaging.

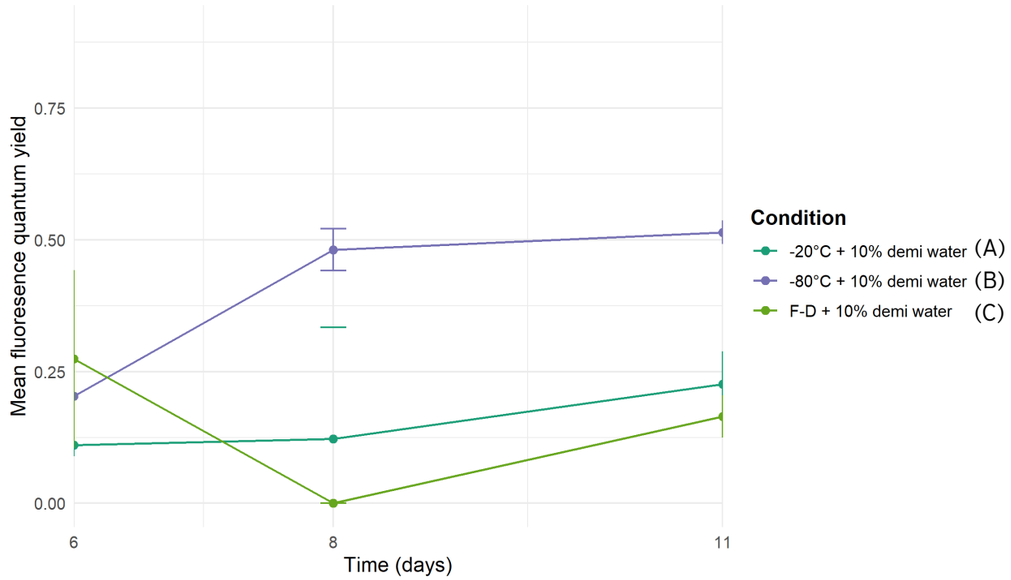

Figure 38: Fluorescence quantum yield of *Scenedesmus* sp. measured over 11 days, with sample group B showing the highest metabolic performance. Time points represent days from the start of the protocol.

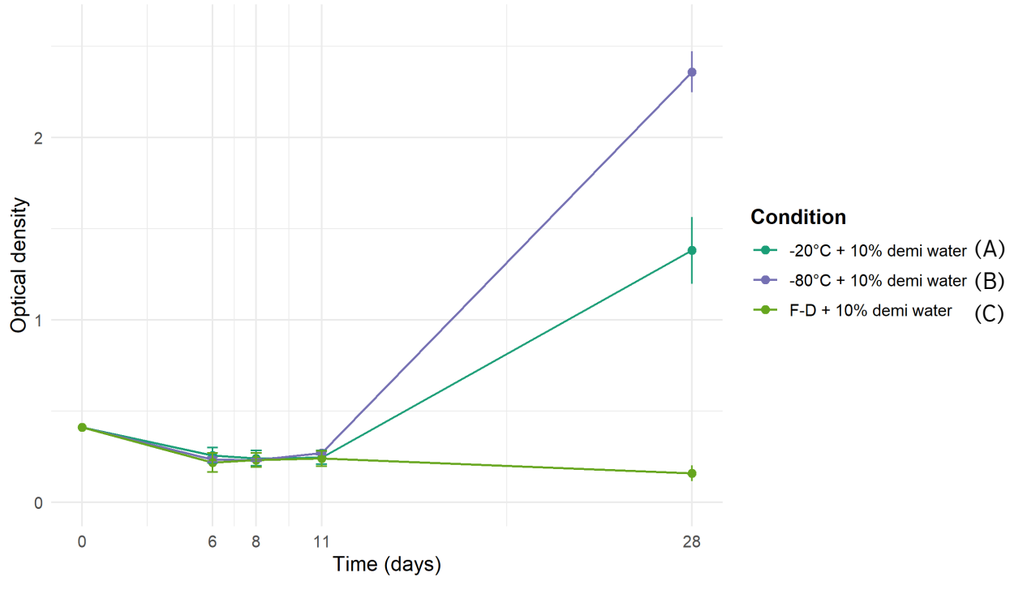

Figure 39: Optical density of *Scenedesmus* sp. measured over 28 days at 430 nm. The samples initially show a slight increase in biomass, with a significant difference observed at day 28, where sample group B exhibits the highest biomass concentration. Time points represent days from the start of the protocol.

4.3.3 Discussion and Conclusion

The results indicate that *Scenedesmus* sp. can retain viability following both freezing and freeze-drying, although recovery and photosynthetic performance depend strongly on the preservation method. The presence of an unidentified brown material after freeze-drying suggests that dehydration may induce cellular stress or pigment degradation, although its exact nature remains unclear, and its impact on photosynthetic efficiency cannot be fully determined.

Rehydrated freeze-dried samples showed recovery of green pigmentation and detectable photosynthetic activity, indicating that a fraction of the microalgal cells remained metabolically active after preservation. However, all treatments exhibited a delay in biomass increase, suggesting a lag phase linked to cellular repair and metabolic reactivation after preservation stress.

Across all conditions, freezing at −80 °C consistently resulted in higher photosynthetic efficiency compared to −20 °C and freeze-drying. This is likely explained by faster solidification of the medium at −80 °C, which reduces ice crystal formation and limits mechanical damage to the cell membrane. In contrast, slower freezing at higher temperatures allows larger ice crystals to form, increasing the likelihood of membrane rupture and cellular damage. The increased viability of Group B is supported by consistently higher fluorescence quantum yield values, indicating more effective preservation of metabolic activity. In contrast, freeze-dried samples showed the lowest photosynthetic performance, despite partial recovery, indicating that dehydration imposes stronger physiological stress than freezing alone.

In conclusion, preservation conditions strongly influence the viability of *Scenedesmus* sp. (SRQ1). Freezing at −80 °C maintains the highest viability and photosynthetic performance, whereas −20 °C and freeze-drying cause greater cellular stress and lower cell recovery. Recovery of metabolic activity is possible under all conditions but depends on the method used (SRQ2). While *Scenedesmus* sp. is able to regain partial photosynthetic activity after both freezing and freeze-drying, recovery is slower and less efficient after freeze-drying, with consistently lower biomass growth and photosynthetic yield compared to frozen samples. Overall, −80 °C freezing provides the most reliable preservation of photosynthetic activity, while freeze-drying results in reduced but not absent metabolic recovery. The next protocol will investigate whether reducing thaw time, while freezing the samples at −80 °C, can improve recovery dynamics by limiting additional stress during the restoration of metabolic processes.

4.4 Thawing Duration

Effect of Thawing Duration Between Freeze-Thaw Cycles on *Scenedesmus* sp. Viability

Overview Thawing Duration

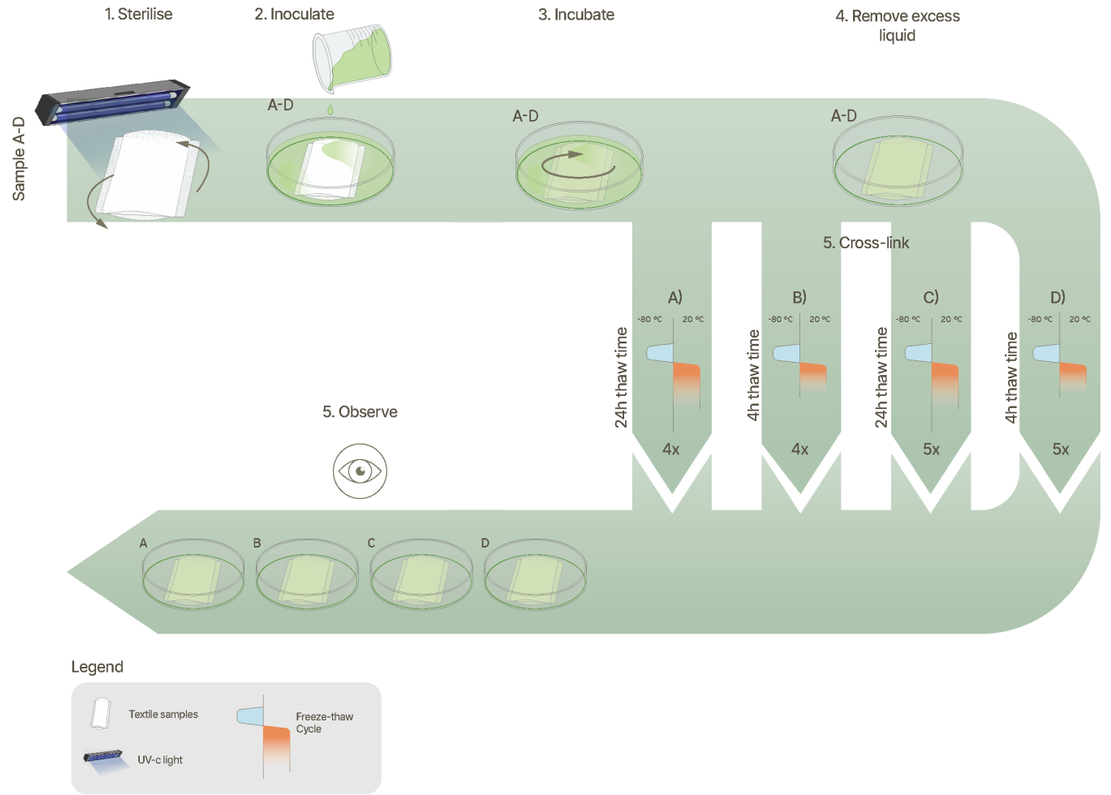

Figure 40: Overview methodology Protocol Thawing Duration

Table 13: Timeline Protocol Thawing Duration

Nr.	Action	Sample group	Protocol day
1	Sterilise with UV-C light for 20 minutes	A-D	1
2	Inoculate sample groups with *Scenedesmus* sp. and Incubate samples on a rotating platform (25°C, 120 rpm)	A-D	1-4
3	Remove the excess liquid	A-D	4
4	Cross-link the samples (24 hours freezing, 24 hours thawing)	A	4-12
		C	4-10
	Cross-link the samples (24 hours freezing, 4 hours thawing)	B	4-14
		D	4-12
5	Observe	A	12-15
		B	10-15
		C	14-17
		D	12-15

For sample groups see Table 14

4.4.1 Introduction

This protocol builds on previous findings showing that *Scenedesmus* sp. viability is strongly influenced by preservation conditions, with −80 °C freezing providing the most reliable recovery, while overall metabolic recovery remains limited and delayed after thawing. It was observed that viability often declined during the thawing phase, suggesting that cellular damage incurred during freezing becomes apparent when metabolic activity resumes, leading to cell death during reactivation.

To investigate this, Protocol Thawing Duration focuses on the effect of thaw duration between freeze-thaw cycles on the viability of *Scenedesmus* sp. The methodology compares regular thawing (24 h) with shorter thawing periods (4 h). It is hypothesised that shorter thaw durations will improve viability, as freezing-induced cellular damage may lead to cell death during the reactivation of metabolic activity. Reducing the thawing time may limit this vulnerable phase and thereby improve post-thaw recovery. Additionally, observations showed that samples fully thaw within a shorter time frame, indicating that extended thawing may be unnecessary.

Based on this rationale, this protocol addresses research question 3, and the following sub-question (SRQs) was defined:

1. How does thaw duration between freeze-thaw cycles (short vs. prolonged) affect the viability and recovery of *Scenedesmus* sp.?

Scenedesmus sp. cultures were cultivated according to the standard cultivation protocol (Appendix 1.1), with an initial optical density of 0.707 measured at a wavelength of 430 nm.

Four experimental groups were prepared, as outlined in Table 14. The textile samples consisted of a multilayer weave (outer layers: 60% cotton, 40% PVA; inner layer: 100% cotton) secured on all sides with a compound twill (Figure 23, Appendix 4.1.1). Prior to inoculation, the textile samples were sterilised using a UV-C sterilisation box (Appendix 1.2). All samples were frozen at −80 °C. Detailed procedural steps are provided in Appendix 3.7.

Each sample was monitored over a nine-day period through visual documentation, with pigment intensity used as a proxy for microalgal growth and viability.

4.4.2 Results

At the start of the experiment, all samples exhibited visible green pigmentation, indicating the presence and viability of *Scenedesmus* sp. within the cotton-hydrogel matrix prior to freezing. Figure 41 shows the appearance of the samples during the freeze-thaw cycles, with images captured during thawing phases.

Differences in pigment intensity were observed between the sample groups. Sample groups A and C exhibited a noticeable reduction in pigment intensity at earlier stages of the freeze-thaw process compared to sample groups B and D. Three days after thawing, sample groups A and C appeared less pigmented overall. In contrast, sample groups B and D retained higher pigmentation during the intermediate cycles, although gradual pigment loss was also observed following completion of the freeze-thaw process. Among these groups, sample Group B maintained higher pigment intensity than sample Group D (Figure 41).

After three days post-freeze-thawing, all samples exhibited a substantial decrease in green pigmentation and slight dehydration of the textile matrix (Figure 41).

Table 14: Samples overview Protocol Thawing Duration

Sample group	Description
A (n=2)	Multilayer woven textile matrix immersed in *Scenedesmus* sp. suspension, subjected to 4 F-T cycles, 24 hours restoration in between F-T cycles
B (n=2)	Multilayer woven textile matrix immersed in *Scenedesmus* sp. suspension, subjected to 4 F-T cycles, 4 hours restoration in between F-T cycles
C (n=2)	Multilayer woven textile matrix immersed in *Scenedesmus* sp. suspension, subjected to 5 F-T cycles, 24 hours restoration in between F-T cycles
D (n=2)	Multilayer woven textile matrix immersed in *Scenedesmus* sp. suspension, subjected to 5 F-T cycles, 4 hours restoration in between F-T cycles

Figure 41: Overview of freeze-thaw samples during thawing. A single representative biological replicate was selected from each sample group for imaging. Sample groups B and D show a less rapid decline in pigmentation compared to sample groups A and C.

4.4.3 Discussion and Conclusion

Thaw duration influenced the short-term viability of *Scenedesmus* sp. within the cotton-hydrogel matrix during freeze-thaw cycles. Samples exposed to shorter thawing periods (4 h) retained higher pigment intensity during intermediate stages compared to samples with prolonged thawing (24 h), suggesting a temporary protective effect. However, this difference was not sustained, as all samples exhibited substantial pigment loss after completion of the freeze-thaw process, regardless of thaw duration or number of F-T cycles.

Post-thaw recovery was limited across all conditions. Although some pigment was retained during intermediate stages, a strong decrease in pigmentation after three days indicated reduced viability and only partial or absent restoration of metabolic activity. This suggests that repeated freeze-thaw cycling introduces increased cellular stress that *Scenedesmus* sp. cannot fully recover from under the tested conditions. In addition, gradual drying of the cotton-hydrogel matrix likely contributed to reduced viability, highlighting the importance of continuous moisture retention for sustained microalgal viability.

In conclusion, *Scenedesmus* sp. viability is only marginally affected by the thaw duration, with shorter thawing (4 h) showing temporary retention of pigment compared to prolonged thawing (24 h), but no improvement in long-term recovery was observed (SRQ1). These results indicate that freeze-thaw cycling remains highly damaging to the microalgae, even under optimised thaw conditions. Building on this, the next protocol will investigate whether the timing of microalgae immobilisation (before vs. after freeze-thaw treatment) influences attachment strength within the hydrogel-textile matrix, as current results suggest that effective hydrogel cross-linking may require conditions that simultaneously reduce microalgal viability.

This page is intentionally left blank

4.5 Time of Inoculation

Effect of Pre- and Post-Cross-linking Inoculation on *Scenedesmus* sp. Attachment in a Cotton-Hydrogel Matrix

Overview Time of Innoculation

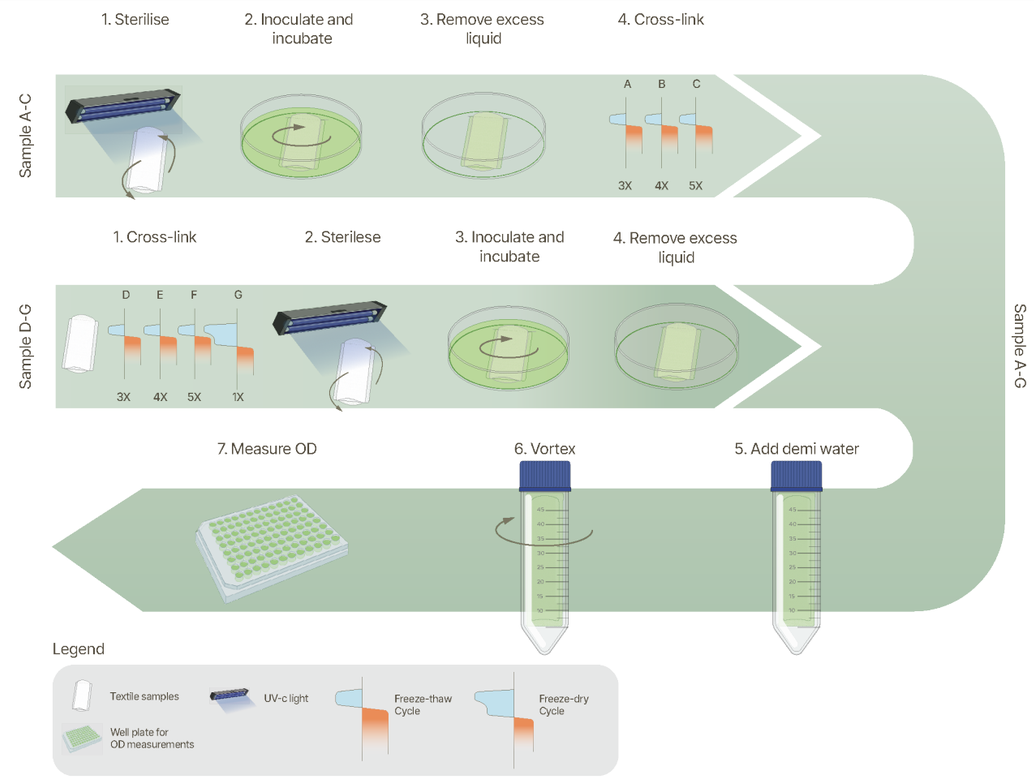

Figure 42: Overview methodology Protocol Time of Innocolation

Table 15: Timeline protocol Time of Inoculation Samples A-C

Nr.	Action	Sample group	Protocol day
1	Sterilise with UV-C light for 20 minutes	A-C	1
2	Inoculate sample groups with *Scenedesmus* sp. and Incubate samples on a rotating platform (25°C, 120 rpm)	A-C	1-4
3	Remove the excess liquid	A-C	4
4	Cross-link the samples (24 hours freezing, 24 hours thawing)	A	4-10
		B	4-12
		C	4-14
5	Add 40 mL demi water	A	10
		B	12
		C	14
6	Vortex samples	A	10
		B	12
		C	14
7	Measure the optical density of the liquid surrounding the textile	A	10
		B	12
		C	14

For sample groups see Table 17

Table 16: Timeline protocol Time of Inoculation Samples D-G

Nr.	Action	Sample group	Protocol day
1	Cross-link the samples (24 hours freezing, 24 hours thawing)	D	1-6
		E	1-8
		F	1-10
		G	1-3
2	Sterilise with UV-C light for 20 minutes	D	6
		E	8
		F	10
		G	3
3	Inoculate sample groups with *Scenedesmus* sp. and Incubate samples on a rotating platform (25°C, 120 rpm)	D	6-9
		E	8-11
		F	10-13
		G	3-6
4	Remove the excess liquid	D	9
		E	11
		F	13
		G	6
5	Add 40 mL demi water	D	9
		E	11
		F	13
		G	6
6	Vortex samples	D	9
		E	11
		F	13
		G	6
7	Measure the optical density of the liquid surrounding the textile	D	9
		E	11
		F	13
		G	6

4.5.1 Introduction

This protocol builds on the findings from the Textile Cross-linking protocol (4.1), which showed no clear relationship between the number of freeze-thaw cycles and the resulting cross-linking strength, as well as the Thawing Duration protocol (4.4), which demonstrated that *Scenedesmus* sp. viability declines significantly after cross-linking, even when shorter thawing periods are applied. Together, these results suggest a conflict between achieving sufficient structural integrity of the cotton-hydrogel matrix and maintaining microalgal viability.

To address this, the present study first investigates whether the timing of microalgal inoculation before or after hydrogel cross-linking affects the ability of *Scenedesmus* sp. to attach to and become immobilised within the textile matrix. All samples were cross-linked at −80 °C, based on previous findings that identified this temperature as the most favourable condition for preserving microalgal viability during freeze-thaw processing (4.3).

Subsequently, the study evaluates the strength of this immobilisation by assessing cell detachment. This is done by immersing the samples in water, subsequently vortexing, and quantifying the number of released cells through optical density measurements. This approach enables comparison of how well different cross-linking and inoculation strategies retain microalgae within the textile structure.

Based on this rationale, this protocol addresses research question 2, and the following sub-questions (SRQs) were defined:

1. How does the timing of microalgal inoculation (before vs. after hydrogel cross-linking) affect the immobilisation of *Scenedesmus* sp. within the textile-hydrogel matrix?
2. How stable is the immobilisation of *Scenedesmus* sp. within the textile-hydrogel system, as indicated by cell detachment under mechanical stress?

Scenedesmus sp. cultures were cultivated according to the standard cultivation protocol (Appendix 1.1), with an initial optical density of 0.873 measured at a wavelength of 430 nm.

Seven experimental groups were prepared following two different methodologies: Groups A-C) where the textile was first immersed in *Scenedesmus* sp. and then cross-linked for varying numbers of cycles, and Groups D-G) where the textile was first cross-linked and subsequently immersed in *Scenedesmus* sp. (Table 16). The textile samples consisted of a multilayer weave (outer layers: 60% cotton, 40% PVA; inner layer: 100% cotton) secured on all sides with a compound twill (Figure 23, Appendix 4.1.1). Prior to inoculation, the textile samples were sterilised using a UV-C sterilisation box (Appendix 1.2). All samples were frozen at −80 °C. Detailed procedural steps are provided in Appendix 3.8.

Sample evaluation was performed by immersing the textile samples in water, vortexing, and measuring the optical density of the surrounding liquid. This value was then compared to the initial optical density used for inoculation, providing a measure of microalgal detachment and the effectiveness of immobilisation.

Table 17: Samples overview Protocol Time of Inoculation

Sample group	Description
A (n=2)	Multilayer woven textile matrix immersed in *Scenedesmus* sp., ***subsequently subjected to*** 3 F-T cycles
B (n=2)	Multilayer woven textile matrix immersed in *Scenedesmus* sp., ***subsequently subjected to 4*** F-T cycles
C (n=2)	Multilayer woven textile matrix immersed in *Scenedesmus* sp., ***subsequently subjected to 5*** F-T cycles
D (n=2)	Multilayer woven textile matrix subjected to 3 F-T cycles, subsequently immersed in *Scenedesmus* sp.
E (n=2)	Multilayer woven textile matrix subjected to 4 F-T cycles, subsequently immersed in *Scenedesmus* sp.
F (n=2)	Multilayer woven textile matrix subjected to 5 F-T cycles, subsequently immersed in *Scenedesmus* sp.
G (n=2)	Multilayer woven textile matrix subjected to 1 F-D cycle, subsequently immersed in *Scenedesmus* sp.

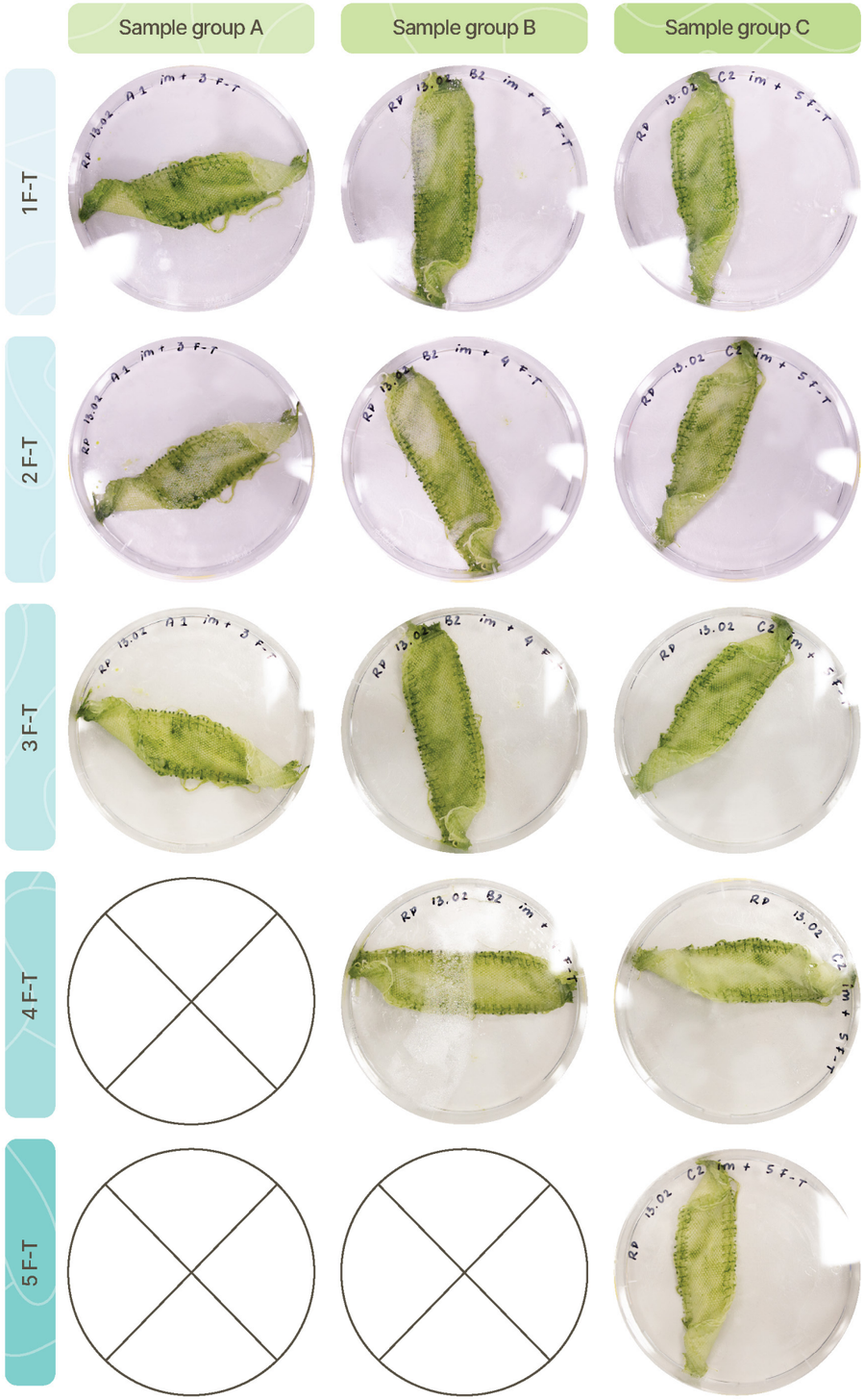

Figure 43: Overview of microalgae-textile biocomposite sample groups A-C during freeze-thawing, captured during the thawing phase. The images illustrate that an increasing number of freeze-thaw cycles leads to reduced pigmentation. A single representative biological replicate was selected from each sample group for imaging.

4.5.2 Results

During cross-linking, sample groups that were immersed in *Scenedesmus* sp. prior to cross-linking exhibited a gradual decrease in pigment intensity, indicating a decline in visible biomass during the process (Figure 43).

Sample groups that were first cross-linked and subsequently immersed in *Scenedesmus* sp. were dried prior to inoculation. Following immersion, these samples absorbed the microalgal suspension at a similar rate to the pre-immersed samples, resulting in a comparable visual appearance (Figure 44).

Following vortexing, the surrounding liquid of all samples exhibited a visible green colour, indicating the release of microalgal cells from the textile matrix. Optical density measurements confirmed that all sample groups released more than 60% of the initially immobilised microalgae cells into the surrounding liquid (Figure 45). No significant differences were observed between the sample groups. However, the freeze-dried sample showed the highest percentage of cell release. Samples subjected to five freeze-thaw cycles with *Scenedesmus* sp. inoculated prior to cross-linking, as well as samples inoculated after cross-linking, showed similar percentages of cell release and exhibited the lowest overall cell loss compared to the other sample groups.

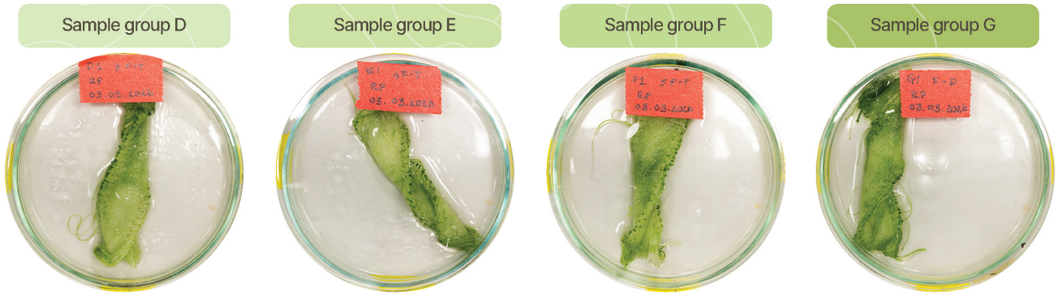

Figure 44: Overview of sample groups D-G during the incubation period, showing immobilisation of microalgal cells within the textile and a reduced number of cells in the surrounding liquid.

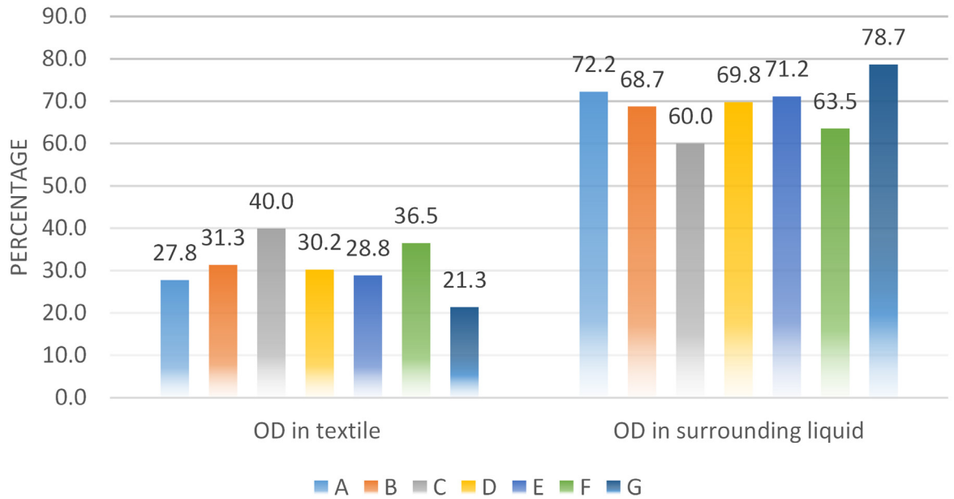

Figure 45: Percentage of microalgal cells released from the textile by vortexing and retained within the textile for samples A-G, showing that samples with a higher number of freeze-thaw cycles exhibit the lowest levels of microalgal detachment (notably sample groups C and F).

4.5.3 Discussion and Conclusion

Freeze-thaw conditions influenced the immobilisation of *Scenedesmus* sp. within the textile-hydrogel matrix. Samples subjected to five freeze-thaw cycles exhibited the lowest release of microalgal cells during vortexing, compared to other conditions, indicating improved immobilisation. In contrast, freeze-dried samples exhibited the highest level of cell release, suggesting weaker attachment within the matrix. However, the effect of cross-linking method was limited, as substantial cell detachment was observed across all sample groups.

The timing of inoculation had a minimal impact on immobilisation performance. Samples inoculated prior to cross-linking and those inoculated after cross-linking showed similar levels of cell retention, indicating that effective immobilisation can be achieved without exposing *Scenedesmus* sp. to freeze-thaw conditions. Despite improvements with increased freeze-thaw cycles, overall immobilisation remained limited, with more than 60% of cells released under mechanical stress, indicating that the majority of biomass was not strongly bound to the matrix.

In conclusion, the timing of microalgal inoculation (before vs. after hydrogel cross-linking) had no significant effect on the immobilisation of *Scenedesmus* sp., as similar levels of cell retention were observed across both approaches (SRQ1). This demonstrates that microalgae can be effectively immobilised after cross-linking, avoiding exposure to damaging freeze-thaw conditions. However, the stability of immobilisation within the textile-hydrogel system remained limited, with more than 60% of cells detaching under mechanical stress across all sample groups (SRQ2). These findings indicate that, while immobilisation is achievable, the binding strength between microalgae and the textile matrix is insufficient for stable retention. Building on this, the next protocol will focus on improving the textile material itself by investigating whether *Scenedesmus* sp. shows a preference for attachment to cotton or PVA yarn, enabling further optimisation of the matrix design to enhance immobilisation strength and overall system performance.

This page is intentionally left blank

4.6 Yarn Attachment

Attachment of *Scenedesmus* sp. to Cotton and PVA Yarn Structures

Overview Yarn Attachment

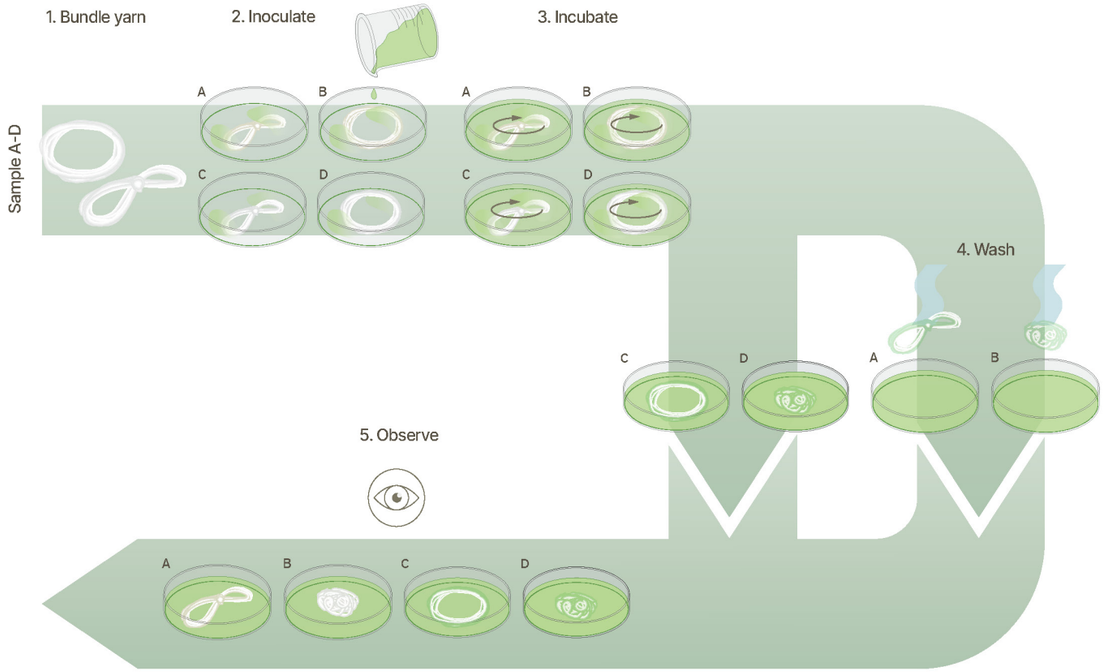

Figure 46: Overview methodology Protocol Yarn Attachment

Table 18: Timeline Protocol Yarn Attachment

Nr.	Action	Sample group	Protocol day
1	Bundle PVA and cotton yarn	A-D	1
2	Inoculate sample groups with *Scenedesmus* sp.	A-D	1
3	Incubate samples on a rotating platform (25°C, 120 rpm)	A-D	1-4
4	Wash samples with demi water	A-B	4
5	Observe	A-D	4-20

For sample groups see Table 19

4.6.1 Introduction

This protocol builds on the findings of Pilot 3 (3.3) and the previous protocol Time of Inoculation (4.5). Pilot 3 indicated that *Scenedesmus* sp. showed a preference for cotton-rich regions within the textile matrix, while the protocol Time of Inoculation demonstrated that, although immobilisation is achievable, the overall attachment strength remains limited. Together, these results highlight the need to further optimise the textile matrix itself to improve immobilisation stability.

To address this, the Protocol Yarn Attachment investigates whether *Scenedesmus* sp. shows a preference for attachment to specific yarn materials within the textile matrix. The protocol focuses on comparing microalgal growth and attachment on cotton and PVA yarns arranged in different bundling configurations.

The aim is to identify material compositions that promote stronger attachment and sustained microalgal growth, thereby informing the design of improved textile matrices for more stable and functional microalgae-textile biocomposites.

Based on this rationale, this protocol addresses research question 1, and the following sub-questions (SRQs) were defined:

1. Does *Scenedesmus* sp. show a preferential attachment to cotton or PVA yarn?
2. How does yarn material (cotton vs. PVA) affect the stability of *Scenedesmus* sp. attachment, as indicated by cell detachment during washing?

Scenedesmus sp. cultures were cultivated according to the standard cultivation protocol (Appendix 1.1).

Yarn samples were either bundled tightly or formed into a circular bundle and immersed fully in the microalgae suspension (Table 18). Detailed procedural steps are provided in Appendix 4.9.

Each sample was monitored over sixteen days through visual documentation, with pigment intensity used as a proxy for microalgal growth and viability.

Table 19: Samples overview Protocol Yarn Attachment

Sample group	Description
A (n=1)	Cotton yarn in a tight bundle, washed with water
B (n=1)	Cotton yarn in a circular bundle, not washed
C (n=1)	PVA yarn in a tight bundle, washed with water
D (n=1)	PVA yarn in a circular bundle, not washed

4.6.2 Results

Clear differences were observed between cotton and PVA yarn in their interaction with *Scenedesmus* sp. Upon immersion, PVA yarns rapidly shrank and compiled into a compact ball-like structure, whereas cotton yarns retained their original form (Figure 47).

Cotton samples absorbed *Scenedesmus* sp. more rapidly and in greater quantities than PVA samples. Microalgal cells appeared to preferentially attach to the rough surface of the cotton fibres, aligning along the fibre structure (Figure 48 A). In contrast, the distribution of *Scenedesmus* sp. within the PVA samples was less defined. Microalgal suspension was observed to drip from PVA yarns, suggesting limited retention, whereas no visible dripping of *Scenedesmus* sp. was observed from cotton samples.

Washing experiments further demonstrated differences in attachment stability. *Scenedesmus* sp. cells were easily washed from PVA yarns by rinsing with demineralised water. In cotton samples, partial detachment occurred during washing. However, complete removal required substantially longer washing times compared to PVA (Figure 47).

Sample configuration influenced microalgal survival and biomass development. Microalgae viability was maintained in yarn configurations that remained hydrated over time. In configurations where cotton yarns remained hydrated, higher biomass growth was observed compared to PVA samples. In contrast, when cotton samples dried more rapidly, both microalgal survival and biomass development were reduced (Figure 49).

Over time, visual inspection suggested that *Scenedesmus* sp. became increasingly immobilised within the PVA yarn, indicating gradual growth or penetration of the microalgae into the polymer structure (Figure 48 B).

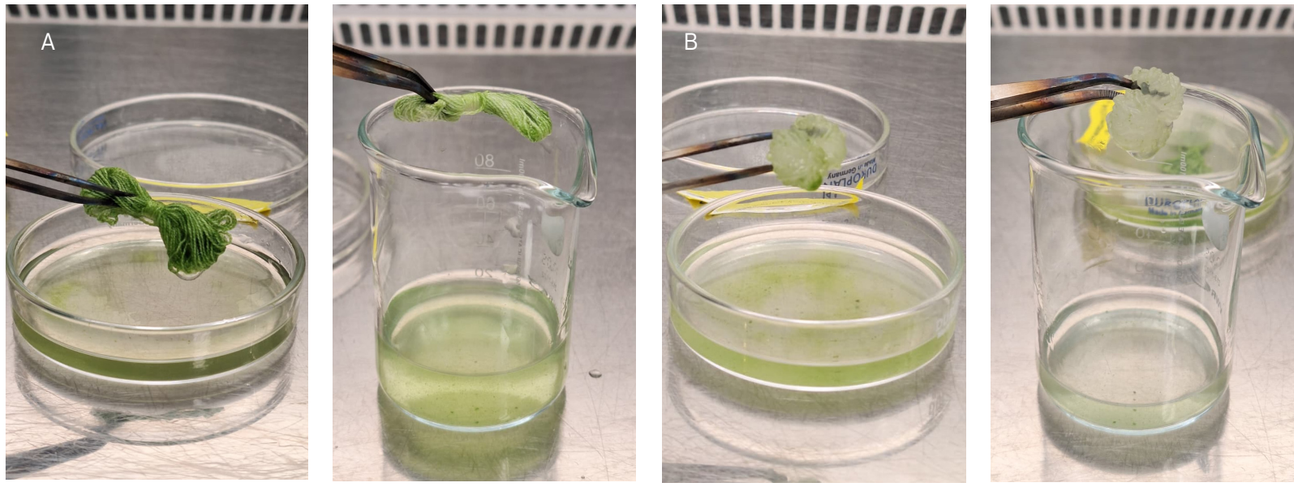

Figure 47: (A) Cotton inoculated with *Scenedesmus* sp. before and after washing; (B) PVA inoculated with *Scenedesmus* sp. before and after washing.

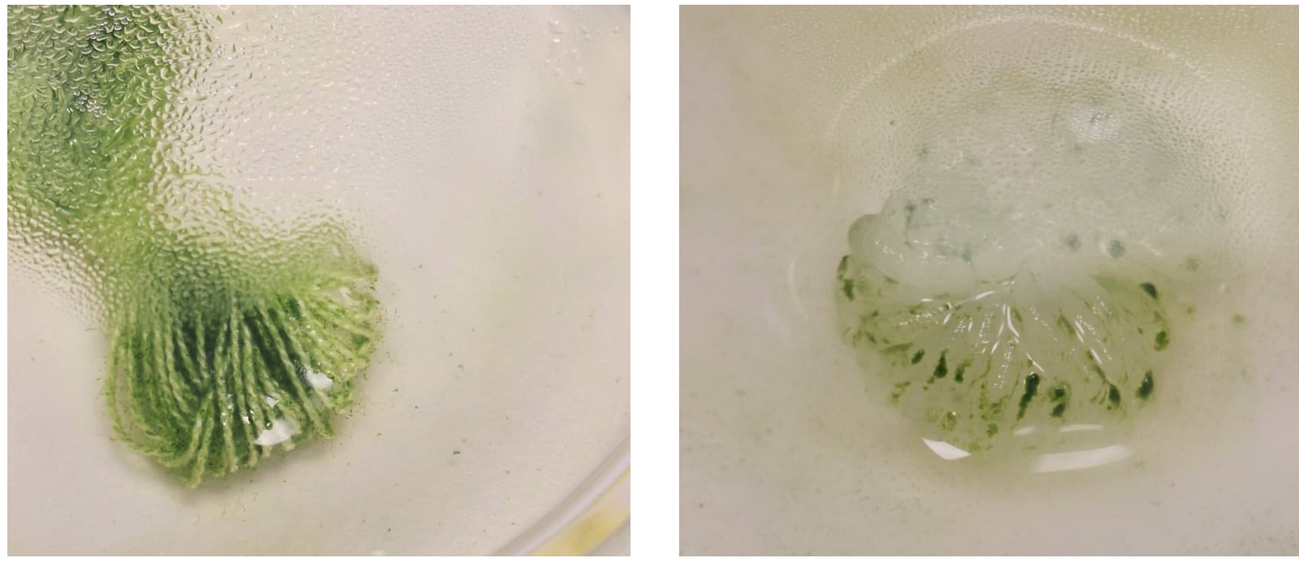

Figure 48: (A) *Scenedesmus* sp. growth in cotton yarn, showing colonisation within the fibre structure; (B) *Scenedesmus* sp. growth in PVA yarn, showing penetration into the material structure.

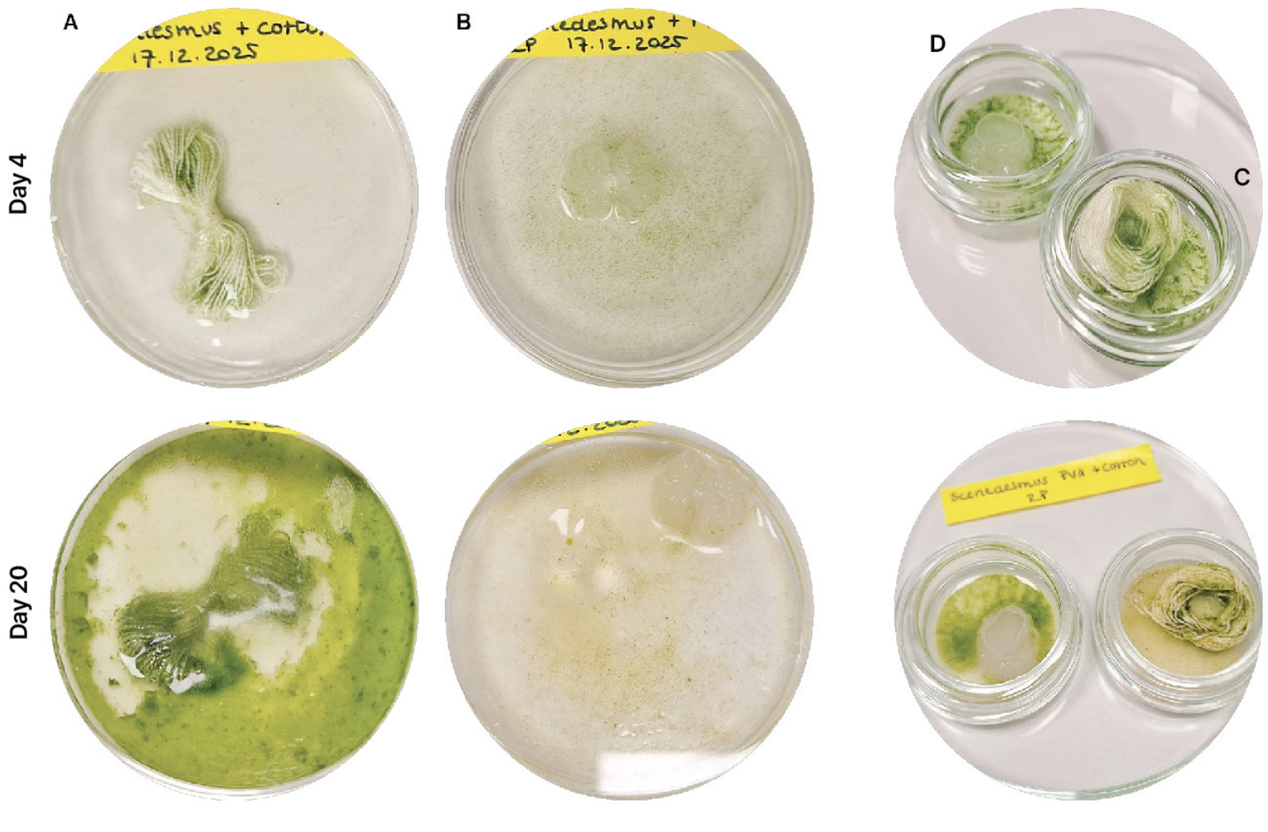

Figure 49: (A) Cotton yarn in a tight bundle, washed with water, showing increased biomass at day 20; (B) PVA yarn in a tight bundle, washed with water, showing no viability at day 20; (C) PVA yarn in a circular bundle, not washed, showing no viability at day 20 due to material drying and lack of nutrient availability; (D) PVA yarn in a circular bundle, not washed, showing increased biomass at day 20. Time points represent days from the start of the protocol.

4.6.3 Discussion and Conclusion

Yarn material influenced the attachment of *Scenedesmus* ***sp.*** within the textile matrix. Cotton yarn showed stronger microalgal attachment compared to PVA yarn, as indicated by higher biomass retention and increased resistance to removal during washing. This is likely related to the rough surface structure of cotton fibres. In contrast, PVA yarn exhibited limited initial retention, with microalgal suspension dripping from the fibres, indicating weaker attachment. It should however, be noted that the hydrogel was not cross-linked, which might have resulted in a different observation.

Moisture retention played a critical role in microalgal survival, consistent with findings from previous protocols. Samples that remained hydrated supported continued viability and biomass development, whereas drying resulted in a rapid decline in visible pigmentation. While cotton supports strong attachment, PVA contributes to moisture retention within the system. This suggests that an optimised ratio of both materials should be reached, as cotton enhances immobilisation and PVA supports moisture availability.

Although initial attachment to PVA was limited, visual observations indicated a gradual increase in microalgal presence within PVA regions over time, suggesting possible growth within the polymer matrix. However, attachment stability remained lower than in cotton samples. Overall, these results indicate that both material properties and hydration conditions influence microalgal attachment and retention.

In conclusion, *Scenedesmus* ***sp.*** shows a clear preference for attachment to cotton over PVA yarn (SRQ1), and attachment to cotton is more stable under washing conditions, whereas PVA exhibits weaker retention and higher cell detachment (SRQ2). These findings confirm that cotton is the primary contributor to effective immobilisation, while PVA plays a supporting role in moisture retention. Building on this, the next protocol will investigate textile systems with varying cotton-PVA ratios to further optimise the matrix design. This will enable evaluation of how material composition influences both microalgal attachment and system performance, including its effect on CO_2 capture.

4.7 Cotton-Hydrogel Ratio

Effect of Different Ratios of Cotton-Hydrogel on the Viability and CO_2 Fixation of *Scenedesmus* sp. in a Multilayer Textile Matrix

Overview Cotton-Hydrogel Ratio

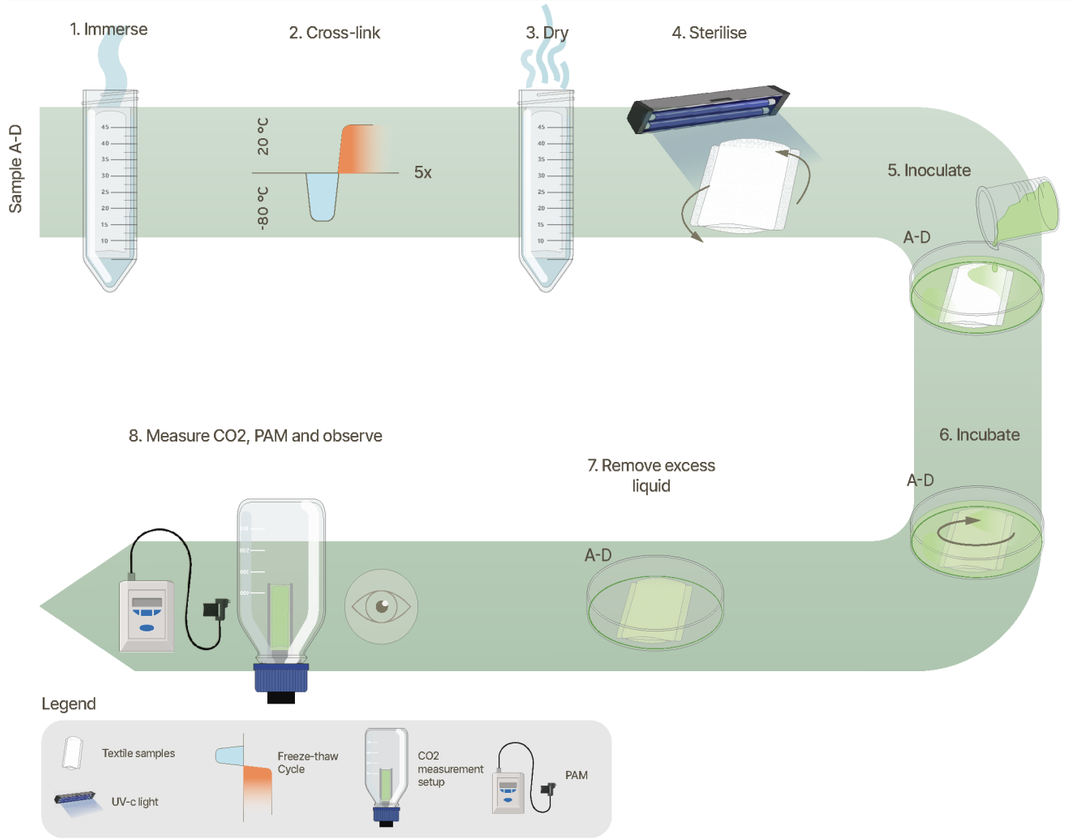

Figure 50: Overview methodology Protocol Cotton-Hydrogel Ratio

Table 20: Timeline Protocol Cotton-Hydrogel Ratio

Nr.	Action	Sample group	Protocol day
1	Immerse textile in 50 mL demi water	A-D	1
2	Cross-link the samples (24 hours freezing, 24 hours thawing)	A-D	1-10
3	Dry the textile samples	A-D	10
4	Sterilise with UV-C light for 20 minutes	A-B	10
5	Inoculate sample groups with *Scenedesmus* sp.	A-D	10
6	Incubate samples on a rotating platform (25°C, 120 rpm)	A-D	10-14
7	Remove the excess liquid	A-D	14
8	Vortex samples and measure the optical density of the liquid surrounding the textile	A-D	27
	Measure CO2	A-D	14-15
	Take measurements with Monitoring Pulse-Amplitude-Modulation	A-D	15, 18, 21, 23
	Observe	A-D	14-21

For sample groups see Table 21

4.7.1 Introduction

This protocol builds on the findings of the Protocol Yarn Attachment (4.6), which demonstrated that *Scenedesmus* sp. shows a preference and stronger attachment to cotton fibres than to PVA, and that moisture retention is a critical factor for sustaining viability within the textile system.

To further optimise the textile matrix, this study investigates different cotton-PVA ratios within a multilayer textile matrix to identify the composition that best supports microalgal attachment, growth, and CO_2 capture. In addition, findings from the Protocol Time of Inoculation (4.5) demonstrated that inoculating *Scenedesmus* sp. prior to cross-linking results in reduced long-term viability, while also confirming that immobilisation is still possible after cross-linking. Based on these findings, the standard procedure was adjusted in the present protocol by first cross-linking the textiles and subsequently inoculating them with *Scenedesmus* sp. to minimise unnecessary exposure to stress conditions during immobilisation.

Based on this rationale, this protocol addresses research questions 1,3 and 4, and the following sub-questions (SRQs) were defined:

1. How does the cotton-PVA ratio within a multilayer textile matrix influence the attachment and distribution of *Scenedesmus* sp.?
2. How does the cotton-PVA ratio affect the viability of *Scenedesmus* sp.?
3. How does the cotton-PVA ratio influence the CO_2 capture performance of the microalgae-textile biocomposite?

Scenedesmus sp. cultures were cultivated according to the standard cultivation protocol (Appendix 1.1), with an initial optical density of 0.656 measured at a wavelength of 430 nm.

Four experimental groups were prepared, representing different cotton-PVA ratios (Table 20). Detailed weaving patterns are provided in Appendix 4.1.1-4.1.4. Prior to inoculation, the textile samples were sterilised using a UV-C sterilisation box (Appendix 1.2). Detailed procedural steps are provided in Appendix 3.10.

Each sample was monitored over a 1.5-week period through visual documentation, with pigment intensity used as a proxy for microalgal growth and viability. Following the visual assessment, the samples were examined microscopically to evaluate the density and distribution of *Scenedesmus* sp. within specific regions of the textile matrix. Additionally, CO_2 measurements and PAM fluorescence analyses were performed to evaluate photosynthetic activity. The CO_2 measurements were conducted over a period of two days, with samples maintained under continuous light to minimise respiratory effects.

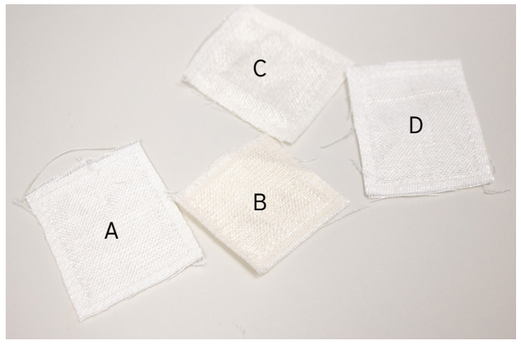

Figure 51: Cotton-hydrogel textile samples groups A-D

Table 21: Samples overview Protocol Cotton-Hydrogel Ratio

Sample group	Description
A (n=4)	Multilayer textile containing 60% cotton, 40% PVA, subjected to 5 F-T cycles, immobilised in *Scenedesmus* sp.
B (n=4)	Multilayer textile containing 69.2% cotton, 30.8% PVA, subjected to 5 F-T cycles, immobilised in *Scenedesmus* sp.
C (n=4)	Multilayer textile containing 84.6% cotton, 15.4% PVA, subjected to 5 F-T cycles, immobilised in *Scenedesmus* sp.
D (n=4)	Multilayer textile containing 53.8% cotton, 46.2% PVA, subjected to 5 F-T cycles, immobilised in *Scenedesmus* sp.

4.7.2 Results

Differences in pigment intensity were observed between the sample groups. Figure 52 shows the development of *Scenedesmus* sp. over a 1.5-week period. Samples with a higher cotton content exhibited a greater distribution of biomass throughout the textile matrix, as indicated by increased and more homogeneous pigment intensity.

In contrast, samples with a higher PVA content showed a non-uniform distribution of microalgae. Higher pigment intensity was observed along the compound edges of the textile, while the multilayer inner structure exhibited limited microalgal growth. These observations were supported by microscopic analysis, which revealed a higher density of *Scenedesmus* sp. in cotton-rich regions compared to PVA-dominant areas (Figure 53).

CO_2 measurements showed a similar trend across sample groups A, B and D. The CO_2 concentration initially decreased from the starting value, followed by stabilisation at approximately 300 ppm (Figure 54). Differences in the rate of CO_2 uptake were observed between samples, as indicated by variations in the slope of the curves (Figure 55), with sample C showing a release of CO_2 instead of carbon capture (Figure 54). The measurement was delayed due to a failure in the CO_2 setup, and the sample was therefore not considered representative. Among the valid samples (A, B, and D), sample B exhibited the steepest decline in CO_2 concentration, indicating the highest uptake rate.

PAM fluorescence measurements initially showed comparable trends across all samples, with cotton-rich textiles exhibiting higher fluorescence quantum yield than samples with higher PVA content (Figure 56). After seven days, several samples showed visible signs of drying (Figure 52), which corresponded with a decrease in fluorescence quantum yield, particularly in the cotton-rich samples (Figure 52 B, C).

Drying was not uniform across all samples and likely resulted from variations in incubator conditions, such as heat distribution or airflow. Samples showing significant dehydration were rehydrated with 5 mL BG11 medium, while others remained unaffected. Following rehydration, cotton-rich samples again showed higher fluorescence quantum yield compared to PVA-rich samples.

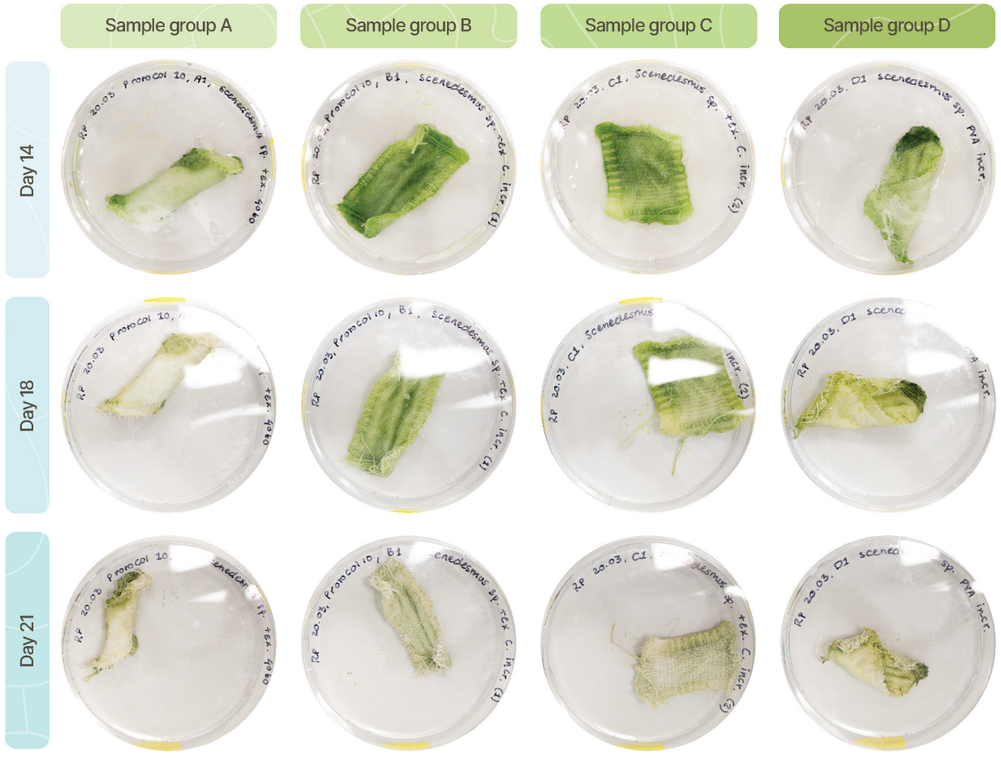

Figure 52: Overview of microalgae-textile biocomposite samples A-D after removal of excess liquid, showing decreased pigmentation across all sample groups and significant drying. A single representative biological replicate was selected from each sample group for imaging. Time points represent days from the start of the protocol.

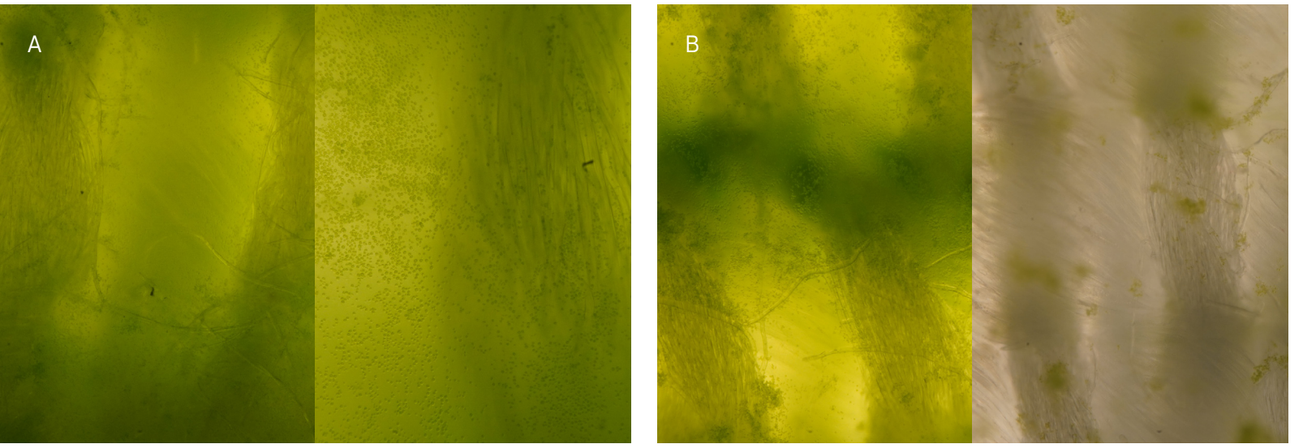

Figure 53: Microscopic images (5× magnification) of immobilised textile samples, showing *Scenedesmus* sp. in the compound twill (left) and multilayer structure (right): (A) biomass distribution in sample group C; (B) biomass distribution in sample group D, showing reduced biomass in the central structure.

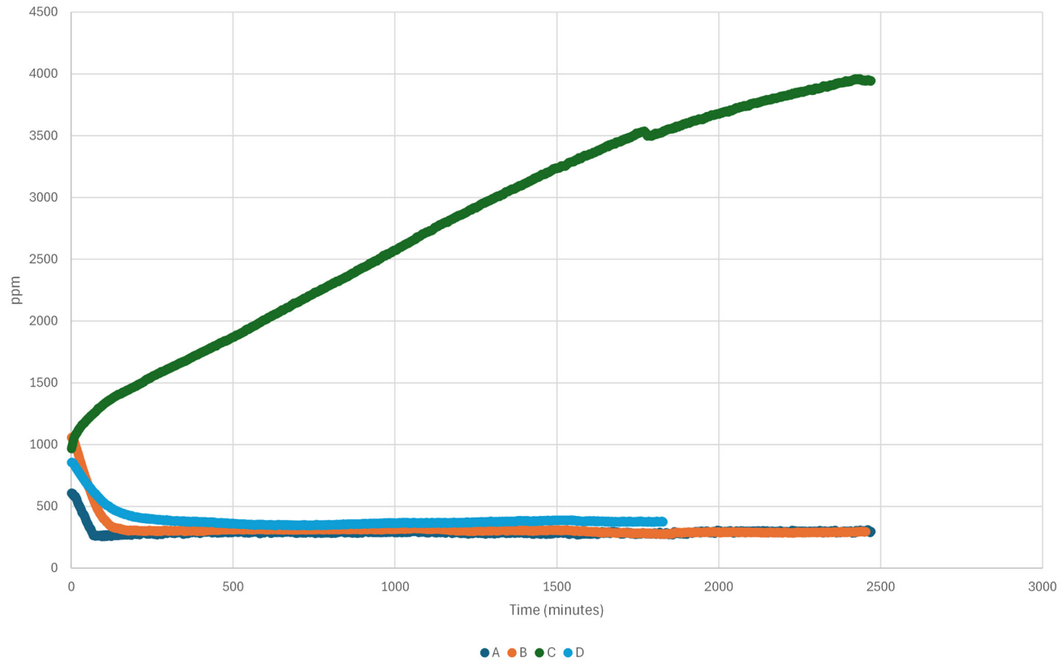

Figure 54: CO_2 measurements of samples A-D, where samples A, B, and D show a decrease in CO_2 concentration reaching an equilibrium around 300 ppm after approximately seven hours, while sample C shows an increase in CO_2 concentration.

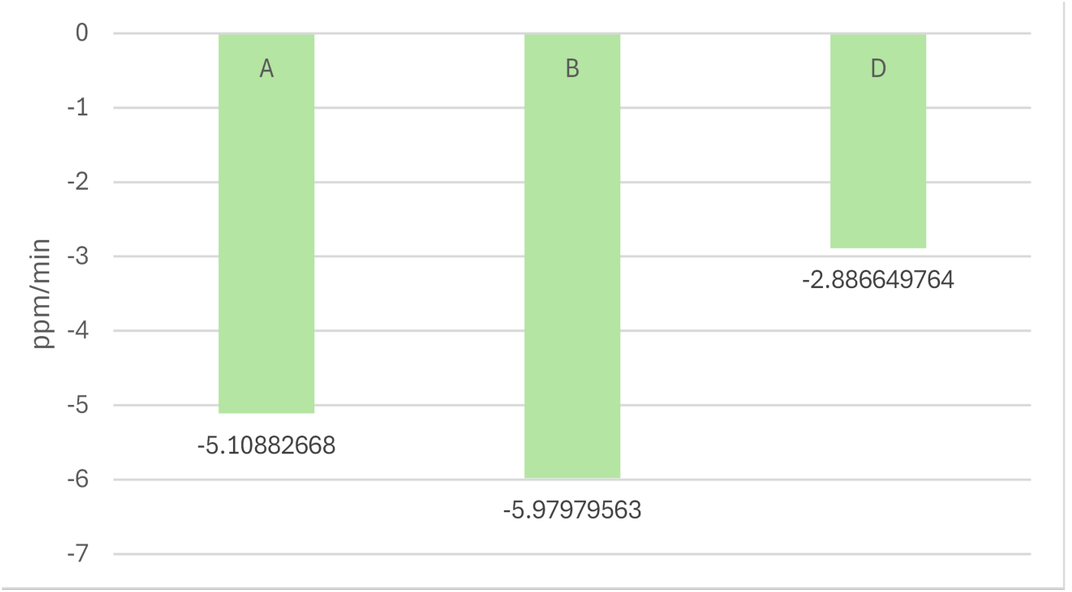

Figure 55: CO_2 uptake rates (ppm/min slope) of samples A, B, and D, where lower values indicate faster CO_2 uptake; sample group B shows the fastest uptake rate.

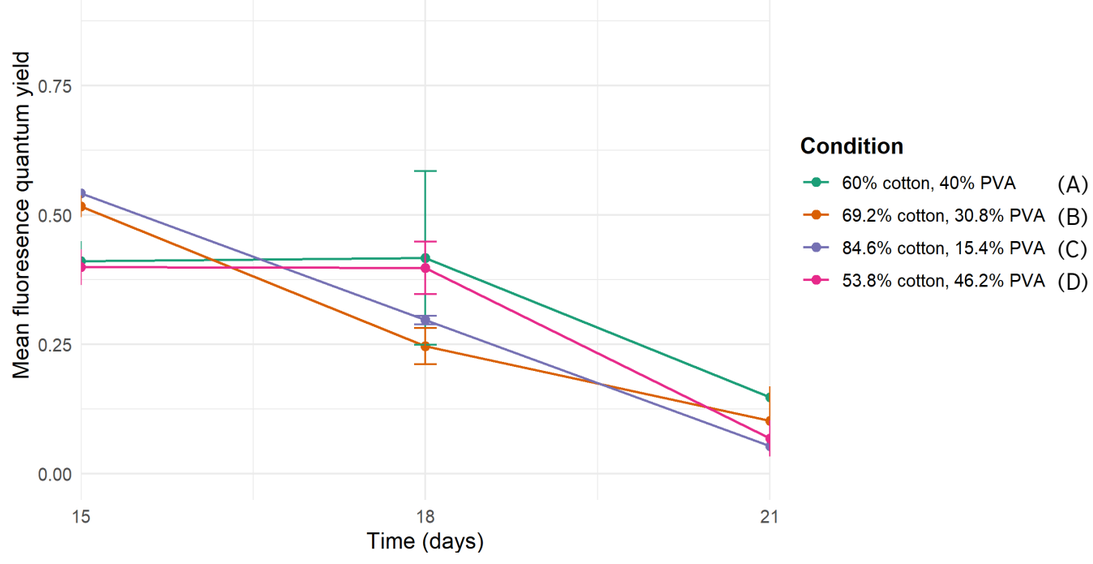

Figure 56: Fluorescence quantum yield of textile samples over six days, showing a decrease in all samples after day18. Time points represent days from the start of the protocol.

4.7.3 Discussion and Conclusion

The cotton-PVA ratio influenced the attachment and distribution of *Scenedesmus* sp. within the textile matrix. Cotton-rich samples exhibited a more homogeneous biomass distribution and higher pigment intensity. In contrast, PVA-rich samples showed a more localised distribution, with microalgae primarily concentrated along the edges of the textile, suggesting limited attachment within the inner structure. These findings are consistent with earlier observations that *Scenedesmus* sp. preferentially attaches to cotton fibres.

The decline in PAM fluorescence over time can be explained by the gradual evaporation of the growth medium, leading to drying of the textile samples and reduced microalgal viability. Cotton-rich samples appeared more affected by this process, likely due to their lower PVA content and, consequently, reduced water retention capacity within the textile matrix. This highlights the importance of balancing cotton content for attachment with sufficient PVA to maintain hydration. Additionally, periodic supplementation of growth medium is required to maintain the viability of the biocomposite.

CO_2 measurements showed an overall decrease followed by stabilisation, suggesting the establishment of a dynamic equilibrium within the closed system. However, sample C is not considered representative due to a failure in the CO_2 measurement setup. The delay in sample measurement likely resulted in the degradation of the textile during the experiment, which may have caused an increase in the recorded CO_2 concentration. Among the valid samples (A, B, and D), sample B exhibited the steepest decline in CO_2 concentration, indicating the highest uptake rate. The increased CO_2 uptake observed in these samples can be attributed to higher biomass levels, as a greater number of active cells enhances photosynthetic activity. The subsequent stabilisation of CO_2 levels may indicate that, as CO_2 becomes limited, a portion of the microalgal population loses viability and releases CO_2 through respiration or decomposition, thereby sustaining the remaining cells.

In conclusion, increasing cotton content improves the attachment and spatial distribution of *Scenedesmus* sp. within the textile matrix (SRQ1), while long-term viability is dependent on sufficient moisture retention, which is enhanced by the presence of PVA (SRQ2). CO_2 capture performance is initially higher in cotton-rich samples due to increased biomass, but declines over time as drying reduces microalgal viability (SRQ3). These findings demonstrate that an optimised balance between cotton and PVA is required to achieve both strong attachment and sustained viability.

Building on these findings, the next protocol will incorporate multilayer textile samples containing 69.2% cotton and 30.8% PVA, subjected to five freeze-thaw cycles. This composition is considered to provide the most suitable balance between microalgal attachment and moisture retention, thereby supporting both biomass growth and overall system stability.

Furthermore, the next protocol will integrate the key findings from previous studies while introducing periodic supplementation of BG11 medium to maintain hydration after inoculation. In addition, a second microalgal strain, *Scenedesmus bacillaris*, will be included to evaluate whether a more defined species exhibits similar attachment, viability, and CO_2 capture behaviour within the optimised textile matrix.

This page is intentionally left blank

4.8 Optimised System Integration

Evaluation of an Optimised Cotton-Hydrogel Matrix Following Freeze-Thaw Cross-linking and Post-Inoculation with *Scenedesmus* sp. and *Scenedesmus bacillaris*

Overview Optimised System Integration

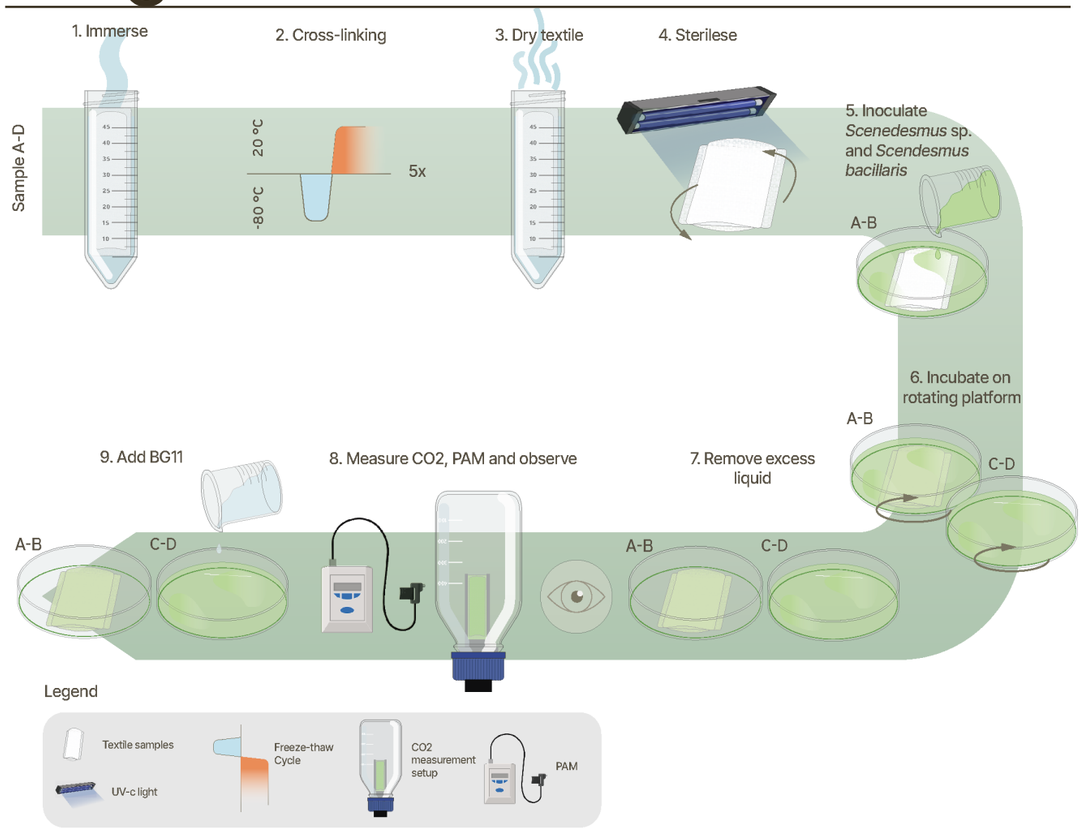

Figure 57: Overview methodology Protocol Optimised System Integration

Table 22: Timeline Protocol Optimised System Integration

Nr.	Action	Sample group	Protocol day
1	Immerse textile in 50 mL demi water	A-D	1
2	Cross-link the samples (24 hours freezing, 24 hours thawing)	A-D	1-10
3	Dry the textile samples	A-D	10
4	Sterilise with UV-C light for 20 minutes	A-B	10
5	Inoculate sample groups with *Scenedesmus* sp.	A-D	10
6	Incubate samples on a rotating platform (25°C, 120 rpm)	A-D	10-12
7	Remove the excess liquid	A-D	12
8	Measure CO2 (24 hours per measurement)	A-D	12-18
	Take measurements with Monitoring Pulse-Amplitude-Modulation	A-D	13, 17, 19, 21
	Observe	A-D	12-21

For sample groups see Table 23

4.8.1 Introduction

This protocol builds on the previous Protocol, Cotton-Hydrogel Ratio (4.7), which showed that cotton enhances attachment and growth of *Scenedesmus* sp., while PVA improves moisture retention. However, imbalances negatively affect viability and CO_2 performance. From these findings, a 69.2% cotton / 30.8% PVA composition subjected to five freeze-thaw cycles was identified as optimal for balancing attachment and moisture retention. Despite the presence of hydrogel in the textile matrix, periodic rehydration with BG11 medium remains necessary to maintain a hydrated environment.

Building on this, the following protocol incorporated key findings from all previous protocols to develop an optimised approach for incorporating microalgae into a multilayer woven textile matrix. Hydrogel cross-linking through repeated freeze-thaw cycles (5 F-T cycles) is applied to ensure structural stability, while post-cross-linking inoculation is used to preserve microalgal viability by avoiding exposure to freezing conditions.

The inoculation strategy is based on findings that immersion of the textile in microalgal suspension promotes homogeneous distribution. In addition, rotational incubation is applied to enhance cell-textile contact and improve attachment. Environmental conditions, including sufficient light intensity and temperatures between 20-30 °C, are maintained to support sustained microalgal growth.

In addition to *Scenedesmus* sp., the species *Scenedesmus bacillaris* is included to evaluate whether different *Scenedesmus* species exhibit similar behaviour within the textile matrix.

The overall aim of this protocol is to evaluate the performance of the optimised microalgae-textile biocomposite system under controlled experimental conditions, focusing on microalgal attachment, viability, and CO_2 capture efficiency.

Based on this rationale, this protocol addresses research questions 1 - 4, and the following sub-questions (SRQs) were defined:

1. How do optimised textile composition (69.2% cotton / 30.8% PVA) and five freeze-thaw cross-linking cycles influence the attachment and viability of *Scenedesmus* sp. within a multilayer woven textile matrix?
2. How does post-cross-linking inoculation combined with rotational incubation affect the distribution and stability of *Scenedesmus* sp. within the textile matrix?
3. How do controlled environmental conditions (light intensity, temperature, and periodic BG11 supplementation) influence the biomass development and CO_2 capture performance of the microalgae-textile biocomposite?
4. How does CO_2 capture in a microalgae-textile biocomposite compare to that of a suspension culture?

Scenedesmus cultures were cultivated according to the standard cultivation protocol (Appendix 1.1). The initial optical densities of *Scenedesmus* sp. and *Scenedesmus bacillaris* were adjusted to approximately 0.400, measured at 430 nm, to ensure comparability between samples.

Four experimental groups were prepared (Table 22). Sample groups A and C each contained five biological replicates: two for visual observation, two for CO_2 measurements, and one spare sample in case of measurement failure. Prior to inoculation, all textile samples were sterilised using a UV-C sterilisation box (Appendix 1.2). Detailed procedural steps and weaving patterns are provided in Appendices 3.11 and 4.1.2.

Table 23: Samples overview Protocol Optimised System Integration

Sample group	Description
A (n=5)	Multilayer textile containing 60% cotton, 40% PVA, subjected to 5 F-T cycles, subsequently inoculated with *Scenedesmus* sp.
B (n=4)	*Scenedesmus* sp. suspension culture
C (n=5)	Multilayer textile containing 60% cotton, 40% PVA, subjected to 5 F-T cycles, subsequently inoculated with *Scenedesmus bacillaris*
D (n=4)	*Scenedesmus bacillaris* suspension culture

Each sample was monitored over a 1.5-week period through visual documentation, with pigment intensity used as a proxy for microalgal growth and viability. Additionally, CO_2 measurements and PAM fluorescence analyses were performed to evaluate photosynthetic activity. The CO_2 measurements were conducted over a period of twelve hours, with samples maintained under continuous light to minimise respiratory effects.

4.8.2 Results

Following cross-linking, the textiles exhibited a noticeable sticky texture, compared to previous protocols. The samples were inoculated at a relatively low optical density, resulting in low visibility of green pigmentation. In previous protocols, higher optical densities were used, leading to more visible biomass development.

Suspension cultures showed a significant visual difference (Figure 58 A), indicating contamination in the *Scenedesmus bacillaris* samples. Based on the colour of the suspension and microscopic observations (Figure 58 B), the contaminant is assumed to be a cyanobacterial species. As a result, findings involving *Scenedesmus bacillaris* are considered inconclusive.

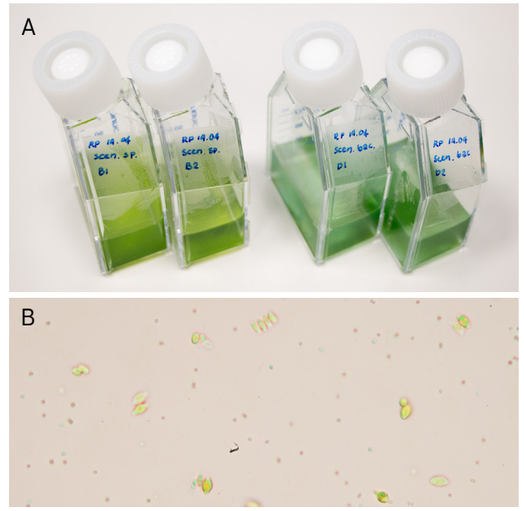

Figure 58: (A) (Left) sample group B with *Scenedesmus* sp.; (Right) sample group D with *Scenedesmus bacillaris*, showing pigment discolouration indicative of contamination. (B) Microscopic image (40× magnification), where the larger cells are *Scenedesmus bacillaris* and the smaller blue cells indicate contamination.

Differences in biomass distribution and growth behaviour were observed between the sample groups (Figure 59). Overall, microalgal growth within the textile matrix was limited, with most biomass accumulating in the surrounding liquid rather than within the textile structure. Higher cell densities were primarily observed at the bottom of the *Petri* dishes, indicating that growth especially occurred in the suspension.

Figure 59: Overview of sample groups A and C, showing consistently high moisture levels and minimal increase in pigmentation in both groups. In sample group C, a shift from green to yellow pigmentation is observed after day 3. A single representative biological replicate was selected from each group for imaging. Time points represent days after inoculation.

The presence of excess liquid resulted from the addition of BG11 medium to prevent drying. However, sealing the *Petri* dishes with parafilm significantly reduced evaporation, causing liquid buildup and submerging the textile samples.

Comparing groups A and C, *Scenedesmus* sp. showed a more homogeneous distribution within the textile matrix than *Scenedesmus bacillaris* (Figure 59). The samples containing *Scenedesmus bacillaris* showed yellow pigmentation instead of green. The results are however inconclusive since the *Scenedesmus bacillaris* samples were contaminated.

Due to repeated CO_2 measurement setup failures, only one replicate per group was analysed (Figure 60). Suspension cultures (groups B and D) showed a decrease in CO_2 concentration, with *Scenedesmus* sp. exhibiting a steeper decline, indicating higher uptake. In contrast, textile samples (groups A and C) showed an increase in CO_2 concentration, suggesting CO_2 production. However, these results should be interpreted with caution due to contamination and deviation in results from previous protocols (4.7).

PAM fluorescence measurements confirmed higher performance in suspension cultures compared to textile samples (Figure 61). The *Scenedesmus* sp. textile samples showed a gradual decline in metabolic activity. In contrast, *Scenedesmus bacillaris* exhibited an initial decrease followed by a partial recovery after day 9. It should be noted that quantum fluorescence yield could only be measured at a limited number of locations within the *Scenedesmus bacillaris* samples, whereas measurements could be taken more consistently across the textile samples containing *Scenedesmus* sp. However, due to contamination, these results remain inconclusive.

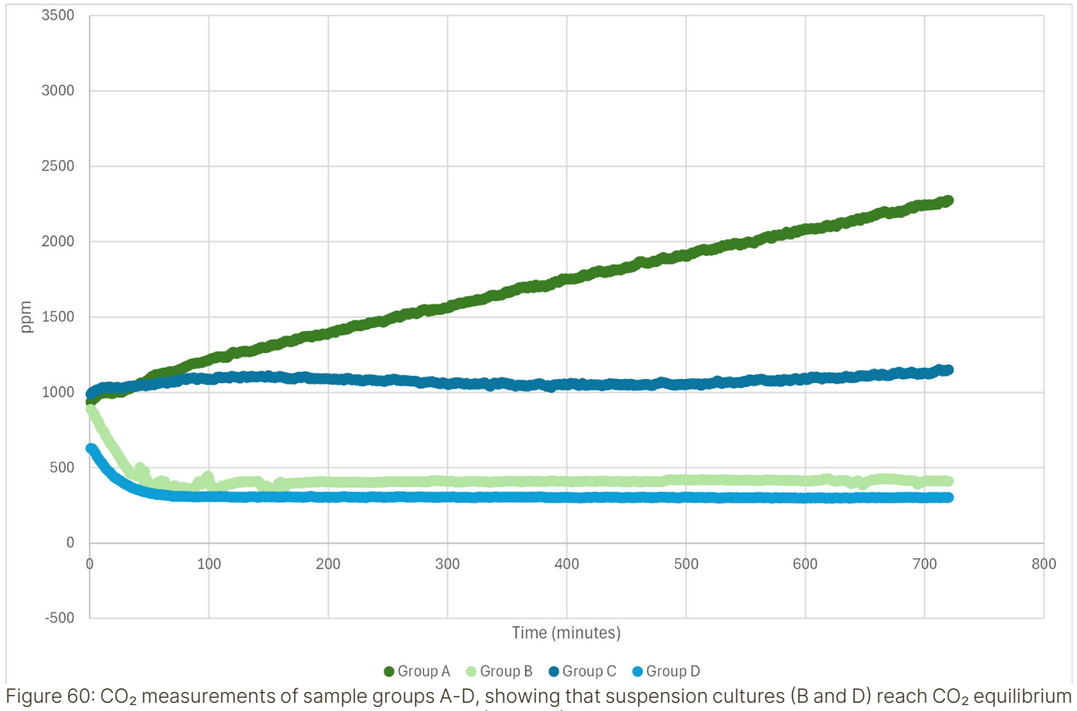

Figure 60: CO_2 measurements of sample groups A-D, showing that suspension cultures (B and D) reach CO_2 equilibrium within approximately one hour, while textile samples (A and C) release CO_2, possibly due to respiration or degradation. Samples B and D represent contaminated conditions.

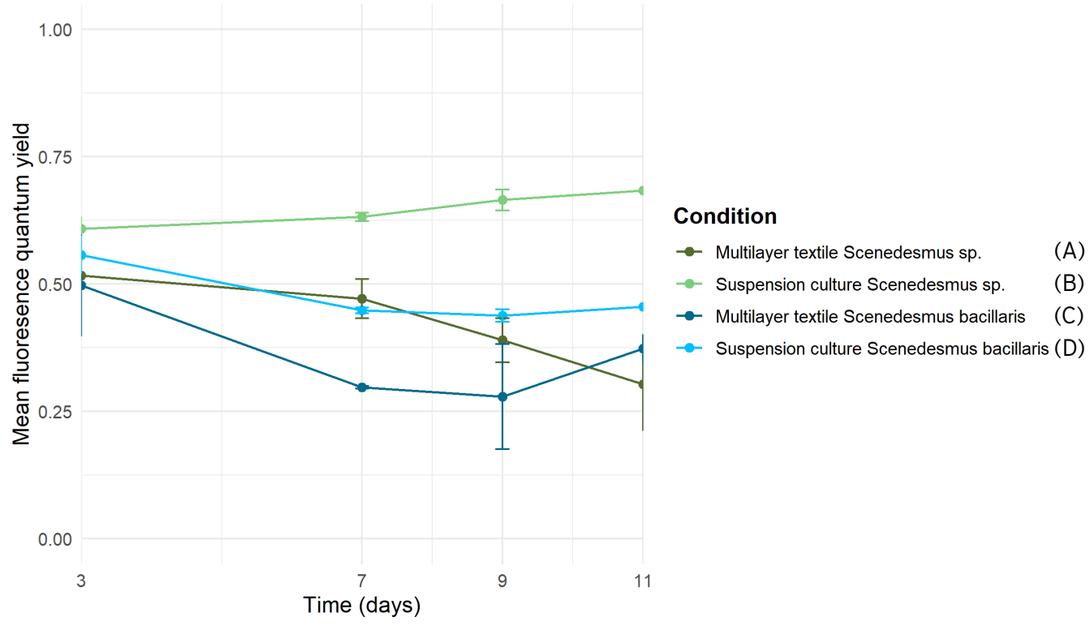

Figure 61: Fluorescence quantum yield of samples A-D, showing a gradual decrease in sample group A, while sample groups C and D initially decrease and then increase. Sample B shows an immediate increase, indicating that the *Scenedesmus* sp. suspension culture has the highest metabolic activity. Samples C and D represent contaminated sample. Time points represent days after inoculation.

4.8.3 Discussion and Conclusion

Although the optimised composition (69.2% cotton / 30.8% PVA) and five freeze-thaw cycles were expected to provide favourable conditions, variation in cross-linking likely affected homogeneous cross-linking throughout the material and material properties, resulting in the sticky matrix. This may have been caused by insufficient cross-linking, increasing surface degradation compared to previous protocols, ultimately reducing effective immobilisation and stability of the system.

Moisture availability again proved to be a critical factor for microalgal survival. However, in this protocol, the use of parafilm significantly reduced evaporation, leading to excess liquid around the textile due to additional BG11 supplementation. As a result, microalgae mainly grew in the surrounding liquid rather than within the textile matrix, likely due to higher nutrient availability. This indicates that controlled hydration strategies are essential and that excessive liquid environments can undermine immobilisation in the textile by shifting growth away from the intended substrate.

The initial optical density also played a key role in biomass development. Due to the slow growth of *Scenedesmus bacillaris*, which necessitated matching the optical density of *Scenedesmus* sp. to ensure comparability between sample groups. Therefore, inoculation was performed at a relatively low optical density, which resulted in limited visible biomass development within the textile. In combination with the larger textile size used in this protocol, the inoculated biomass was insufficient relative to the available surface area, further contributing to low cell density and reduced immobilisation in the textile matrix.

Differences in biomass growth between samples were further complicated by contamination in the *Scenedesmus bacillaris* cultures. The observed yellow colouration and altered growth behaviour suggest reduced viability, potentially caused by interspecific competition for nutrients with the contaminating microorganism. Alternatively, the contaminant may not have been suited to the textile environment, for example due to unfavourable pH conditions. As a result, comparisons involving *Scenedesmus bacillaris* remain inconclusive.

CO_2 capture results were inconsistent with previous protocols (4.7). While suspension cultures showed similar CO_2 performance to Protocol Cotton-Hydrogel Ratio, with Group B outperforming Group D. The slower CO_2 capture of Group D may have been influenced by contamination, particularly if the contaminant was a photosynthetic species such as cyanobacteria. In contrast, textile samples containing *Scenedesmus* sp. showed CO_2 production rather than uptake, deviating from earlier findings. This is likely due to insufficient biomass growth or possible contamination, highlighting the sensitivity of the biocomposites' performance to biological and experimental conditions.

PAM fluorescence measurements supported these observations. Textile samples containing *Scenedesmus* sp. showed a decline in metabolic activity, indicating an unfavourable growth environment. In contrast, *Scenedesmus bacillaris* samples showed an increase in fluorescence yield over time. However, this is likely attributed to improved measurement calibration rather than actual biological recovery. Measurement variability was further increased by non-homogeneous biomass distribution within the textile.

In conclusion, the optimised textile composition and cross-linking strategy did not consistently result in improved attachment and viability under the conditions of this protocol, primarily due to variations in cross-linking quality and low initial biomass density (SRQ1). Post-cross-linking inoculation combined with rotational incubation did not lead to stable immobilisation, as microalgae preferentially grew in the surrounding liquid rather than attaching to the textile. Indicating that nutrient distribution and moisture control are critical factors in achieving effective immobilisation (SRQ2). Controlled environmental conditions, including reduced evaporation due to parafilm and additional BG11 supplementation, negatively influenced system performance by promoting suspended growth and limiting textile colonisation. Ultimately reducing CO_2 capture capacity and metabolic activity (SRQ3).

CO_2 capture performance of the microalgae-textile biocomposite was lower than that of suspension cultures, with textile samples showing limited uptake or CO_2 production, likely due to low biomass density and reduced viability within the textile matrix (SRQ4).

The subsequent protocol was initially designed as an additional exploration of *Scenedesmus* sp. viability across different weaving structures. However, due to failures in the CO_2 measurement setup, a selection of these samples was repurposed to further evaluate and compare CO_2 uptake between textile-based systems and suspension cultures. This shift in focus highlights the need for robust experimental setups and reinforces the importance of validating CO_2 capture performance across different system configurations.

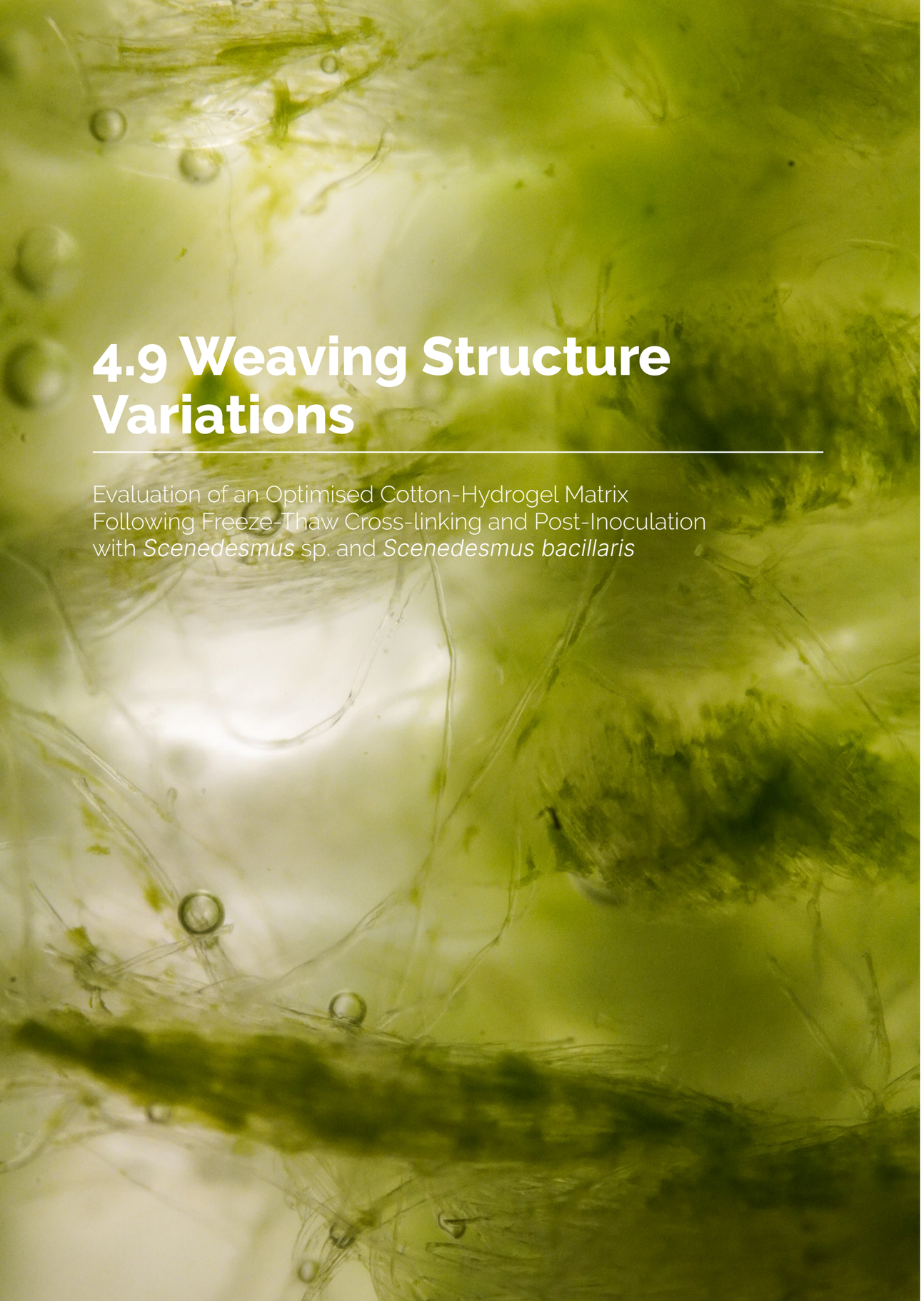

4.9 Weaving Structure Variations

Evaluation of an Optimised Cotton-Hydrogel Matrix Following Freeze-Thaw Cross-linking and Post-Inoculation with *Scenedesmus* sp. and *Scenedesmus bacillaris*

Overview Weaving Structure Variations

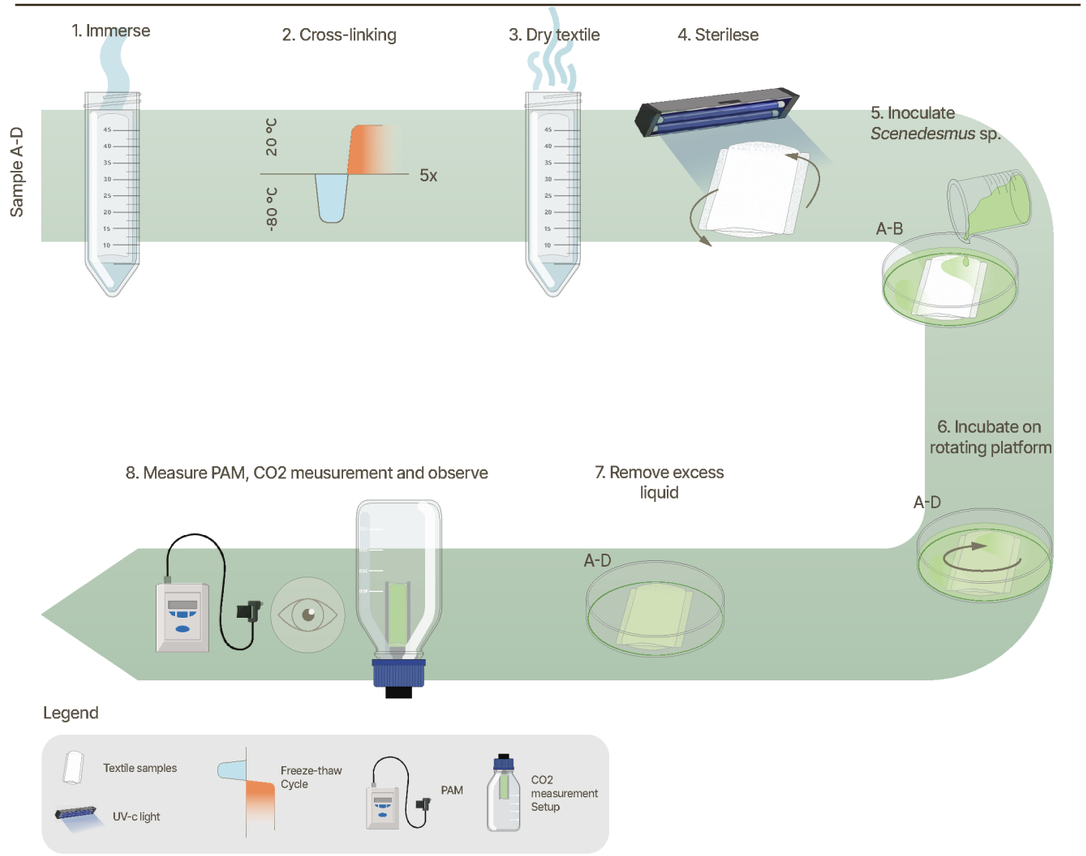

Figure 62: Overview methodology Protocol Weaving Structure Variations

Table 24: Timeline Protocol Weaving Structure Variations

Nr.	Action	Sample group	Protocol day
1	Immerse textile in 50 mL demi water	A-D	1
2	Cross-link the samples (24 hours freezing, 4 hours thawing)	A-D	1-7
3	Dry the textile samples	A-D	7-8
4	Sterilise with UV-C light for 20 minutes in each side	A-B	8
5	Inoculate sample groups with *Scenedesmus* sp.	A-D	8
6	Incubate samples on a rotating platform (25°C, 120 rpm)	A-D	8-10
7	Remove the excess liquid	A-D	10
8	Measure CO2	A-D	11, 15
	Take measurements with Monitoring Pulse-Amplitude-Modulation	A-D	9, 11, 14
	Observe	A-D	8-15

For sample groups see Table 25

4.9.1 Introduction

This final protocol was meant as a short, exploratory study to further investigate opportunities for optimisation of the textile matrix. Previous results for the Protocol Cotton-Hydrogel Ratio (4.7) indicate that matrix design plays a critical role in microalgal attachment and growth, suggesting that additional improvements may be achieved by modifying the structural configuration of the textile.

The primary aim of this protocol was therefore to evaluate new matrix designs by varying the number of textile layers and introducing structures with increased three-dimensional geometry. These modifications were intended to increase the available surface area and, consequently, enhance biomass growth within the textile and gas exchange.

In addition to cotton-hydrogel samples, samples incorporating recycled denim were included. Recycled denim yarns typically consist of shorter, mechanically processed fibres, resulting in a more irregular, fibrillated structure with increased surface roughness and a higher number of exposed fibre ends. This was expected to provide additional attachment of microalgae, potentially supporting increased biomass growth compared to conventional cotton yarns.

Due to failures encountered in the previous CO_2 measurement protocol (4.8), a subset of the samples in this study was repurposed to also evaluate CO_2 uptake performance. As a result, this protocol not only serves an exploratory function in assessing textile design variations but also contributes to the comparative analysis of CO_2 capture between textile-based systems and suspension cultures.

Based on this rationale, this protocol addresses research questions 1 and 4, and the following sub-questions (SRQs) were defined:

1. How does yarn type (cotton vs. recycled denim) influence the attachment and biomass growth of *Scenedesmus* sp. within the textile-hydrogel matrix?
2. How does the textile structure (number of layers and 3D structure) affect biomass growth of *Scenedesmus* sp. within the matrix?
3. How does CO_2 capture in a microalgae-textile biocomposite compare to that of a suspension culture?

Scenedesmus cultures were cultivated according to the standard cultivation protocol (Appendix 1.1), with an initial optical density of 0.876 measured at a wavelength of 430 nm.

Table 25: Samples overview Protocol Optimised System Integration

Sample group	Description
A (n=2)	Three-layer textile matrix, 60% cotton, 40% PVA (Appendix 4.1.2). Subjected to 5 F-T cycles, subsequently inoculated with *Scenedesmus* sp.
B (n=2)	Two-layer textile matrix, containing cotton and PVA (Appendix 4.1.5), subjected to 5 F-T cycles, subsequently inoculated with *Scenedesmus* sp.
C (n=2)	Six-layer textile matrix, containing cotton and PVA (Appendix 4.1.6), subjected to 5 F-T cycles, subsequently inoculated with *Scenedesmus* sp.
D (n=2)	Waffle weave textile matrix, containing cotton and PVA (Appendix 4.1.7), subjected to 5 F-T cycles, subsequently inoculated with *Scenedesmus* sp.
E (n=2)	Three-layer textile matrix, containing recycled denim, cotton and PVA (Appendix 4.1.2). Subjected to 5 F-T cycles, subsequently inoculated with *Scenedesmus* sp.
F (n=2)	Two-layer textile matrix, containing recycled denim, cotton and PVA (Appendix 4.1.5), subjected to 5 F-T cycles, subsequently inoculated with *Scenedesmus* sp.
G (n=2)	Six-layer textile matrix, containing recycled denim, cotton and PVA (Appendix 4.1.6), subjected to 5 F-T cycles, subsequently inoculated with *Scenedesmus* sp.
H (n=2)	Waffle weave textile matrix, containing recycled denim, cotton and PVA (Appendix 4.1.7), subjected to 5 F-T cycles, subsequently inoculated with *Scenedesmus* sp.
I (n=2)	*Scenedesmus* sp. suspension culture

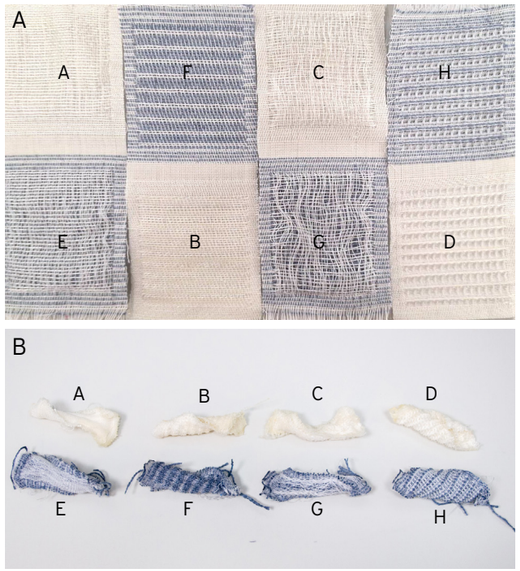

Figure 63: Weaving structures of sample groups A-H, where the white samples consist of cotton and PVA, and the blue samples consist of cotton, recycled denim, and PVA. (A) Before cross-linking ; (B) After cross-linking.

Nine experimental groups were prepared, representing different structures and material groupings (Table 25, Figure 63). Detailed weaving patterns are provided in Appendix 4.1.2, 4.1.5-4.1.7. Prior to inoculation, the textile samples were sterilised using a UV-C sterilisation box (Appendix 1.2). Detailed procedural steps are provided in Appendix 3.12.

Each sample was monitored over a one-week period through visual documentation, with pigment intensity used as a proxy for microalgal growth and viability. Cotton samples and recycled denim samples could not visually be compared because the blue denim causes the samples to appear darker. Therefore, sample groups were compared within the same material composition group.

Additionally, the quantum fluorescence yield was analysed to evaluate photosynthetic activity. Due to time constraints, CO_2 measurements were only conducted for sample groups A and I. The measurement duration was reduced to four hours to prevent decomposition within the closed setup, allowing the samples to be reused for subsequent observation and PAM measurements. The samples were maintained under continuous light to minimise respiratory effects.

4.9.2 Results

Following inoculation with a high optical density, all samples exhibited visible green pigmentation after one day of immersion in the suspension culture. Within the textile matrices, microalgal cells showed a clear preference for cotton yarns, which appeared more intensely pigmented compared to other materials.

Over the course of one week, no significant increase in pigmentation was observed across the samples, suggesting limited visible biomass development over time (Figure 64). Moisture retention remained stable due to the use of parafilm. However, slight drying was observed around day 8.

PAM fluorescence measurements showed similar quantum fluorescence yield values across all sample groups, with only minor variations (Figure 65). A gradual decrease in fluorescence yield was observed over time, with sample group H exhibiting the lowest values. When comparing samples with identical weaving structures but different materials (A+E, B+F, C+G, D+H), no consistent differences in the rate of decline were identified. Similarly, no clear distinction was observed between cotton (A-D) and recycled denim (E-H) samples, indicating comparable performance under the tested conditions.

Two CO_2 measurements were conducted: the first at day 4 after inoculation and the second at day 8. In both cases, a textile sample was compared with a suspension culture. (Figure 66) Both measurements showed a decrease in CO_2 concentration for both textile and suspension samples (Figure 67, 68). In the first measurement, the textile exhibited a slower CO_2 uptake compared to the suspension culture, as indicated by a less steep decline in CO_2 concentration (Figure 67). Both samples reached a concentration equilibrium of approximately 300 ppm after about two hours. In the second measurement (Figure 68), Overall uptake rates were lower, with the suspension culture reaching equilibrium approximately two hours into the measurement period, while the textile sample had not yet stabilised after four hours.

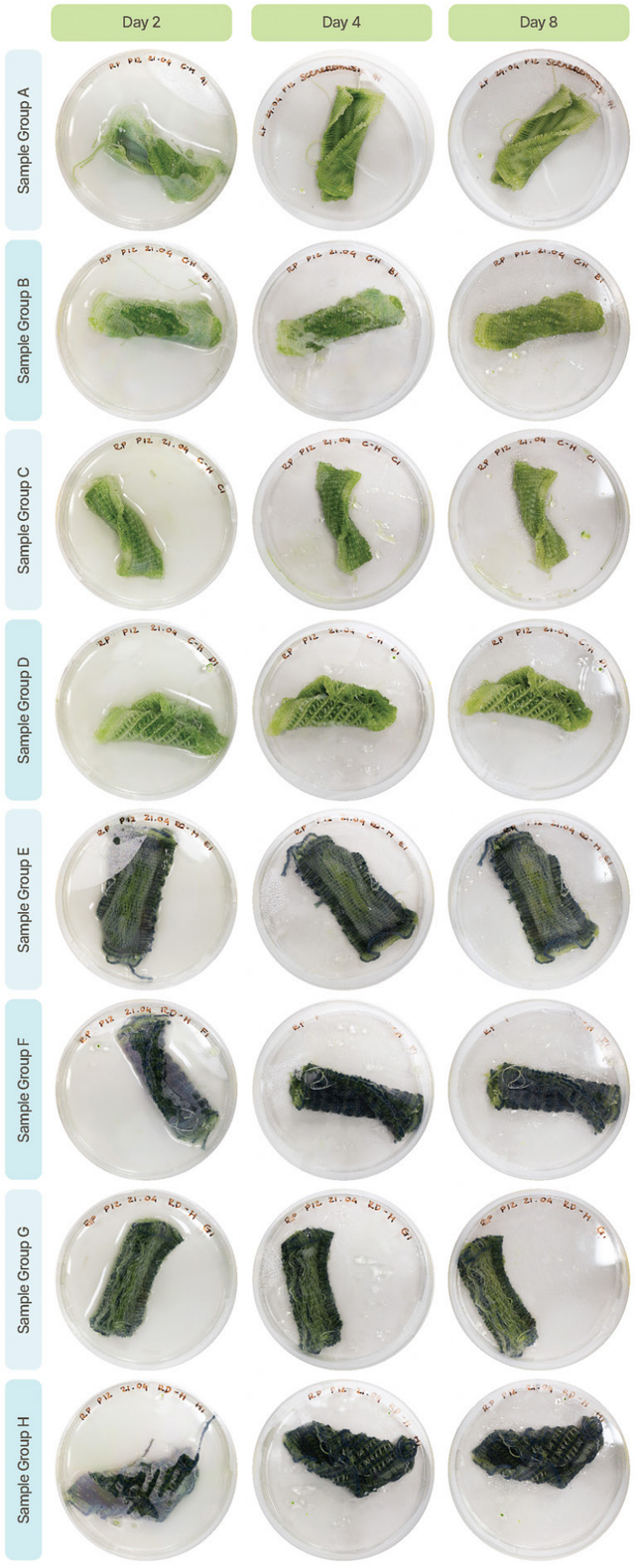

Figure 64: Overview of sample groups A-H. A single representative biological replicate was selected from each group for imaging. No significant increase in pigmentation is observed over the 6-day period. Time points represent days after inoculation.

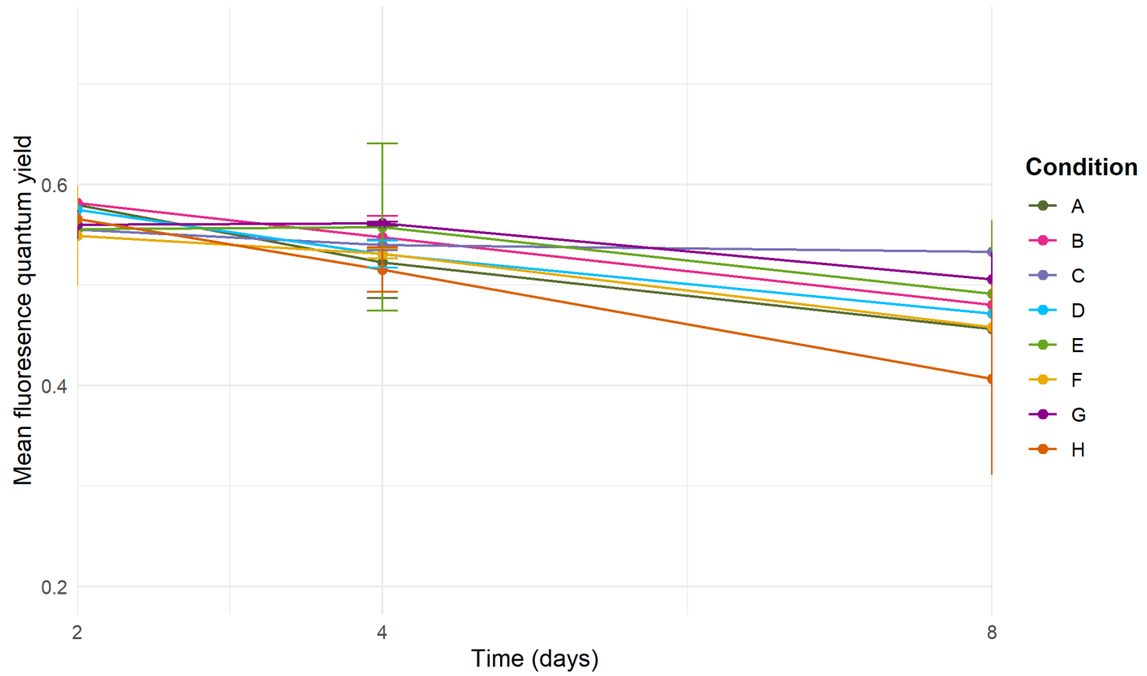

Figure 65: Fluorescence quantum yield measurements of sample groups A-H, showing a gradual decrease in metabolic activity across all samples. No clear outperforming sample is observed. Time points represent days after inoculation.

Figure 66: Optimised CO_2 measurement setup with suspended sensors for both microalgae-textile biocomposites and suspension cultures, with samples showing high pigmentation indicative of high viability.

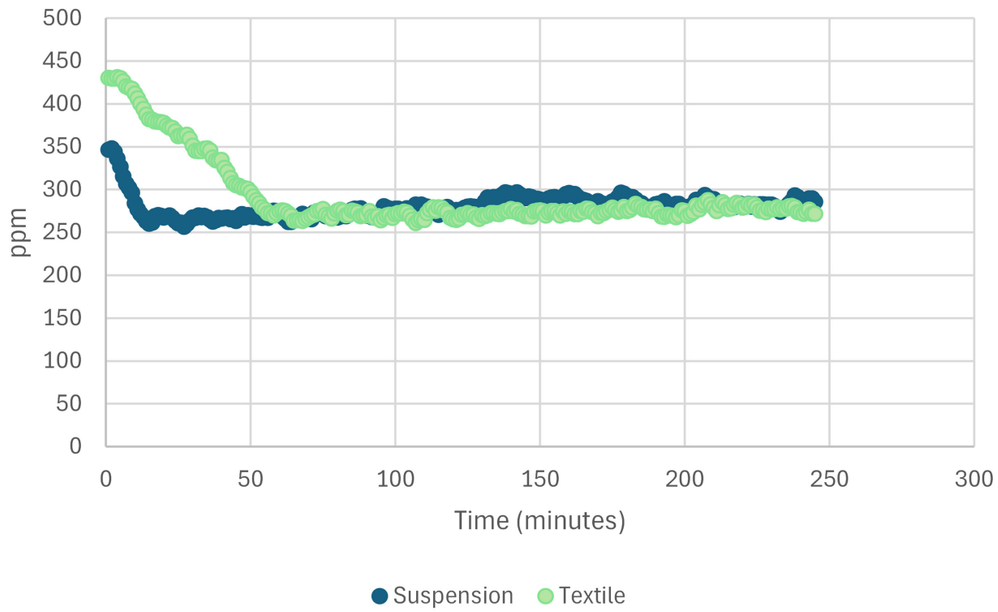

Figure 67: Results of the first CO_2 measurement, showing that both the microalgae-textile biocomposite and the suspension culture reach equilibrium after approximately one hour, with the suspension culture exhibiting a faster CO_2 uptake.

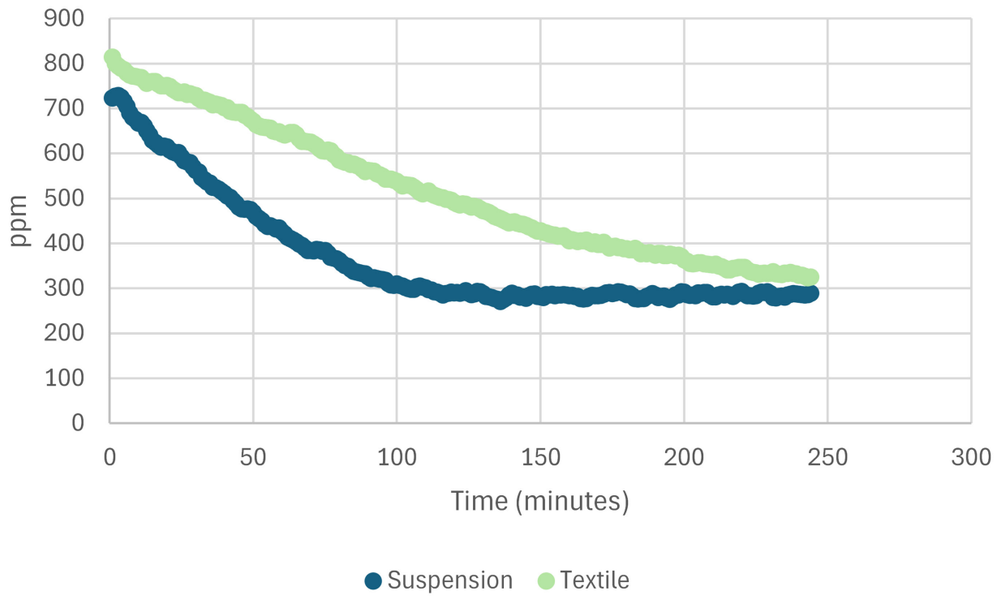

Figure 68: Results of the secondary CO_2 measurement, showing that the suspension culture reaches equilibrium after approximately two hours, whereas the microalgae-textile biocomposite does not reach equilibrium within the measurement timeframe, indicating faster CO_2 uptake in the suspension culture.

4.9.3 Discussion and Conclusion

The absence of a significant increase in pigmentation over time is likely related to the high initial optical density, which resulted in already strongly pigmented samples at the start of the experiment. This reduces the visual detectability of further biomass growth, even if biological activity is present. In future protocols, this growth can be assessed microscopically by quantifying the number of cells per unit surface area of the textile.

Although parafilm effectively maintained moisture levels, the slight drying observed after day 8 may have contributed to the gradual decline in quantum fluorescence yield. In addition, nutrient depletion within the closed system may have further limited metabolic activity. These results suggest that, under controlled laboratory conditions, rehydration may still be necessary, but less frequently than expected. Potentially on a weekly basis rather than at shorter intervals.

The relatively small differences in quantum fluorescence yield between samples indicate that the tested textile configurations provide comparable environments for *Scenedesmus* sp. viability. However, the overall decreasing trend suggests that long-term stability remains a challenge, likely influenced by the combined effects of drying and nutrient limitation. A longer experimental duration is required to confirm these observations and to further evaluate whether one material structure outperforms the other.

During CO_2 measurements, samples A1 and A2 were placed in a gas-tight container for a four-hour period at a constant light intensity, restricting normal gas exchange. This may have influenced metabolic activity and affected the measured quantum fluorescence yield. In addition, the removal of excess liquid after two days of immersion and prior to measurement likely resulted in biomass loss. Leading to differences in optical density between the textile (Group A) and suspension samples (Group I). As CO_2 uptake is directly related to biomass concentration, this introduces uncertainty in the comparison.

Despite these limitations, both CO_2 measurements indicate that the textile-based system exhibits slower CO_2 uptake compared to the conventional suspension culture. In the first measurement, both systems showed a rapid initial uptake followed by a quick stabilisation of CO_2 levels, consistent with the behaviour observed in protocol Cotton-Hydrogel Ratio (4.7).

In the second measurement, the slower CO_2 absorption may be partly attributed to a higher initial CO_2 concentration, which likely required more time for sequestration by the microalgae. Again, the textile system showed lower CO_2 uptake than the suspension culture. This is likely related to differences in biomass as well as reduced microalgal viability due to limited nutrient availability, as no additional growth medium was supplied in the four days between measurements.

When compared to Pichaya [47], who reported significantly higher CO_2 absorption rates in microalgae-textile biocomposites than in suspended cultures, the results of this study do not align. Instead, the textile system consistently showed slower CO_2 uptake than the suspension culture under the tested conditions. Compared to the CO_2 uptake reported by Oh et al. [56] for microalgae-hydrogel systems, which averaged 16.7 ppm per hour, the textile system in this study exhibited a substantially higher average CO_2 capture rate of 160 ppm per hour. However, this comparison should be interpreted with caution, as the optical density within the textile matrix was not determined and may have been higher than in the samples studied by Oh et al. [56], potentially contributing to the increased CO_2 uptake.

In conclusion, yarn type does not show a clear influence on biomass growth or attachment under the tested conditions, as both cotton and recycled denim exhibited comparable microalgal performance (SRQ1). The textile structure also did not result in a measurable improvement in biomass growth within the given timeframe, with all structures showing similar trends in pigmentation and metabolic activity (SRQ2). In terms of functional performance, CO_2 capture in the textile system was consistently lower than in suspension cultures, as indicated by slower uptake rates and delayed stabilisation (SRQ3). These findings suggest that, while the textile matrix can support microalgal activity, further optimisation of biomass retention, nutrient availability, and system conditions is required to enhance overall performance.

4.9 Summary of Key Findings

This chapter synthesises the main findings of all experimental protocols by explicitly addressing each research question in relation to microalgae-textile biocomposite performance, including attachment, viability, and CO_2 capture.

4.10.1 Textile Design: Material Composition and Weaving Structure

Answering RQ1 (How do textile architecture and material composition influence microalgal attachment and spatial distribution within the textile matrix?), the results show that both material composition and weaving structure play a significant role in microalgal attachment and distribution.

Cotton fibres promote strong microalgal attachment and more homogeneous biomass distribution due to their rough, fibrous surface, whereas PVA primarily contributes to moisture retention but shows weaker attachment. This reveals a trade-off between attachment and hydration: increasing cotton content enhances biomass growth and retention but increases susceptibility to drying, while higher PVA content improves moisture retention but limits effective immobilisation.

Within the tested configurations, a multilayer composition of 69.2% cotton and 30.8% PVA provided the most balanced performance. In addition, textile architecture influences spatial distribution, as increased structural complexity and surface area enhance biomass growth, provided sufficient moisture is maintained.

Further exploration of textile design showed that quantum fluorescence trends were comparable across samples with different weaving structures, indicating that multiple textile configurations can support similar short-term microalgal viability. However, long-term stability remains limited by factors such as drying and nutrient depletion.

4.10.2 Hydrogel Cross-linking

Addressing RQ2 (How do hydrogel cross-linking methods and preservation conditions affect structural integrity and the viability of *Scenedesmus* sp.?), the findings indicate that cross-linking methods strongly influence both material properties and biological performance.

Both freeze-thaw and freeze-drying methods successfully produce structurally stable cotton-hydrogel textile matrices. However, freeze-drying resulted in more distinct structural features without providing an improvement in microalgal immobilisation performance. Cross-linking methods also alter the material properties of the textile matrix: freeze-drying produces a more flexible, paper-like structure, whereas freeze-thawing results in a denser structure that becomes increasingly rigid upon drying.

Increasing the number of freeze-thaw cycles does not significantly enhance cross-linking strength beyond a threshold. Five freeze-thaw cycles were sufficient to achieve structural stability and resulted in the lowest cell detachment, indicating the most effective immobilisation under the tested conditions.

Hydrogel integration is essential for maintaining moisture retention within the textile system and significantly improves microalgae viability compared to non-hydrogel textiles.

Variability in cross-linking quality can negatively affect both structural homogeneity and immobilisation performance, indicating that consistent processing conditions are critical for reliable material behaviour.

4.10.3 Microalgae Viability

Addressing RQ3 (To what extent can the textile-hydrogel system support stable microalgal viability and long-term biomass retention?), the results show that the system supports initial viability and biomass establishment, but long-term stability remains highly condition-dependent.

Scenedesmus sp. viability is highly sensitive to processing conditions, particularly freezing and dehydration. Repeated freeze-thaw cycles significantly reduce metabolic activity and limit recovery capacity, indicating cellular stress.

Scenedesmus sp. can be immobilised both before and after cross-linking. However, when immobilised prior to cross-linking, the microalgae are exposed to the cellular stress caused by freezing and therefore show reduced viability. Post-cross-linking inoculation is preferred, as it better preserves microalgal viability by avoiding exposure to freezing stress during the immobilisation process.

Among the tested preservation conditions prior to inoculation, freezing at −80 °C provides the highest preservation of both viability and photosynthetic performance. In contrast, freeze-drying introduces greater stress and results in reduced recovery compared to freezing-thawing methods. The addition of a cryoprotectant further affects long-term viability negatively, likely due to cytotoxicity or metabolic stress effects.

Thaw duration shows only a limited influence on overall recovery, with shorter thawing periods providing temporary benefits but no sustained improvement. Across all conditions, recovery remains partial and delayed, indicating that microalgae require significant time to restore metabolic function after preservation.

Moisture availability is a critical factor for maintaining viability, as drying of the system leads to a rapid decline in metabolic activity. In addition, microalgal viability, growth, and CO_2 uptake are strongly dependent on environmental conditions, including light intensity, temperature, nutrient availability, and water content. Under suboptimal conditions, metabolic activity shifts from photosynthesis towards respiration and decay, limiting long-term stability.

4.10.4 Immobilisation

Addressing RQ1-RQ3, the results confirm that *Scenedesmus* sp. can be successfully immobilised within both cotton and cotton-hydrogel textile matrices, demonstrating the feasibility of microalgae cultivation within a textile-based matrix. It should be noted that attachment remains suboptimal, as approximately 60% of the microalgal cells detach under applied mechanical stress. Rotational incubation was found to enhance microalgal attachment by increasing contact between cells and the textile surface, leading to improved initial immobilisation.

Microalgae can be effectively immobilised after hydrogel cross-linking, thereby avoiding exposure to damaging freeze-thaw conditions. Although the timing of inoculation (before vs. after cross-linking) does not significantly affect immobilisation efficiency, post-cross-linking inoculation is preferred due to its positive effect on microalgal viability.

Excess moisture availability can shift microalgal growth from the textile matrix to the surrounding liquid, demonstrating that controlled hydration is essential for maintaining effective immobilisation within the material.

Despite successful attachment, the overall immobilisation strength remains limited. Material composition plays a key role, with cotton acting as the primary contributor to stable attachment, while PVA supports the system indirectly through improved moisture retention.

4.10.5 CO_2 Capture Performance

Finally, addressing RQ4 (How does the microalgae-textile biocomposite perform in terms of CO_2 uptake compared to conventional suspension cultures?), the results show that CO_2 uptake is directly linked to microalgal viability and biomass density within the textile matrix, with a higher biomass resulting in increased CO_2 uptake due to enhanced photosynthetic activity.

Measurements indicated an initial decrease in CO_2 concentration followed by stabilisation, suggesting the establishment of a dynamic equilibrium within the system. Among the valid samples, differences in uptake rate were observed, with the highest performance corresponding to samples with greater biomass presence.

Over time, CO_2 uptake decreased as drying reduced microalgal viability and metabolic activity. Under suboptimal conditions, systems may shift from net CO_2 uptake to CO_2 production, indicating loss of photosynthetic function and degradation of the material.

Reliable CO_2 assessment depends on stable environmental conditions and a consistent experimental setup, as measurement limitations and system variability can significantly influence data interpretation. In particular, CO_2 measurements are highly sensitive to environmental factors such as temperature, pressure, and humidity, which can affect measurement accuracy and data reliability.

Textile-based systems consistently exhibited slower CO_2 uptake rates compared to suspension cultures, indicating that microalgae viability and potentially lower effective biomass density constrain overall performance. This contrasts with the findings of Pichaya [47], who reported faster CO_2 absorption in microalgae-textile biocomposites than in suspended cultures, suggesting that the performance of the current system is not yet optimised. It is therefore likely that the biocomposite approach still has potential for improvement in matrix design, biological components, or environmental conditions.

This page is intentionally left blank

Chapter 5

Material Application

5.1 Material Benchmarking

To obtain a clearer understanding of the application potential of the microalgae-textile biocomposite, an overview of existing algal and textile-based applications was analysed (Table 26, 27).

Table 26: Material benchmarking

Category	Cultivation	Cultivation	Cultivation	Cultivation	Wastewater
Name	The Coral	AIReactor	Solar Bio-panel	Photo.Synth.Etica	The Indus project
Manufacturer	Hyunseok An	EcoLogicStudio	Greenfluidics	ecoLogicStudio and Climate KIC	Barlett School of Architecture
Picture material/origin		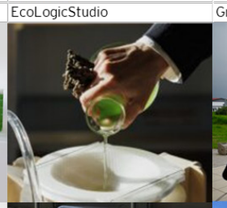	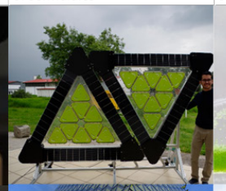		
Picture application	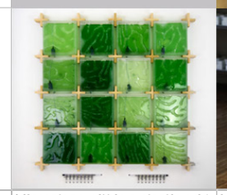		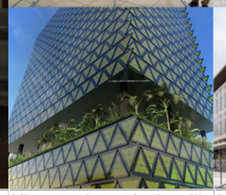		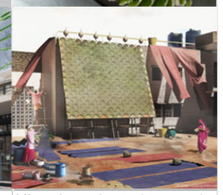
Composition	Microalgae within a plastic grid	Microalgae, in a wooden structure	Microalgae in combination with nanofluids	Microalgae	Microalgae, clay and seaweed-based hydrogel
Living/Non-living	Living	Living	Living	Living	Living
Discription	Wall-mounted Photobioreactor consisting of individual square culture cells, that can be used as a food source grown in your house	An indoor photobioreactor capable of absorbing carbon dioxide and pollutants while oxygenating the air	Integrating CO2 capturing, the production of oxygen, and the production of energy through the use of micro-algae	Curtain functioning as a photobioreactor. Unfiltered urban air enters the installation at the bottom and air bubbles rise. There, the bubbles come into contact with veracious microbes that capture CO2 molecules and air pollutants.	A tile-based, modular bioreactor wall system that cleans water through bioremediation. The project focuses on the rural community of artisans in India, enabling them to regenerate water for reuse within their manufacturing processes.
Application	Photobioreactor, Consumption	Photobioreactor, Air purifier	Photobioreactor panels integrated into architecture	Photobioreactor as a shading system on a building	Photobioreactor, wastewater cleaning tiling system
Goal	New food source, carbon capture	Carbon capture, air purifying	Carbon capture	Carbon capture	Carbon capture, manufacturing waterwater cleaning
Source	[64]	[70]	[65]	[66]	[67]

Category	Material	Material	Microalgae-textile	Macroalgae-textile	Microalgae-textile
Name	SEAmpathy	The Seaweed Archives	Plant and Algae T-shirt	AlgaeFabrics	Biogarmentry
Manufacturer	Daniel Elkayam	Studio Tang	Vollebak	Studio Tjeerd Veenhoven	Roya Aghighi
Picture material/origin		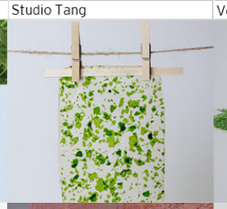			
Picture application				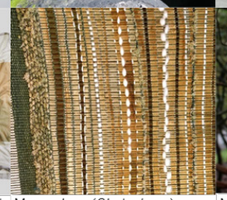	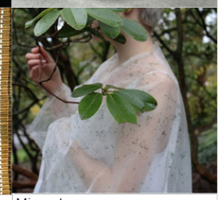
Composition	Macroalgae	Macroalgae and agar	Pulped eucalyptus, spruce, and beech wood and macro- and microalgae	Macroalgae (Cladophora)	Mircoalgae
Living/Non-living	Living	Non-living	Non-living	Non-living	Living
Discription	A shell for algae that on the one hand transforms it into a material for the formation of spheres of fibres, and on the other, allows gas exchange and the continuation of living material	Seaweed was used as a building element for architectural application	The dye of the t-shirt slowly fades over time. When you're finished with your T-shirt, you can put it in the compost or bury it in the ground, where it fully composts and biodegrades within 12 weeks.	The macoalgae had a high percentage of cellulose, and drying it can be spun into yarn. The macroalgae areot alive anymore	clothes made from algae that turn carbon dioxide into oxygen via photosynthesis, as a more sustainable alternative to fast fashion.
Application	Material	Building material	Textile, Textile Dye	Textiles	Textile
Goal	Create a living material that can perform photosynthesis	Estethics	Less textile waste and less harmful dye	Textile alternative	Perform photosynthesis and create a more sustainable alternative
Source	[68]	[69]	[71]	[72]	[58]

Table 27: Material benchmarking

Category	Dye	Dyes	Textile	Textile	Textile
Name	Living Shoes	Algadye	Knitted Façade	Hybrid adaptive sunshade	WaterSolve
Manufacturer	Jessica Ties	Tocco Earth	Studio Petra Vonk	Lanfranco et al.	WaterSolve
Picture material/origin			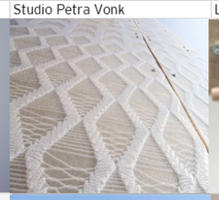		
Picture application		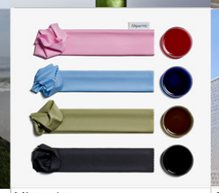		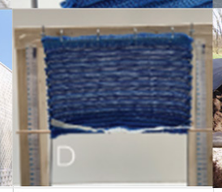	
Composition	Microalgae, hemp	Microalgae	Composite plate and textile	Textile, shape memory alloy	Textile
Living/Non-living	Living	Non-living	Non-living	Non-living	Non-living
Discription	Culturing microalgae cells on textiles for carbon-capturing, photosynthetic materials. Microalgae were added to printing ink, creating a living material	Reduce water usage by 98 and cut greenhouse gas (GHG) emissions by 70-74 compared to conventional dye and ink production	The goal of the façade was to create a unique look that also served as solar protection	Design of a two-component passive dynamic sunshade that combines Shape Memory Alloys (SMAs) and knitted textile	Large geotextile tubes, filled with sludge or agriculture wastewater, that separate solids from water
Application	Textiles Dye	Textiles Dye	Façade	Façade	Wastewater treatment textile filter system
Goal	Less harmful dye	Less harmful dye	Esthethics, solar protection	Adaptive façade	Wastewater treatment
Source	[73]	[77]	[74]	[75]	[76]

5.1.1 Microalgae-Textile Biocomposite as a Cultivation System

One of the primary outcomes of integrating microalgae within a cotton-hydrogel textile matrix is the creation of a viable growth environment. Compared to conventional cultivation systems, this approach presents several advantages. Open pond systems are prone to contamination, experience significant water loss through evaporation, and provide limited environmental control, while also requiring large surface areas, limiting scalability. In contrast, photobioreactors offer controlled conditions but are associated with high construction, operational, and energy costs [44].

The microalgae-textile biocomposite offers an alternative by combining a large effective surface area, provided by the woven structure, with a relatively compact spatial footprint. The textile allows horizontal or suspended placement, reducing land requirements. Although water loss remains a limitation, as observed in the Protocol Textile Cross-linking (4.1), the presence of cross-linked hydrogel likely reduces evaporation compared to open systems by retaining moisture within the matrix. Additionally, the system has the potential to operate under natural environmental conditions, reducing energy demand compared to closed photobioreactors.

If effective harvesting methods are developed, the microalgal biomass could be extracted and applied in downstream applications such as natural dyes, biofuels, or bioplastics (1.2).

5.1.2 Microalgae-based Garments and Accessories

Existing examples demonstrate that microalgae can be incorporated into wearable textiles (Table 26), such as in the Biogarmentry project [58]. However, maintaining microalgal viability in wearable applications remains challenging. The material is exposed to fluctuating environmental conditions, including light intensity, temperature, and pH, which can negatively affect growth.

In addition, the material requires controlled maintenance conditions, including sufficient light-dark cycles and regular nutrient supply. Washing and standard textile use conditions are incompatible with microalgal survival. Furthermore, the cotton-hydrogel matrix exhibits a moist and adhesive surface, limiting its suitability for direct contact applications such as clothing or accessories.

5.1.3 Microalgae-based Interior Application

Microalgae have been applied in interior systems, primarily in suspension-based photobioreactors such as The Coral and AIReactor (Table 26). Textile-based interior applications, such as divider screens, proposed by Mancini [49], are conceptually possible. However, practical limitations reduce feasibility.

The material requires a hydrated environment and is sensitive to handling, making it unsuitable for high-contact applications. Additionally, non-sterile indoor conditions increase the risk of contamination, including fungal growth. Likely resulting in health risks in an indoor environment. Limited and inconsistent light availability indoors further constrains microalgal performance unless artificial lighting is introduced and controlled.

5.1.4 Microalgae-based Exterior Application

Exterior applications show stronger potential. Existing systems demonstrate the integration of microalgae into building façades, where they function as photobioreactors (Table 26). A similar approach could be applied using textile-based systems.

The biocomposite could contribute to façade systems by combining CO_2 capture with additional functions, such as water filtration. Rainwater, which may contain pollutants such as PFAS and heavy metals [59], [60], could potentially serve as a nutrient source. Textile-based façade systems have already been explored, supporting the feasibility of such integration [74]. In addition, the material could be applied in green roof systems, providing both biological activity and surface coverage.

5.1.5 Microalgae in Agriculture

The microalgae-textile biocomposite may also have possible applications in agricultural systems. Textile-based filtration systems, such as WaterSolve (Table 27), demonstrate the potential of textiles in water treatment. A similar system incorporating microalgae could combine cultivation, CO_2 capture, and wastewater treatment.

Microalgae are capable of removing nutrients such as nitrogen and phosphorus, as well as other contaminants, from agricultural wastewater [21]. The material could also contribute to soil improvement and fertility. Additionally, when applied in soil, the biodegradable textile structure may assist in erosion control, eventually decomposing over time [21].

5.1.6 Microalgae Wastewater Treatment

Microalgae are known to play a role in wastewater treatment processes, particularly in secondary and tertiary treatment stages [61]. In these stages, microalgae can remove nutrients, heavy metals, and organic pollutants. Pollutants can bind to the surface of algal cells, enabling the material to function as a biofilter. Even non-living algal biomass can contribute to pollutant removal through biosorption processes [62].

However, several limitations exist. The effectiveness of pollutant removal depends on the specific microalgal species. Additionally, the hydrogel component primarily functions as an immobilisation medium and does not directly contribute to filtration performance. As observed in Protocol 9, immobilisation within the textile matrix remains insufficient to fully prevent cell loss. Long-term immersion in water also accelerates the degradation of the cotton fibres, limiting durability.

5.1.7 Conclusion

Based on the analysis of potential applications, exterior applications currently present the most suitable context for the microalgae-textile biocomposite. These environments provide more stable conditions for maintaining hydration, access to natural light, and reduced physical interaction, supporting both microalgal viability and functional performance.

5.2 Microalgae-Textile Material Application

During the material benchmarking, it became evident that exterior applications represent the most feasible and effective use for the microalgae-textile biocomposite. This is primarily because the microalgae can utilise natural sunlight, avoiding the need for energy-intensive artificial lighting as required in photobioreactors. Additionally, rainwater could serve both as a water supply and a source of nutrients for microalgal growth. However, periods of dryness would necessitate the implementation of a supplemental hydration system to maintain algal viability.

Several potential exterior applications can be envisioned, including use as a green roof, a sunshade screen, or a façade system that could simultaneously provide shading. Each option presents advantages and limitations:

Green roof: While the biocomposite could be placed on a roof surface, light would primarily penetrate from one side. This reduces the efficiency of the multilayer textile, as algal growth would be concentrated only on the sun-exposed side, consistent with observations by Oh et al. [56].

Sunshade screen: A hanging textile may be suboptimal, as gravity could cause microalgae to leak from the matrix. Encasing the textile between glass panels could mitigate this issue and reduce evaporation of the growth medium. However, this configuration may restrict CO_2 capture, which is the primary goal of the system.

Façade system: Suspending the biocomposite along the exterior of a building would maximise available surface area for light exposure, potentially increasing CO_2 capture compared to the other applications. Incorporating a rotational mechanism to track the sun could further enhance light utilisation while doubling as a dynamic shading system.

Overall, exterior façade applications appear most promising, as they combine high surface exposure, potential for enhanced CO_2 capture, and integration with architectural shading systems.

The building Echo on the Delft University of Technology campus was selected as a case study for applying the microalgae-textile biocomposite. This building was chosen because its existing overhanging roof provides an ideal opportunity to showcase the potential installation of biocomposite screens (Figure 69).

The screen would be mounted on a rotating axis, allowing it to orient towards the direction of incoming sunlight (Figure 70). If one side of the screen demonstrates reduced performance compared to the other, the panel can be rotated 180° to optimise light exposure and maintain more uniform microalgal activity.

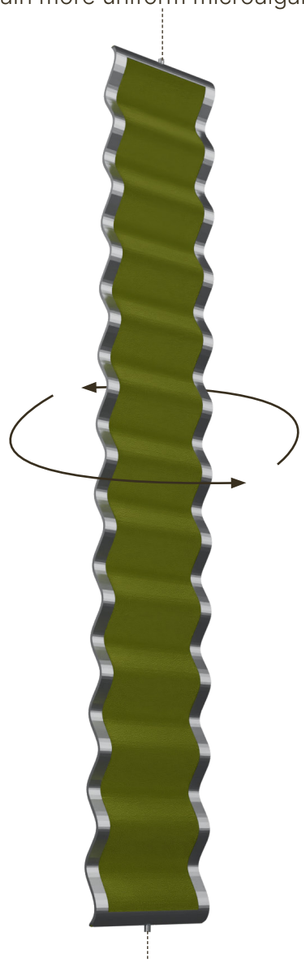

Figure 70: Microalgae-textile biocomposite façade sunshade screen, illustrating its rotational capability to follow the sun and provide favourable light conditions for the microalgae.

Maintaining adequate hydration is essential, as the microalgae will otherwise dry out rapidly. Therefore, the system should incorporate two types of sensors: one to detect the position of the sun and control the rotation of the screen, and a second to monitor the moisture content of the textile, enabling timely hydration to sustain microalgal viability. When the moisture content drops below a critical level, additional growth medium can be supplied at the top of the screen through a tubing system (Figure 71), allowing it to percolate through the textile under the influence of gravity.

Figure 69: Application of the microalgae-textile biocomposite as a façade sunshade screen, visualised on the façade of the Echo building on the campus of Delft University of Technology [78], [79].

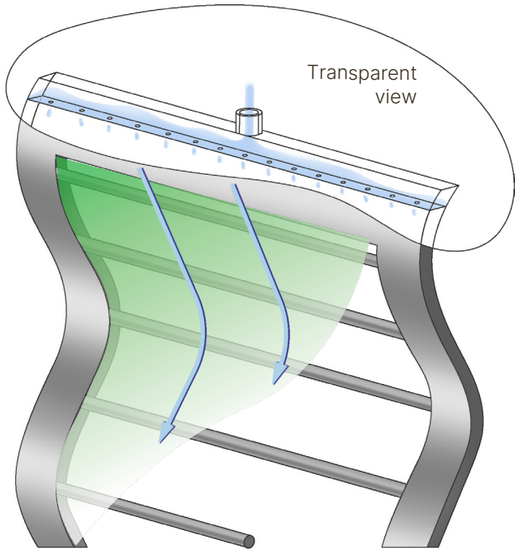

Figure 71: Moisture retention system allowing controlled dripping of growth medium through the textile to maintain hydration and support viability of the microalgae-textile biocomposite.

Due to gravitational forces, moisture within the textile matrix naturally flows downward, resulting in uneven hydration across the textile. To address this, the textile should be designed with a gradient in material composition. The upper section of the textile should contain a higher proportion of hydrogel to retain moisture and ensure sufficient hydration for microalgae located at the top. In contrast, the lower section should incorporate a higher percentage of cotton, as this material has been shown to provide stronger microalgal attachment (4.6), thereby reducing the risk of cells detaching and leaking into the surrounding environment.

Despite these design strategies, complete prevention of leakage is not feasible. Therefore, a drainage system should be integrated at the bottom of the textile to collect excess liquid and detached biomass, preventing uncontrolled release into the environment.

To maximise surface area and enhance light exposure, the textile should not be positioned as a flat plane, but rather shaped into a wave-like configuration. This increases the effective surface area available for microalgal growth while avoiding sharp angles that could limit light penetration. The desired shape can be achieved using a supporting steel frame with horizontal rods that guide and stabilise the textile (Figure 72).

The textile can be woven with integrated channels or openings, allowing it to be tensioned over these rods so that the structural frame remains embedded and visually concealed within the textile matrix (Figure 73).

The disadvantages of a large-scale application are discussed in the Chapter 6.

Figure 72: Stainless steel frame supporting the microalgae-textile biocomposite, secured by vertical rods. The integrated channels within the woven structure allow the textile to be tensioned across the rods.

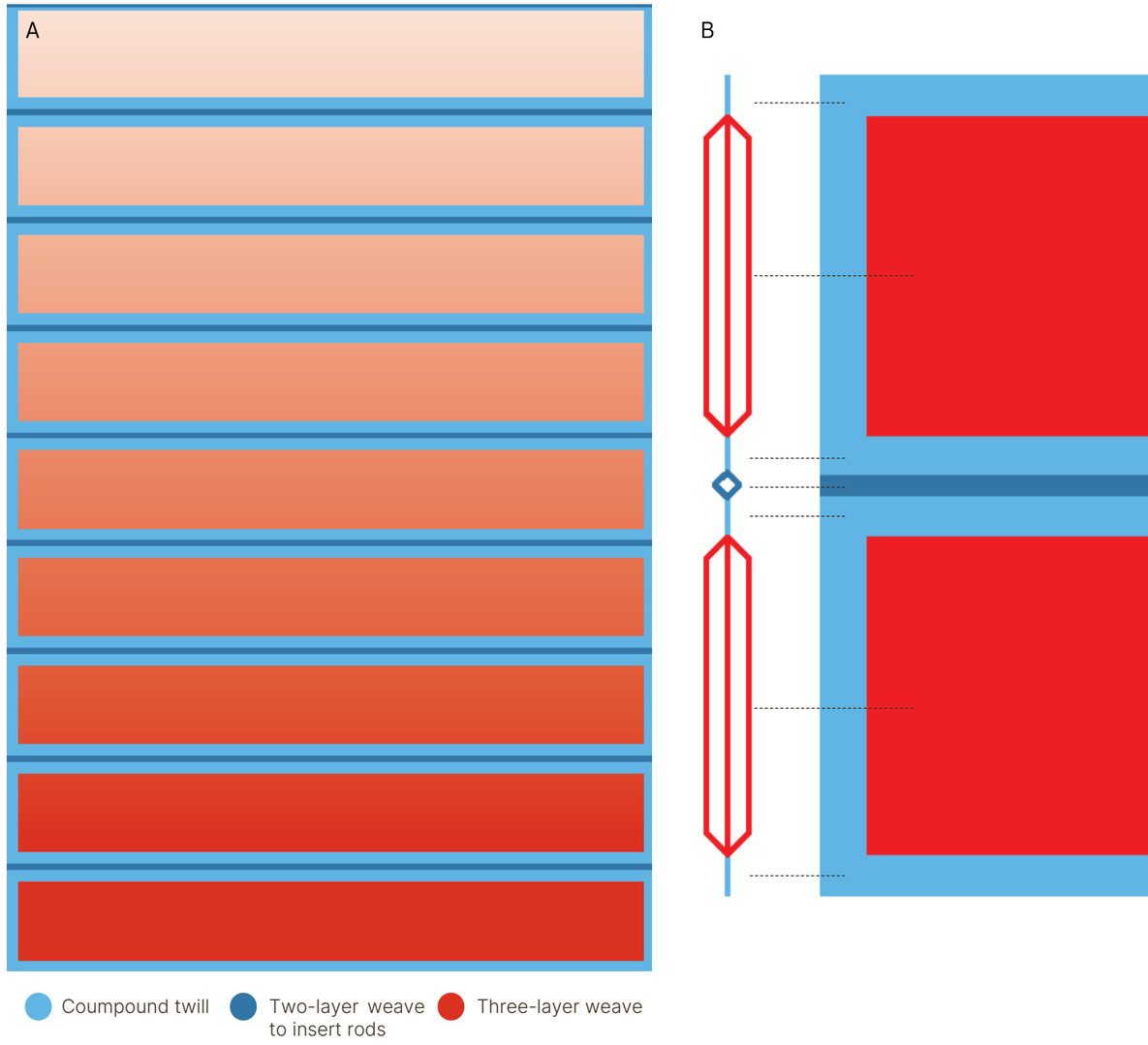

Figure 73: (A) Section of the weaving structure visualised with different colours representing the various weaving patterns. (B) Cross-section of the weaving structure, illustrating its multilayered structure.

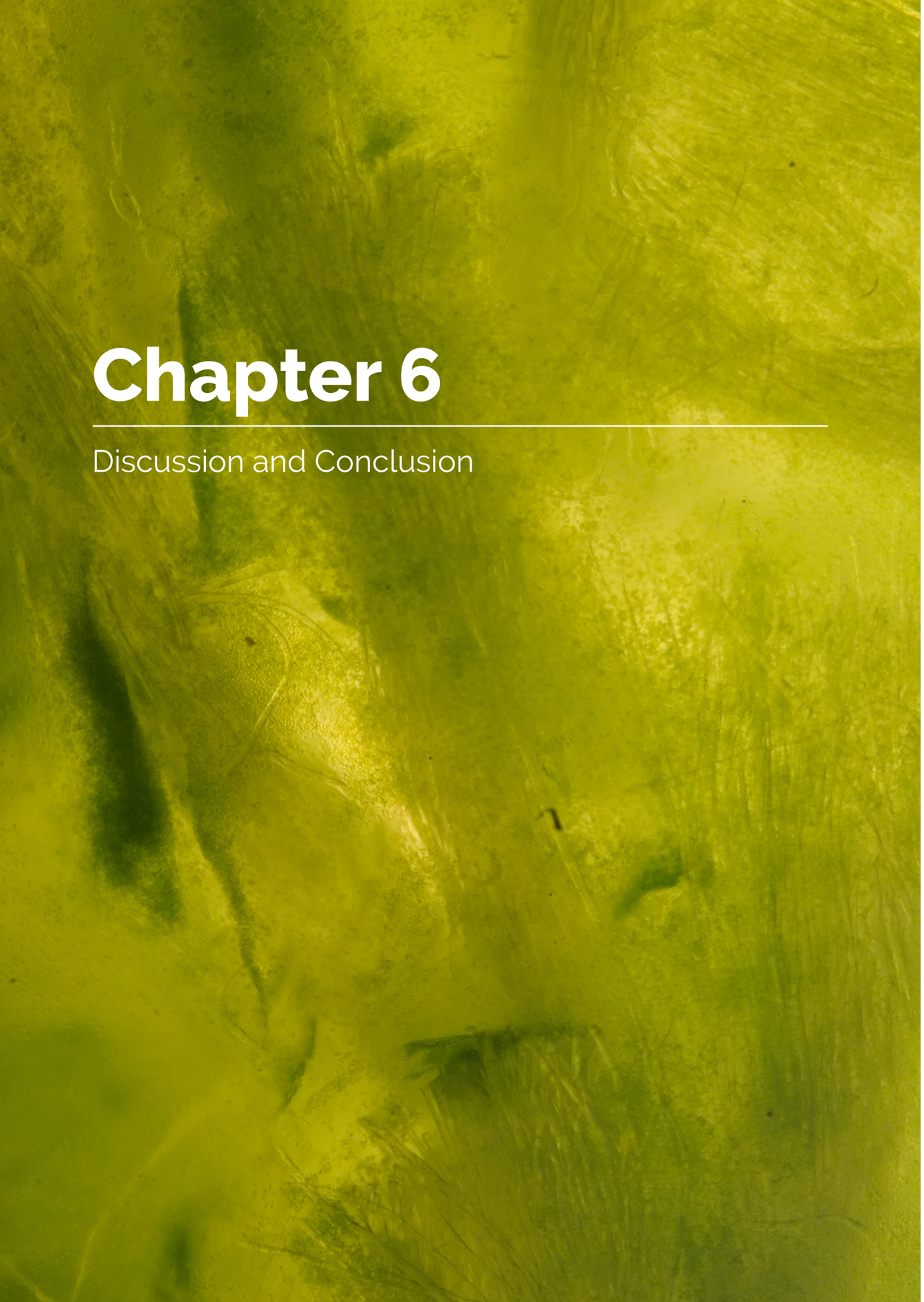

Chapter 6

Discussion and Conclusion

In this section, the findings of this study are interpreted in relation to the performance and behaviour of the textile-hydrogel-microalgae system. The complexities and opportunities emerging from the results are discussed, along with the broader implications for designing with living systems in biodesign. The limitations of the study are also critically addressed.

This research investigates a multilayer cotton-hydrogel textile matrix in which microalgae are integrated. In this system, material structure, hydrogel cross-linking, moisture availability, and biological viability are tightly interdependent. Rather than functioning as separate variables, these components collectively determine system behaviour. As a result, system performance emerges from the interaction between biological and material factors, rather than from any single parameter in isolation.

6.1 Thematic discussion

6.1.1 Weaving Structure and Material Composition

Within this interdependent system, the textile matrix itself forms the primary interface between the biological and material components of the biocomposite. The weaving structure and material composition define not only the physical environment in which the microalgae are embedded but also regulate key factors such as surface roughness, moisture distribution, and structural stability. As such, the textile does not act merely as a supporting material but as an active design parameter that directly influences microalgal attachment, spatial distribution, and overall system performance. The following section examines the role of weaving structure and material composition across different scales.

6.1.1.1 Design Scale

At the design level, woven textile matrices offer a high degree of flexibility and control. A wide range of material configurations can be achieved by altering fibre composition, yarn ratios, and weaving patterns, allowing the textile to be engineered to optimise microalgal viability. This distinguishes textile-based systems from naturally grown matrices, such as a loofah [48], where structure and material properties are naturally optimised for different purposes and therefore largely uncontrollable.

Furthermore, the integration of hydrogel within the textile enables additional optimisation through variation in cotton-hydrogel ratios throughout the textile, allowing simultaneous optimisation of attachment and moisture retention.

This design freedom presents significant opportunities but also introduces challenges. While it is possible to tailor the textile to specific biological and functional requirements, doing so requires specialised knowledge in textile design as well as an understanding of biological constraints. The interdependence between structure, material composition, and microalgal behaviour makes the design process complex and as such, optimising one variable may lead to negative effects. Additionally, designing for living systems requires anticipating dynamic changes over time, such as drying or biomass growth, which are not typically considered in conventional textile design.

6.1.1.2 Fabrication Scale

From a fabrication perspective, the use of relatively standard industrial jacquard weaving techniques enables the production of textile matrices at larger scales. This presents a clear advantage over approaches in which textiles are coated with hydrogel [47], which are often difficult to scale due to issues with uniformity, adhesion, and processing time. By integrating the hydrogel directly into the weaving structure, the material becomes inherently scalable and more compatible with existing textile manufacturing processes.

However, challenges remain in ensuring consistency and reproducibility during fabrication. Variations in weaving tension or material distribution may lead to uneven performance across samples. In addition, incorporating hydrogel into the textile structure introduces complexity in handling and processing, particularly sterilisation.

6.1.1.3 Application Scale

At the application level, textile-based microalgae systems offer several opportunities. The flexibility of textiles allows for a wide range of applications. This adaptability enables the material to be tailored to specific architectural contexts, including variation in material ratios across the textile to respond to environmental conditions or design requirements.

Moreover, implementing such systems at a building scale contributes to sensitisation, by making living materials visible and accessible to the public. Unlike conventional carbon capture systems, which are often located in remote or industrial settings, textile-based systems can be integrated into everyday environments [74]. This proximity may increase public awareness and acceptance of nature-based solutions for carbon capture. In addition, textile-based systems require less space and offer the potential for interactive integration into the built environment compared to conventional approaches such as open ponds or photobioreactors (PBRs) [44], enabling more efficient use of urban spaces. Unlike traditional systems, textile configurations can be incorporated into architectural elements such as façades, walls, or shading structures, where they can respond dynamically to environmental conditions (e.g., light, humidity, or airflow). This allows for real-time interaction with both the surrounding environment and users, for example through visible changes in biomass growth, colour, or system performance. Furthermore, such systems can be designed to integrate with building management strategies, contributing to functions such as shading or educational engagement.

Despite these advantages, several challenges must be addressed. The durability of the textile system under real-world conditions remains uncertain, as exposure to environmental factors such as temperature fluctuations, UV radiation, and moisture variation may accelerate material degradation and reduce system performance. Maintenance and repair also present challenges, particularly when microalgae are immobilised within the textile, making replacement or cleaning more complex at larger scales.

Overall, while woven textile matrices provide a highly adaptable and scalable platform for microalgae integration, successful real-world application depends on resolving challenges related to durability, maintenance, and long-term microalgae performance.

6.1.2 Hydrogel Cross-linking

Within the microalgae-textile biocomposite, hydrogel cross-linking regulates the internal structure and functional behaviour of the textile matrix. The cross-linking method defines the mechanical properties and water retention capacity of the hydrogel, thereby directly influencing moisture availability and the stability of the microalgal environment. The following section examines the role of hydrogel cross-linking across different scales.

6.1.2.1 Design Scale

At the design level, the integration of hydrogel into the textile matrix significantly enhances moisture retention, which is essential for sustaining microalgal viability over time. The hydrogel functions as a water reservoir within the structure, reducing rapid dehydration compared to non-hydrogel systems.

This creates opportunities to design living materials that maintain biological activity for longer periods.

6.1.2.2 Fabrication Scale

From a fabrication perspective, hydrogel cross-linking introduces significant complexity into the production process. The use of repeated freeze-thaw cycles results in long processing times and limits throughput. This makes rapid or large-scale production more challenging compared to conventional textile fabrication methods.

In addition, the fabrication workflow requires multiple stages, including soaking prior to cross-linking and controlled drying afterwards. These steps introduce practical challenges, such as handling fragile, water-saturated textiles and ensuring uniform cross-linking throughout the material. The drying phase in particular may require substantial space and controlled conditions, which can become a logistical constraint.

Another challenge lies in maintaining consistency across samples, as variations in freezing conditions, thawing duration, or moisture content can influence the final material properties and, consequently, system performance.

6.1.2.3 Application Scale

At the application level, several limitations emerge related to the behaviour of the hydrogel in open environments. Although the hydrogel improves moisture retention, it does not provide sufficient immobilisation strength, resulting in the potential leakage of microalgae from the textile matrix. Under real-world conditions, gravity and environmental exposure may further increase this effect, leading to the release of microalgae into the surrounding environment.

This raises both ecological and human-related concerns. Excessive release of microalgae could disrupt local ecosystems, while uncontrolled exposure in built environments may pose hygiene or safety considerations.

In addition, maintaining sufficient moisture levels becomes more challenging outside controlled laboratory conditions. In open environments, water evaporates more rapidly from the textile, reducing microalgal viability over time. Unlike experimental settings, where textiles can be fully submerged, rehydration in application contexts is limited to surface wetting or passive absorption, which may not sufficiently restore moisture levels. Therefore, the textile and its surrounding system need to be optimised to better retain and manage moisture. This could involve not only the use of hydrogels with improved water retention properties, but also the integration of system-level strategies such as controlled water distribution or enclosure strategies. By limiting direct exposure to air and sunlight, moisture can be retained within the textile for longer periods, supporting sustained microalgal viability.

Overall, while hydrogel cross-linking is essential for enabling moisture retention and structural stability, its integration introduces challenges related to fabrication complexity, limited immobilisation strength, and environmental performance. Addressing these challenges is critical for translating laboratory-scale systems into viable real-world applications.

6.1.3 Microalgae Viability

Microalgae viability is a critical factor regulating the performance and longevity of the microalgae-textile biocomposite. As a living system, its functionality depends on maintaining suitable environmental conditions that support viability, growth, and metabolic activity. Unlike purely material-driven systems, biological behaviour introduces variability and uncertainty, making viability a complex and multi-factorial challenge.

At the current stage, the research remains primarily laboratory-based, and it is therefore unclear how microalgae will respond to dynamic and less controlled real-world environments. While experimental conditions allow for stable temperature, light, and moisture levels, these parameters fluctuate significantly in application contexts. As a result, the long-term viability and performance of the system outside controlled settings remain uncertain.

Microalgal viability is influenced by a wide range of interacting factors, including light intensity, temperature, moisture availability, nutrient access, and gas exchange. Environmental conditions such as excessive heat or insufficient light may constrain photosynthesis, while rain can have both beneficial and disruptive effects, potentially rehydrating the system and supplying nutrients [59], [60], but also risking the physical washout of cells from the textile matrix. These overlapping influences make it difficult to predict system behaviour under variable outdoor conditions.

Moisture availability remains a critical limitation, as the system may require more frequent or intensive hydration than initially expected, potentially reducing its advantage compared to open ponds and photobioreactors (PBRs) [44]. Open ponds are low-cost and simple to operate but suffer from poor environmental control, high evaporation, and are particularly prone to biological contamination from bacteria, fungi, and competing algae species, which can reduce productivity. PBRs mitigate these issues through controlled conditions, but at the expense of higher energy use, cost, and infrastructure.

The biocomposite approach could offer intermediate benefits by reducing energy demand, cost, and spatial footprint relative to both systems. However, if it requires sustained or tightly managed moisture to maintain viability, these advantages may be limited. Like open ponds, it may also be vulnerable to contamination in real-world conditions, where colonisation by other microorganisms could impact microalgal viability and CO_2 capture performance, adding further uncertainty to long-term reliability.

A fundamental challenge lies in the nature of microalgae as living organisms. Their behaviour cannot be fully controlled or predicted in the same way as conventional materials. Biological constraints, adaptive responses, and potential viability loss must be considered as part of the design process.

Finally, the integration of living organisms into design systems necessitates interdisciplinary expertise. Ongoing monitoring and maintenance of microalgal viability require knowledge from fields such as microbiology and biotechnology. This highlights the importance of involving domain experts to ensure the system remains functional and effective over time.

Overall, while microalgae viability enables the core functionality of the biocomposite, it also introduces significant uncertainty related to environmental responsiveness, contamination, maintenance requirements, and biological limitations. Addressing these challenges is essential for transitioning from controlled experimental setups to robust, real-world applications.

6.1.4 CO2 capturing capacity

The CO_2 capturing capacity of the microalgae-textile biocomposite is a central performance indicator, yet current findings show significant variability and uncertainty. While the system demonstrates potential for carbon sequestration (4.9), the results are highly fluctuating, indicating that the design still requires further optimisation to achieve stable and predictable CO_2 uptake.

It was found that, in this configuration, the suspension culture exhibited a faster CO_2 uptake than the microalgae-textile biocomposite (4.9). Although both systems rely on microalgal photosynthetic activity, differences in biomass distribution, light exposure, and effective surface area likely influence overall performance. As such, direct comparison remains challenging, particularly given variations in measurement conditions and system configurations. This outcome also differs from the findings of Pichaya [47], who reported faster CO_2 absorption in microalgae-textile biocomposites compared to suspended cultures, suggesting that the present system is not yet optimised and may still have significant potential for improvement.

Experimental observations within this study suggest that CO_2 uptake can occur rapidly in small, controlled environments (4.7, 4.9), such as laboratory containers, where conditions are stable and optimised for photosynthetic activity. Based on these findings, it is assumed that, when scaled up, the system could potentially sequester a substantial amount of CO_2. However, this assumption remains unverified, as scaling introduces additional complexity in terms of light distribution and environmental variability.

A critical limitation is that CO_2 capture efficiency is highly sensitive to environmental and operational variables, including light intensity, moisture availability, nutrient supply, microalgal density, and overall environmental conditions (4.1-4.9). Under unfavourable or fluctuating conditions, the balance between photosynthesis and respiration may change, and microalgae can become net CO_2 producers. Complicating the assessment of the system's carbon-capturing capacity, particularly in outdoor settings where temperature, light, and moisture cannot be tightly controlled. These factors make system performance difficult to isolate and predict, and this challenge is further amplified at larger scales, where accurately quantifying CO_2 uptake becomes increasingly complex.

Another unresolved aspect is the end-of-life behaviour of the textile system. Over time, the biocomposite may become saturated with biomass, raising questions about how the captured carbon is managed or stored. It remains unclear whether the system functions as a long-term carbon sink.

Overall, while the microalgae-textile biocomposite shows promising CO_2 capture potential at small laboratory scales, its performance remains highly variable and context-dependent. Key uncertainties relate to scalability and environmental factors. Addressing these challenges is essential to validate the system's effectiveness as a reliable carbon capture capacity in real-world applications.

6.2 Limitations and Recommendations for Future Research

Although the study offers valuable insights, it was subject to several limitations that influenced both the experimental process and the interpretation of results. One of the main constraints was the CO_2 measuring setup, which proved unreliable measurements as the system broke down multiple times, resulting in missing data and limiting the completeness of the dataset. In addition, the availability of only two measurement setups restricted data validation. Therefore, future research should incorporate more CO_2 measurement setups specifically optimised for wet environments, as well as additional complementary CO_2 measurement techniques to validate and strengthen the reliability of the results. In addition, a more in-depth investigation into the differences in CO_2 capture performance between a microalgae-textile biocomposite and a suspension culture is recommended to better understand the advantages of a microalgae-textile biocomposite.

Material and fabrication constraints also affected the consistency and scalability of the work. The TC2 weaving machine, being shared and frequently repaired, introduced variability in yarn distribution and density across samples, which may have influenced material performance. Its limitation to cotton warp yarns further restricted the exploration of alternative material compositions that could potentially enhance microalgal attachment or moisture behaviour. In addition, the lack of larger lab equipment, such as larger *Petri* dishes, limited the ability to scale the textile system and evaluate more realistic application sizes. Therefore, future research should explore alternative material compositions, potentially by using a different jacquard loom capable of varying the warp yarns. Expanding the material scope would also be valuable, including the investigation of different textile structures, weaving patterns, hydrogels, and fibre types to improve both microalgal attachment and overall system performance. In addition, acquiring supplementary laboratory equipment would enable the production of samples on a larger scale.

Time was another significant limitation, as the study focused on identifying suitable combinations of variables to optimise microalgae viability. While this allowed for controlled short-term experimentation, it did not permit investigation of long-term viability or performance. Similarly, the study was initially restricted to *Scenedesmus* ***sp.***, meaning that the potential advantages of other microalgae species could not really be explored. Advanced tools such as SEM microscopy could have been used for a deeper analysis of the hydrogel structure and microalgae immobilisation. Future research should therefore build on these limitations and opportunities by extending the experimental timeframe to assess long-term microalgae viability and system performance. It should also expand beyond *Scenedesmus* ***sp.*** to evaluate a broader range of microalgae species, which may offer improved adaptation or CO_2 capture efficiency. In addition, access to advanced analytical tools such as SEM microscopy should be prioritised to enable more detailed investigation of hydrogel structure and immobilisation.

A key first step is to validate the viability of the microalgae-textile biocomposite system. This should be achieved by enhancing CO_2 capture performance such that uptake rates exceed those of conventional suspension cultures. Efficient immobilisation of microalgal cells within the textile matrix must be ensured, with minimal to no cell detachment observed. In addition, viability should be evaluated over extended operational periods. The material should also demonstrate effective moisture retention, thereby reducing the need for external moisture supplementation while sustaining microalgal metabolic activity.

Once these baseline performance criteria are established, the system should be upscaled to assess its behaviour under more realistic, larger-scale conditions. End-of-life pathways should also be investigated, including biomass harvesting and conversion into value-added products, to mitigate the risk of re-releasing captured carbon. Furthermore, the degradation behaviour of the textile matrix should be evaluated under relevant environmental factors, such as UV exposure, temperature fluctuations, and weather.

If system viability is confirmed, subsequent development should focus on interdisciplinary and application-driven challenges. Collaboration with textile designers, biologists, and biotechnologists will be essential to develop a coherent design framework and integrate domain-specific expertise. In addition, engagement with fabrication specialists is required to evaluate the manufacturability of the material system. This includes assessing multi-step fabrication processes such as sterilisation, cross-linking, and immobilisation.

6.3 Conclusion

Overall, this study shows that a multilayer cotton-hydrogel-microalgae biocomposite seems to have potential as a nature-based solution for CO_2 capture. However, the results are still highly variable and strongly influenced by biological, material, and environmental factors. Due to limitations in measurement accuracy and the lack of long-term observations, combined with the unpredictability of living systems, it is still not possible to draw definitive conclusions about its overall performance or real-world effectiveness. Further research is therefore essential before the true potential can be reliably determined.

Acknowledgement

I would like to express my sincere gratitude to my chair and mentors, Joana Martins and Holly McQuillan, for their invaluable guidance, support, and encouragement throughout the development of my graduation thesis. By sharing their expertise, they enabled me to gain deeper insights into biotechnology, engineered living materials, textiles, and their integration with industrial design. Our weekly meetings were consistently insightful and played an essential role in helping me set and achieve new goals.

I would also like to thank Yi Song, Tobias van Grinsven, and Joren Wierenga for their support during my lab work. Their advice on how to approach experiments and maintain a controlled working environment was extremely valuable, and they were always willing to assist whenever needed.

Finally, I am especially grateful to Martin Verwaal for his help in creating my CO_2 measuring setup. First, by assisting with the coding and later by assembling the hardware. Everyone mentioned above showed great understanding and kindness, helping me navigate through my thesis and guiding me to my graduation.

Furthermore, I am thankful to my family and friends for their constant motivation, encouragement, and support.

This page is intentionally left blank

References

[1] S. Pandey, I. Narayanan, R. Vinayagam, R. Selvaraj, T. Varadavenkatesan, and A. Pugazhendhi, 'A review on the effect of blue green 11 medium and its constituents on microalgal growth and lipid production', J. Environ. Chem. Eng., vol. 11, no. 3, p. 109984, Jun. 2023, doi: 10.1016/j.jece.2023.109984.

[2] 'Biopolymers'. Accessed: Feb. 19, 2026. [Online]. Available: https://www.sciencedirect.com/science/chapter/monograph/pii/B9780123821782000134

[3] G. Bell, 'Replicates and repeats', BMC Biol., vol. 14, p. 28, Apr. 2016, doi: 10.1186/s12915-016-0254-5.

[4] 'What is biotechnology?', Biotech Campus Delft. Accessed: Feb. 19, 2026. [Online]. Available: https://www.biotechcampusdelft.com/en/about-the-campus/biotechnology/

[5] 'What is carbon sequestration? | U.S. Geological Survey'. Accessed: Feb. 19, 2026. [Online]. Available: https://www.usgs.gov/faqs/what-carbon-sequestration

[6] 'Centrifugal/centripetal and coriolis accelerations | Science | Research Starters | EBSCO Research', EBSCO. Accessed: Feb. 19, 2026. [Online]. Available: https://www.ebsco.com

[7] 'Cryoprotectant - an overview | ScienceDirect Topics'. Accessed: Feb. 19, 2026. [Online]. Available: https://www.sciencedirect.com/topics/medicine-and-dentistry/cryoprotectant

[8] 'Chemical Crosslinking - an overview | ScienceDirect Topics'. Accessed: Feb. 19, 2026. [Online]. Available: https://www.sciencedirect.com/topics/engineering/chemical-crosslinking

[9] Y. Wang, Y. Liu, J. Li, Y. Chen, S. Liu, and C. Zhong, 'Engineered living materials (ELMs) design: From function allocation to dynamic behavior modulation', Curr. Opin. Chem. Biol., vol. 70, p. 102188, Oct. 2022, doi: 10.1016/j.cbpa.2022.102188.

[10] 'What is a Fluorescence Spectrometer?' Accessed: Mar. 04, 2026. [Online]. Available: https://www.edinst.com/resource/what-is-a-fluorescence-spectrometer/

[11] S. Group, 'Fluorescence quantum yield measurement | JASCO Global', JASCO Inc. Accessed: Mar. 04, 2026. [Online]. Available: https://www.jasco-global.com/solutions/fluorescence-quantum-yield-measurement/

[12] S. A. Bernal-Chávez et al., 'Enhancing chemical and physical stability of pharmaceuticals using freeze-thaw method: challenges and opportunities for process optimization through quality by design approach', J. Biol. Eng., vol. 17, p. 35, May 2023, doi: 10.1186/s13036-023-00353-9.

[13] M. D. Figueroa-Pizano et al., 'Effect of freeze-thawing conditions for preparation of chitosan-poly (vinyl alcohol) hydrogels and drug release studies', Carbohydr. Polym., vol. 195, pp. 476-485, Sep. 2018, doi: 10.1016/j.carbpol.2018.05.004.

[14] 'Freeze-thaw hydrogel fabrication method: basic principles, synthesis parameters, properties, and biomedical applications - IOPscience'. Accessed: Mar. 04, 2026. [Online]. Available: https://iopscience.iop.org/article/10.1088/2053-1591/acb98e

[15] D. Nowak and E. Jakubczyk, 'The Freeze-Drying of Foods—The Characteristic of the Process Course and the Effect of Its Parameters on the Physical Properties of Food Materials', Foods, vol. 9, no. 10, p. 1488, Oct. 2020, doi: 10.3390/foods9101488.

[16] D. Whaley, K. Damyar, R. P. Witek, A. Mendoza, M. Alexander, and J. R. Lakey, 'Cryopreservation: An Overview of Principles and Cell-Specific Considerations', Cell Transplant., vol. 30, p. 0963689721999617, Mar. 2021, doi: 10.1177/0963689721999617.

[17] O. US EPA, 'Overview of Greenhouse Gases'. Accessed: Mar. 05, 2026. [Online]. Available: https://www.epa.gov/ghgemissions/overview-greenhouse-gases

[18] Ambika and P. P. Singh, '11 - Natural polymer-based hydrogels for adsorption applications', in Natural Polymers-Based Green Adsorbents for Water Treatment, S. Kalia, Ed., Elsevier, 2021, pp. 267-306. doi: 10.1016/B978-0-12-820541-9.00008-9.

[19] 'Materials Degradation - an overview | ScienceDirect Topics'. Accessed: Mar. 05, 2026. [Online]. Available: https://www.sciencedirect.com/topics/materials-science/materials-degradation

[20] L. Barsanti and P. Gualtieri, 'Is exploitation of microalgae economically and energetically sustainable?', Algal Res., vol. 31, pp. 107-115, Apr. 2018, doi: 10.1016/j.algal.2018.02.001.

[21] A. Melnikova et al., 'AlgalTextile - a new biohybrid material for wastewater treatment', Biotechnol. Rep., vol. 33, p. e00698, Mar. 2022, doi: 10.1016/j.btre.2021.e00698.

[22] 'The Ultimate Guide to Nature-Based Carbon Removal (N-CDR)'. Accessed: Mar. 05, 2026. [Online]. Available: https://www.sirona.tech/guide/nature-based-carbon-removal

[23] 'Optical Density - an overview | ScienceDirect Topics'. Accessed: Mar. 05, 2026. [Online]. Available: https://www.sciencedirect.com/topics/engineering/optical-density

[24] 'Biogeochemistry of Terrestrial Net Primary Production', pp. 1-35, Jan. 2007, doi: 10.1016/B0-08-043751-6/08130-5.

[25] S. White, A. Anandraj, and F. Bux, 'PAM fluorometry as a tool to assess microalgal nutrient stress and monitor cellular neutral lipids', Bioresour. Technol., vol. 102, no. 2, pp. 1675-1682, Jan. 2011, doi: 10.1016/j.biortech.2010.09.097.

[26] M. Bercea, 'Recent Advances in Poly(vinyl alcohol)-Based Hydrogels', Polymers, vol. 16, no. 14, Jul. 2024, doi: 10.3390/polym16142021.

[27] '*Scenedesmus* - an overview | ScienceDirect Topics'. Accessed: Mar. 05, 2026. [Online]. Available: https://www.sciencedirect.com/topics/biochemistry-genetics-and-molecular-biology/*Scenedesmus*

[28] 'Climate change: atmospheric carbon dioxide | NOAA Climate.gov'. Accessed: Dec. 04, 2025. [Online]. Available: https://www.climate.gov/news-features/understanding-climate/climate-change-atmospheric-carbon-dioxide

[29] 'Climate change: global temperature | NOAA Climate.gov'. Accessed: Dec. 07, 2025. [Online]. Available: https://www.climate.gov/news-features/understanding-climate/climate-change-global-temperature

[30] O. US EPA, 'Overview of Greenhouse Gases'. Accessed: Dec. 08, 2025. [Online]. Available: https://www.epa.gov/ghgemissions/overview-greenhouse-gases

[31] K. Abbass, M. Z. Qasim, H. Song, M. Murshed, H. Mahmood, and I. Younis, 'A review of the global climate change impacts, adaptation, and sustainable mitigation measures', Environ. Sci. Pollut. Res., vol. 29, no. 28, pp. 42539-42559, Jun. 2022, doi: 10.1007/s11356-022-19718-6.

[32] U. Nations, 'Causes and Effects of Climate Change', United Nations. Accessed: Dec. 09, 2025. [Online]. Available: https://www.un.org/en/climatechange/science/causes-effects-climate-change

[33] 'Glossary:Carbon sink'. Accessed: Dec. 09, 2025. [Online]. Available: https://ec.europa.eu/eurostat/statistics-explained/index.php?title=Glossary:Carbon_sink

[34] European Commission. Joint Research Centre., GHG emissions of all world countries: 2025. LU: Publications Office, 2025. Accessed: Dec. 08, 2025. [Online]. Available: https://data.europa.eu/doi/10.2760/9816914

[35] Y. Chen, R. Wu, and P.-C. Hsu, 'Perspective on distributed direct air capture: what, why, and how?', Npj Mater. Sustain., vol. 3, no. 1, p. 12, May 2025, doi: 10.1038/s44296-025-00056-w.

[36] 'Carbon sequestration: we take a closer look at nature-based solutions | VINCI'. Accessed: Dec. 18, 2025. [Online]. Available: http://www.vinci.com/en/emag/carbon-sequestration-we-take-closer-look-nature-based-solutions

[37] S. Ruan, Y. Jiang, A. Wang, X. Zhang, Y. Lin, and S. Liang, 'Carbon sequestration pathways in microorganisms: Advances, strategies, and applications', Eng. Microbiol., vol. 5, no. 2, p. 100196, Jun. 2025, doi: 10.1016/j.engmic.2025.100196.

[38] ‘Biotechnology - an overview | ScienceDirect Topics’. Accessed: Mar. 11, 2026. [Online]. Available: https://www.sciencedirect.com/topics/agricultural-and-biological-sciences/biotechnology

[39] B. Academy, ‘What Is Biodesign?’, Biodesign Academy. Accessed: Mar. 11, 2026. [Online]. Available: https://www.biodesign.academy/p/what-is-biodesign

[40] Y. Wang, Y. Liu, J. Li, Y. Chen, S. Liu, and C. Zhong, ‘Engineered living materials (ELMs) design: From function allocation to dynamic behavior modulation’, Curr. Opin. Chem. Biol., vol. 70, p. 102188, Oct. 2022, doi: 10.1016/j.cbpa.2022.102188.

[41] E. S. J. Thoré, K. Muylaert, M. G. Bertram, and T. Brodin, ‘Microalgae’, Curr. Biol., vol. 33, no. 3, pp. R91-R95, Feb. 2023, doi: 10.1016/j.cub.2022.12.032.

[42] W. Ma, L.-N. Liu, Q. Wang, D. Duanmu, and B.-S. Qiu, ‘Editorial: Algal photosynthesis’, Front. Microbiol., vol. 13, p. 1112301, Jan. 2023, doi: 10.3389/fmicb.2022.1112301.

[43] M. M. Hoque et al., ‘Microalgae: Green Engines for Achieving Carbon Sequestration, Circular Economy, and Environmental Sustainability—A Review Based on Last Ten Years of Research’, Bioengineering, vol. 12, no. 9, p. 909, Sep. 2025, doi: 10.3390/bioengineering12090909.

[44] M. Egbo, A. Okoani, and I. Okoh, ‘Photobioreactors for microalgae cultivation-An Overview’, Dec. 2018.

[45] ‘Algae biorefinery: strategies for a sustainable industry’, in Algae Materials, Academic Press, 2023, pp. 399-433. doi: 10.1016/B978-0-443-18816-9.00020-4.

[46] O. Spain and C. Funk, ‘Detailed Characterization of the Cell Wall Structure and Composition of Nordic Green Microalgae’, J. Agric. Food Chem., vol. 70, no. 31, pp. 9711-9721, Aug. 2022, doi: 10.1021/acs.jafc.2c02783.

[47] P. In-na, J. Lee, and G. Caldwell, ‘Living textile biocomposites deliver enhanced carbon dioxide capture’, J. Ind. Text., vol. 51, no. 4_suppl, pp. 5683S-5707S, Jun. 2022, doi: 10.1177/15280837211025725.

[48] P. In-na, A. A. Umar, A. D. Wallace, M. C. Flickinger, G. S. Caldwell, and J. G. M. Lee, ‘Loofah-based microalgae and cyanobacteria biocomposites for intensifying carbon dioxide capture’, J. CO2 Util., vol. 42, p. 101348, Dec. 2020, doi: 10.1016/j.jcou.2020.101348.

[49] M. Mancini, ‘Living Textiles: Exploring Microalgae Growth on 3D Woven Structures in Design’, TU Delft, Mar. 2025, [Online]. Available: https://resolver.tudelft.nl/uuid:ca5cf3c0-c0c3-4143-ab4c-c4eb40b7b78f

[50] ‘Material Driven Design (MDD): A Method to Design for Material Experiences’, International Journal of Dsign. Accessed: Jan. 27, 2026. [Online]. Available: https://www.ijdesign.org/index.php/IJDesign/article/view/1965/693

[51] S. Dow et al., ‘Parallel Prototyping Leads to Better Design Results, More Divergence, and Increased Self-Efficacy’, Comput-Hum Interact Artic. ACM Trans. Comput.-Hum. Interact., vol. 17, Jul. 2011, doi: 10.1145/1879831.1879836.

[52] I. Koskinen, F. T. Binder, and J. Redström, ‘Lab, Field, Gallery, and Beyond’, Artifact, vol. 2, no. 1, pp. 46-57, Mar. 2008, doi: 10.1080/17493460802303333.

[53] M. Prieto-Guevara, J. Alarcón-Furnieles, C. Jiménez-Velásquez, Y. Hernández-Julio, J. Espinosa-Araujo, and V. Atencio-García, ‘Cryopreservation of the Microalgae *Scenedesmus* sp.’, Cells, vol. 12, no. 4, p. 562, Feb. 2023, doi: 10.3390/cells12040562.

[54] S. Sasaki, S. Miyauchi, and R. Takigawa, ‘Freeze-Dried PVA Hydrogels with Superior Mechanical Properties: A Rapid Alternative to Conventional Methods’, Langmuir ACS J. Surf. Colloids, vol. 41, no. 48, pp. 32569-32575, Dec. 2025, doi: 10.1021/acs.langmuir.5c04416.

[55] P. Ali, D. Fucich, A. A. Shah, F. Hasan, and F. Chen, ‘Cryopreservation of Cyanobacteria and Eukaryotic Microalgae Using Exopolysaccharide Extracted from a Glacier Bacterium’, Microorganisms, vol. 9, no. 2, p. 395, Feb. 2021, doi: 10.3390/microorganisms9020395.

[56] J. Oh et al., ‘Growth, Distribution, and Photosynthesis of Chlamydomonas Reinhardtii in 3D Hydrogels’, Adv. Mater., vol. 36, no. 2, p. 2305505, Jan. 2024, doi: 10.1002/adma.202305505.

[57] ‘How does an NDIR CO2 Sensor Work?’, CO2 Meter. Accessed: Feb. 03, 2026. [Online]. Available: https://www.co2meter.com/blogs/news/how-does-an-ndir-co2-sensor-work

[58] J. Sims, ‘The Future Of Fashion Is Here: Biogarments That Are ALIVE’. Accessed: Mar. 29, 2026. [Online]. Available: https://theethicalist.com/biogarments-luxury-clothes-alive/

[59] K. A. Coates and P. de B. Harrington, ‘Contamination levels of per- and polyfluoroalkyl substances (PFAS) in recent North American precipitation events. A review’, Water Res., vol. 266, p. 122390, Nov. 2024, doi: 10.1016/j.watres.2024.122390.

[60] Y. Deng, ‘Pollution in rainwater harvesting: A challenge for sustainability and resilience of urban agriculture’, J. Hazard. Mater. Lett., vol. 2, p. 100037, Nov. 2021, doi: 10.1016/j.hazl.2021.100037.

[61] ‘Wastewater Treatment | Essential Guide’. Accessed: Mar. 29, 2026. [Online]. Available: https://www.aquatechtrade.com/water-stories/wastewater/wastewater-essential-guide

[62] P. Kundu, N. Dutta, and S. Bhattacharya, ‘Application of microalgae in wastewater treatment with special reference to emerging contaminants: a step towards sustainability’, Front. Anal. Sci., vol. 4, Dec. 2024, doi: 10.3389/frans.2024.1513153.

[63] S. Farrukh, K. Mustafa, A. Hussain, and M. Ayoub, ‘Synthesis and Applications of Carbohydrate-Based Hydrogels’, 2018, pp. 1-24. doi: 10.1007/978-3-319-76573-0_49-1.

[64] ‘Grow your own algae in an indoor micro-algae farm’, MaterialDistrict. Accessed: Mar. 29, 2026. [Online]. Available: https://materialdistrict.com/article/indoor-micro-algae-farm/

[65] ‘Electricity-generating and CO2-absorbing bio-panels’, MaterialDistrict. Accessed: Mar. 29, 2026. [Online]. Available: https://materialdistrict.com/article/electricity-generating-and-co2-absorbing-bio-panels/

[66] ‘Bio-digital urban curtain captures CO2 from the air’, MaterialDistrict. Accessed: Mar. 29, 2026. [Online]. Available: https://materialdistrict.com/article/bio-digital-urban-curtain-co2/

[67] ‘Algae and hydrogel coated tiles to clean water’, MaterialDistrict. Accessed: Mar. 29, 2026. [Online]. Available: https://materialdistrict.com/article/algae-hydrogel-coated-tiles-clean-water/

[68] ‘Biophilic design with living and dead algae’, MaterialDistrict. Accessed: Mar. 29, 2026. [Online]. Available: https://materialdistrict.com/article/biophilic-design-living-dead-algae/

[69] ‘Algae by Studio Tång - Future Materials Bank’. Accessed: Mar. 29, 2026. [Online]. Available: https://www.futurematerialsbank.com/material/algae-5/

[70] ‘An air purifier powered by algae’, MaterialDistrict. Accessed: Mar. 29, 2026. [Online]. Available: https://materialdistrict.com/article/an-air-purifier-powered-by-algae/

[71] ‘Plant and algae T-shirt biodegrades within 12 weeks’, MaterialDistrict. Accessed: Mar. 29, 2026. [Online]. Available: https://materialdistrict.com/article/plant-algae-t-shirt-12-weeks/

[72] ‘Studio Tjeerd Veenhoven | Algae Fabrics’. Accessed: Mar. 29, 2026. [Online]. Available: https://www.tjeerdveenhoven.com/portfolio_page/algae-fabrics/

[73] ‘“Living” shoes made with microalgae ink’, MaterialDistrict. Accessed: Mar. 29, 2026. [Online]. Available: https://materialdistrict.com/article/living-shoes-made-with-microalgae-ink/

[74] ‘Intriguing use of materials and fascinating technology applications’, Studio Petra Vonk | Textile Design Studio. Accessed: Mar. 29, 2026. [Online]. Available: https://www.petravonk.nl/work/project-one-ephnc-nk2c4-7flb6

[75] V. Lanfranco, A. L. Navaro, and M. Popescu, ‘Design of a hybrid adaptive sunshade with a knitted textile and shape memory alloy’, Text. Intersect. Conf. Ser., Sep. 2023, [Online]. Available: https://dl.designresearchsociety.org/textileintersections/textileintersections2023/researchpapers/3

[76] ‘Agriculture’, WaterSolve Geotextile Bags Tubes & Dredging Company. Accessed: Mar. 29, 2026. [Online]. Available: https://www.gowatersolve.com/agriculture-water-treatment/

[77] R. Krebs, ‘From Algae to Fabric: The Development of Algaeing’s Microalgae Dyes’, Tocco Earth. Accessed: Mar. 29, 2026. [Online]. Available: https://tocco.earth/article/algaeing-microalgae-dyes

78] C. Harrouk, ‘UNStudio Designs a Multifunctional and Flexible Education Building for TU Delft in the Netherlands’, ArchDaily. Accessed: Apr. 30, 2026. [Online]. Available: https://www.archdaily.com/941954/unstudio-designs-a-multifunctional-and-flexible-education-building-for-tu-delft-in-the-netherlands

79] ‘Echo | UNS’ Energy-Positive and Circular Building at TU Delft’. Accessed: Apr. 30, 2026. [Online]. Available: https://www.unstudio.com/projects/echo/

AI use

Artificial intelligence (ChatGPT and Copilot) was used in this thesis as a supporting tool to improve the clarity and readability of the written findings. In particular, AI-assisted editing was applied to help structure and refine technical descriptions, ensuring that the results are communicated in a clear and understandable manner for the reader. However, it is important to emphasise that all experimental work, data collection, and data analysis were conducted independently by the author. The AI tool was not used to generate, modify, or interpret any experimental data, but solely to assist in improving the linguistic and structural presentation of the text.

This page is intentionally left blank

Appendixes

Appendix 1 | Standard protocols

1.1 Standard cultivation protocol

1.1.1 Materials

- *Scenedesmus* sp. or *Scenedesmus bacillaris*
- BG11 growth media, Gibco
- Incubator Memmert, 25 °C

1.1.2 Method

Part of the *Scenedesmus* sp. stock culture was transferred into an Erlenmeyer flask, with the flask size selected according to the required culture volume for each protocol. BG11 growth medium was subsequently added to reach the desired final volume. The Erlenmeyer flask was sealed with a sterile foam plug to maintain sterile conditions while allowing sufficient gas exchange for algal growth. Cultures were maintained either at room temperature or in a temperature-controlled incubator. In both conditions, a 16 h light / 8 h dark photoperiod was applied to support photosynthetic activity. Once per day, the flask was subjected to orbital shaking to ensure homogeneous distribution of *Scenedesmus* within the growth medium, as the microalgal cells tended to settle at the bottom.

1.2 UV-C Sterilisation

1.2.1 Material

- Philips UV-C Sterilisation Box

1.2.2 Method

To sterilise the textile samples, as well as the CO_2 measurement setup caps and the textile holder, all components are exposed to a single 20-minute cycle in a UV-C sterilisation box. The samples are placed on a hanging rack to ensure irradiation from all sides. Afterwards, the samples are taken out of the sterilisation box with a sterile forceps.

1.3 Plate reader

1.3.1 Materials

- Fluorescence Spectrometer, Agilent BioTek Synergy LX
- Well plate, 24 wells / 96 wells
- *Scenedesmus* sp. or *Scenedesmus bacillaris*

1.3.2 Method

Depending on the well plate format, the appropriate volume of culture was pipetted into each well as specified in Table 28. Prior to measuring the optical density, the plate was gently shaken to resuspend settled *Scenedesmus* cells and ensure a homogeneous suspension. Absorbance (optical density, OD) was subsequently measured according to the parameters listed in Table 29.

Table 28: Volumes well plate

Well plate	Volume (µL)
24	2000
96	200

Table 29: Procedure details Fluorescence Spectrometer

Shake	Double Orbital: 3:00 (MM:SS)
	Frequency: 282 cpm (3 mm)
Read	Absorbance Endpoint
	Full Plate
	Wavelengths: 430, 650
	Read Speed: Normal, Delay: 100 msec, Measurements/Data Point: 8

1.4 PAM

1.4.1 Materials

- Monitoring Pulse-Amplitude-Modulation (PAM), WALZ Junior-PAM chlorophyll fluorometer
- *Scenedesmus* sp. or *Scenedesmus bacillaris*

1.4.2 Method

Suspension *Scenedesmus* samples were transferred to cell culture flasks to ensure a flat and uniform contact surface between the microalgae and the PAM sensor. Textile samples were measured through the *Petri* dish. Prior to measurement, samples were dark-adapted for 3 minutes. Following dark adaptation, the fluorescence quantum yield was measured under dark conditions.

The PAM measurement settings are shown in Figure 74. Note that the gain was adjusted to '3' in protocol 10, because the measured quantum fluorescence yield was too high to be measured with gain '4'.

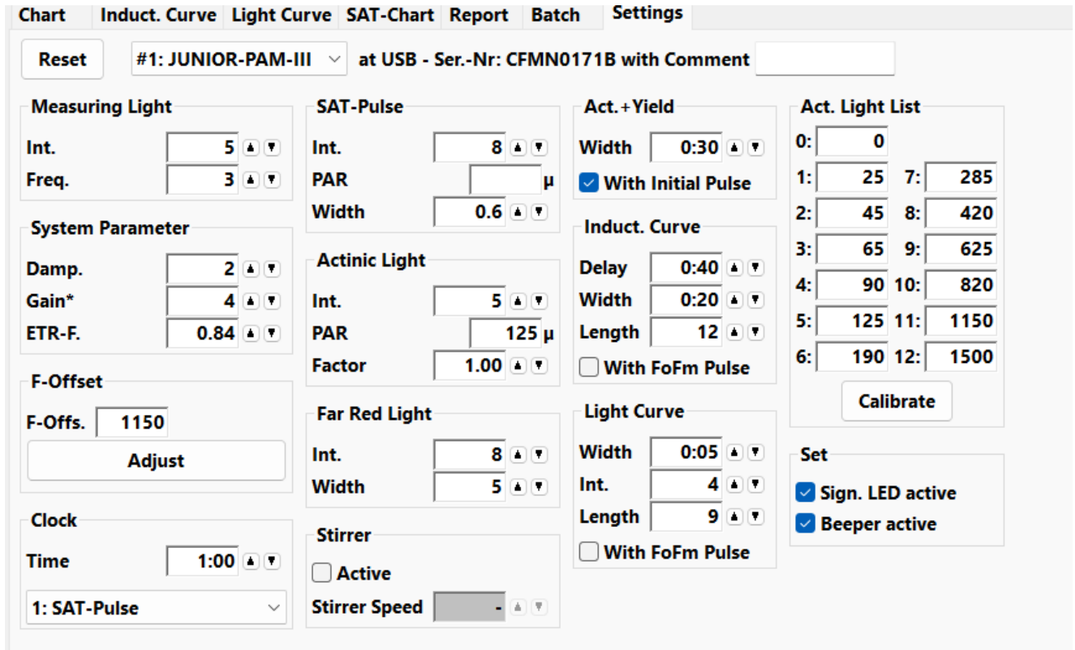

Figure 74: Settings PAM in WinContril-3

Appendix 2 | CO2 measurement setup

2.1 CO2 sensor comparison

Table 30: CO2 sensor comparison

Sensor	Type	CO□ Measurement Range	Accuracy	Output	Response Time	Notes	Suitability for Algae Setup
Sensirion SCD30	NDIR	400–10,000 ppm	±(30 ppm + 3% reading)	I²C, UART	2–10 s	Well-documented, widely used in labs	Excellent. High accuracy, good for small/medium ranges, compact, easy to integrate
SparkFun PASCO□V01	Photoacoustic Spectroscopy	0–32,000 ppm	±(30 ppm + 3% reading 400–5,000 ppm)	I²C, UART, PWM	~3 s	Very precise, slightly more expensive, needs 12V power	Excellent. High precision, ideal for research, compact, can be wireless
MH-Z19B	NDIR	0–5,000 ppm	±50 ppm	UART, PWM	~20 s	Low-cost, hobbyist sensor	Good for rough measurements, not very precise, slow response
SCD41	NDIR (Sensirion)	0–40,000 ppm	±(30 ppm + 3% reading 400–1,000 ppm)	I²C	~5 s	Compact, low power, includes temperature/humidity sensor	Very good. Accurate, small, low power, adds environmental data
MQ-135	Metal Oxide	0–10,000 ppm	±200–300 ppm (very rough)	Analog voltage	~60 s	Cheap, sensitive to many gases, needs calibration	Poor. Too inaccurate and slow for scientific algae measurements
Adafruit SGP3G	MOx / VOC sensor	400–10,000 ppm (indirect, via VOC correlation)	±30 ppm (CO□eq, estimated)	I²C	1–5 s	Not direct CO□ sensor, gives CO□ equivalent	Can track trends, but not reliable absolute CO□ measurement
ENS 160	Metal Oxide VOC/CO□eq	400–10,000 ppm (CO□eq)	±50 ppm (CO□eq, estimated)	I²C	5 s	Similar to SGP3G	Good for indoor air quality monitoring, not for precise algae CO□ uptake
MH-Z19C	NDIR	0–5,000 ppm	±50 ppm	UART, PWM	20 s	Low-cost, simple	Same as MH-Z19B, hobbyist-level accuracy

2.2 Circuit CO2 measuring setup

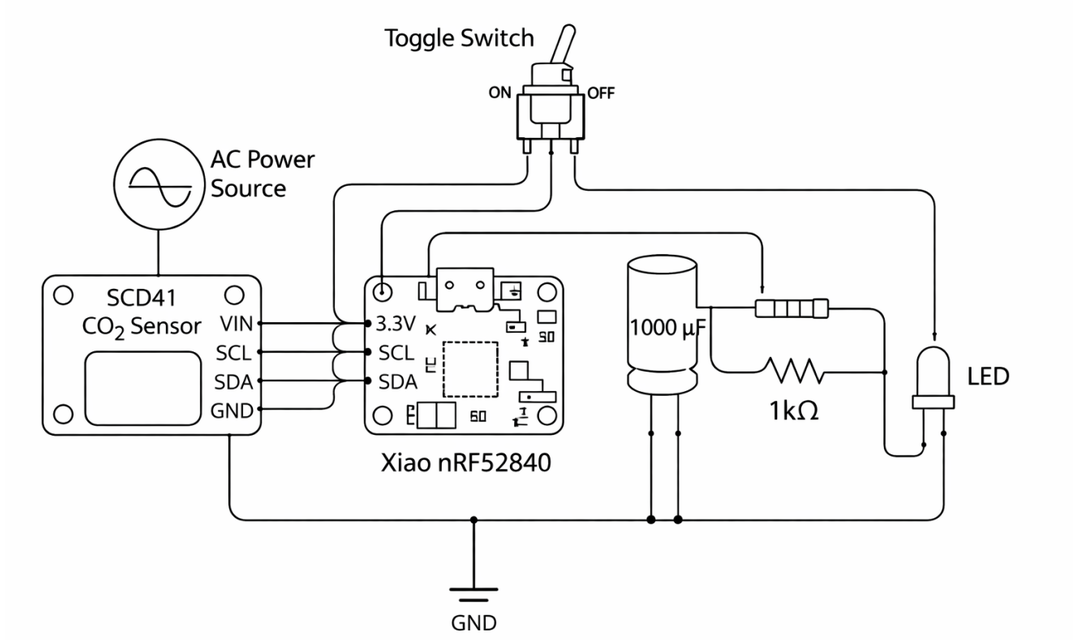

Figure 75: Circuit of the CO_2 measurement setup

2.3 Code CO2 measuring setup

```
import time
import board
import digitalio
import adafruit_scd4x
import setTime


# ------------------------------------------------
# CONFIG
# ------------------------------------------------
MEASURE_INTERVAL = 60
LED_BLINK_INTERVAL = 0.5
LOG_FILE = "/filename.csv"


CO2_OFFSET = -120  # ppm


# ------------------------------------------------
# LED (XIAO active-low)
# ------------------------------------------------
led = digitalio.DigitalInOut(board.LED_BLUE)
led.direction = digitalio.Direction.OUTPUT


def led_on(): led.value = False
def led_off(): led.value = True
def led_toggle(): led.value = not led.value


# ------------------------------------------------
# RTC
# ------------------------------------------------
setTime.set_rtc_time(2026, 5, 7, 0, 0, 0)


# ------------------------------------------------
# I2C + SENSOR
# ------------------------------------------------
i2c = board.I2C()
scd4x = None


# --- NEW: store initial temperature ---
initial_temp_K = None
```

```
def init_scd4x():
    global scd4x
    try:
        scd4x = adafruit_scd4x.SCD4X(i2c)

        scd4x.stop_periodic_measurement()
        time.sleep(1)

        scd4x.automatic_self_calibration = False

        scd4x.start_periodic_measurement()

        print("SCD4x initialized (ASC OFF)")
        return True

    except Exception as e:
        print("SCD4x init failed:", e)
        scd4x = None
        return False

init_scd4x()

# ------------------------------------------------
# SAFE SENSOR READ WITH TEMP CORRECTION
# ------------------------------------------------
def read_scd4x():
    global scd4x, initial_temp_K

    if scd4x is None:
        return None

    try:
        if not scd4x.data_ready:
            return None

        raw_co2 = scd4x.CO2 + CO2_OFFSET
        temp_C = scd4x.temperature
        hum = scd4x.relative_humidity

        # Convert to Kelvin
        temp_K = temp_C + 273.15

        # Store initial temperature once
        if initial_temp_K is None:
            initial_temp_K = temp_K
            print("Initial temperature stored:", temp_C, "°C")

        # Apply ideal gas correction
        corrected_co2 = raw_co2 * (initial_temp_K / temp_K)

        return (corrected_co2, temp_C, hum)

    except (OSError, RuntimeError) as e:
        print("I2C error:", e)
        try:
            scd4x.stop_periodic_measurement()
        except Exception:
            pass
        scd4x = None
        time.sleep(1)
        init_scd4x()
        return None

# ------------------------------------------------
# FILE
# ------------------------------------------------
try:
    with open(LOG_FILE, "x") as f:
        f.write("Timestamp,CO2(ppm),Temperature(C),Humidity(%)\n")
except OSError:
    pass

# ------------------------------------------------
# TIMING
# ------------------------------------------------
last_measure_time = time.monotonic()
last_led_toggle = time.monotonic()
sensor_started = False

co2_sum = 0.0
```

```
temp_sum = 0.0
hum_sum = 0.0
sample_count = 0

# ------------------------------------------------
# MAIN LOOP
# ------------------------------------------------
while True:
    now_mono = time.monotonic()
    now_rtc = time.localtime()

    sample = read_scd4x()
    if sample:
        co2, temp, hum = sample

        if not sensor_started:
            sensor_started = True
            led_on()
            last_led_toggle = now_mono
            print("Sensor active → LED blinking")

        co2_sum += co2
        temp_sum += temp
        hum_sum += hum
        sample_count += 1

    if sensor_started and (now_mono - last_led_toggle >= LED_BLINK_INTERVAL):
        led_toggle()
        last_led_toggle = now_mono
        if led.value:
            print(now_rtc.tm_sec, co2, temp, hum)

    if now_mono - last_measure_time >= MEASURE_INTERVAL:

        if sample_count > 0:

            avg_co2 = co2_sum / sample_count
            avg_temp = temp_sum / sample_count
            avg_hum = hum_sum / sample_count

            timestamp = "{:04d}-{:02d}-{:02d} {:02d}:{:02d}:{:02d}".format(
                now_rtc.tm_year, now_rtc.tm_mon, now_rtc.tm_mday,
                now_rtc.tm_hour, now_rtc.tm_min, now_rtc.tm_sec
            )

            print("------ AVERAGED SAMPLE ------")
            print("Time:", timestamp)
            print("Samples averaged:", sample_count)
            print(f"CO2 avg: {avg_co2:.1f} ppm")
            print(f"Temp avg: {avg_temp:.2f} °C")
            print(f"Hum avg : {avg_hum:.2f} %\n")

            with open(LOG_FILE, "a") as f:
              f.write(f"{timestamp},{avg_co2:.1f},{avg_temp:.2f},{avg_hum:.2f}\n")

            co2_sum = temp_sum = hum_sum = 0.0
            sample_count = 0

        last_measure_time = now_mono

    time.sleep(0.05)
```

Appendix 3 | Protocols Technical characterisation

3.1 Pilot 1 | Assessment of *Scenedesmus* sp. Viability in Plain Cotton Textiles after Freezing Conditions

3.1.1 Materials

- *Scenedesmus* sp.
- BG11
- Plain cotton textile samples
- Incubator Memmert, 25 °C

3.1.2 Method

Plain cotton textile samples (50 × 70 mm) were prepared from 100% cotton fabric and sterilised under UV-C light for 20 min per side.

Four experimental groups were established (Table 31). For groups A and D, 20 mL of *Scenedesmus* sp. culture (OD = 0.540, λ = 680 nm) was inoculated. For group B, *Scenedesmus* sp. cultures were centrifuged at 4000 rpm for 3 min at room temperature. The supernatant was removed, and approximately 5 mL of concentrated microalgal suspension was pipetted onto the surface of the textile samples. Group C received 20 mL of BG11 medium.

All samples were incubated under orbital shaking at 120 rpm for 3 days to promote microalgal attachment. Following incubation, excess liquid was removed from the textile samples.

Samples were subsequently frozen at −20 °C for 24 h and then thawed under standard incubation conditions (Appendix 1.1).

Microalgal immobilisation and growth were assessed over a 14-day period through visual documentation, with pigment intensity used as a proxy for microalgal viability and proliferation.

Table 31: Sample overview Pilot 1

Sample group	Description
A (n=2)	Single-layer textile immersed in *Scenedesmus* sp. suspension
B (n=2)	Centrifuged *Scenedesmus* sp. pipetted onto the single-layer textile surface
C (n=1)	Single-layer textile-only control group immersed in BG11 medium
D (n=2)	*Scenedesmus* sp. suspension culture control group

3.2 Pilot 2 | Assessment of *Scenedesmus* sp. Viability and CO_2 Monitoring in Multilayer Textile Matrices

3.2.1 Materials

- *Scenedesmus* sp.
- Multilayer woven textiles, consisting of outer layers of 60% cotton and 40% PVA in a plain weave, and an inner layer of 100% cotton, with compound twill edges (Appendix 4.1.1)
- BG11
- Incubator Memmert, temperature 25 °C
- CO2 measurement setup

3.2.2 Method

Multilayer woven textile samples (50 × 70 mm), composed of a cotton-hydrogel matrix (outer layers: 60% cotton, 40% PVA; inner layer: 100% cotton), were prepared and sterilised under UV-C light for 30 min per side. The textile structure was secured with a compound twill on two sides (Appendix 4.2, Figure 76).

Four experimental groups were established (Table 32)

For groups A and D, 20 mL of *Scenedesmus* sp. culture (OD = 0.050, λ = 680 nm) was inoculated. For group B, 20 mL of *Scenedesmus* sp. culture (OD = 0.050, λ = 680 nm) was pipetted between the textile layers to achieve localised inoculation. Group C received 20 mL of BG11 medium.

All samples were incubated under orbital shaking at 120 rpm for 3 days to promote microalgal attachment. Following incubation, excess liquid was removed, and the samples were incubated for an additional 3 days without surrounding liquid.

Subsequently, 15 mL of *Scenedesmus* sp. culture (OD = 0.102, λ = 680 nm) was added to groups A and B. Samples were incubated again under the same conditions, after which excess liquid was removed.

All samples were then frozen at −20 °C for approximately two months to induce hydrogel cross-linking. Following the freezing period, samples were thawed at room temperature and transferred to the CO_2 measurement setup. CO_2 concentration was monitored continuously over a period of 3 days.

Microalgal viability was assessed through visual documentation, with pigment intensity used as a proxy for growth and metabolic activity.

Table 32: Sample overview Pilot 2

Sample group	Description
A (n=2)	Multilayer textile immersed in *Scenedesmus* sp. suspension
B (n=2)	*Scenedesmus* sp. pipetted onto the multilayer textile surface
C (n=1)	Multilayer textile-only control group immersed in BG11 medium
D (n=2)	*Scenedesmus* sp. suspension culture control group

3.3 Pilot 3 | Assessment of *Scenedesmus* sp. Viability in Plain Cotton Textiles after Freezing Conditions

3.3.1 Material

- *Scenedesmus* sp.
- Multilayer woven textiles, consisting of outer layers of 60% cotton and 40% PVA in a plain weave, and an inner layer of 100% cotton, with compound twill edges (Appendix 4.1.1)
- BG11
- Incubator Memmert, temperature 25°C
- CO2 measurement setup

3.3.2 Method

Multilayer woven textile samples (360 × 40 mm), composed of a cotton-hydrogel matrix (outer layers: 60% cotton, 40% PVA; inner layer: 100% cotton), were prepared, and the textile samples were sterilised using a UV-C sterilisation box (Appendix 1.2)

Two experimental groups were established (Table 33).

For all samples, 200 mL of *Scenedesmus* sp. culture (OD = 0.660 at λ = 430 nm) was inoculated into a cell cultivation flask. Textile samples were fully immersed in the algal suspension to ensure homogeneous distribution of microalgal cells within the textile matrix.

All samples were incubated under orbital shaking at 125 rpm for 3 days to promote microalgal attachment and distribution. Following incubation, excess liquid was removed from the textile samples.

Samples were subsequently frozen at −20 °C for 24 h to induce hydrogel cross-linking. After freezing, samples were thawed at room temperature and transferred to the CO_2 measurement setup. CO_2 concentration was monitored continuously over a period of 3 days.

All samples were maintained under standard cultivation conditions during measurement (Appendix 1.1). Microalgal viability was assessed through visual documentation, with pigment intensity used as a proxy for growth and metabolic activity.

Table 33: Sample overview Pilot 3

Sample group	Description
A (n=2)	Multilayer textile immersed in *Scenedesmus* sp. suspension
B (n=2)	*Scenedesmus* sp. suspension culture control group

3.4 Textile Cross-linking | Effect of Freeze-Thaw and Freeze-Drying Techniques on Hydrogel Cross-linking in Multilayer Cotton-PVA Textiles

3.4.1 Materials

- Multilayer woven textiles, consisting of outer layers of 60% cotton and 40% PVA in a plain weave, and an inner layer of 100% cotton, with compound twill edges (Appendix 4.1.1)
- Freeze dryer, Buchi Lyovapor L-200
- Incubator Memmert, temperature 30 °C, 43.3%rh

3.4.2 Method

Multilayer woven textile samples (80 × 20 mm) composed of a cotton-hydrogel matrix (outer layers: 60% cotton, 40% PVA; inner layer: 100% cotton) were used to investigate hydrogel cross-linking via freeze-thaw and freeze-drying treatments. All samples were secured on all sides with a compound twill structure.

A total of 18 samples were prepared and divided into six experimental groups (Table 34). Samples A-E were subjected to one to five freeze-thaw cycles, respectively, while samples in group F were subjected to a single freeze-drying cycle.

Prior to cross-linking, samples were weighed and placed in Falcon tubes, followed by immersion in 50 mL demineralised water for 24 h to ensure full hydration. After hydration, excess water was removed by draining the samples.

Freeze-thaw cycles were performed at −20 °C, with each cycle consisting of 24 h of freezing followed by 24 h of thawing at room temperature. This procedure was repeated according to the number of cycles assigned to each group (A-E).

For freeze-drying (Group F), samples were first frozen at −80 °C for 24 h and subsequently freeze-dried at −60 °C under a pressure of 0.1 mbar for 93 h.

Following cross-linking, all samples were reweighed to assess mass changes. Structural properties were evaluated through tactile assessment and microscopic analysis (40× magnification) to examine surface morphology and potential degradation.

Samples were then incubated at 30 °C without caps to allow gradual drying. After drying, samples were rehydrated by immersion in 50 mL demineralised water for 24 h to evaluate water absorption capacity.

Subsequently, samples were incubated again at 30 °C, and their mass was recorded at 15-minute intervals to monitor water loss over time.

Table 34: Sample overview Protocol Textile Cross-linking

Sample group	Description
A (n=3)	1 Freeze-thaw cycle
B (n=3)	2 Freeze-thaw cycles
C (n=3)	3 Freeze-thaw cycles
D (n=3)	4 Freeze-thaw cycles
E (n=3)	5 Freeze-thaw cycles
F (n=3)	1 Freeze-drying cycle

3.5 Cryoprocessing *Scenedesmus* sp. 1 | Effect of Freeze-Thawing and Freeze-Drying with Cryoprotectant on *Scenedesmus* sp. Viability

3.5.1 Materials

- *Scenedesmus* sp.
- Glycerol
- Demineralise water
- BG11
- Filter 0.22 µm
- Monitoring Pulse-Amplitude-Modulation (PAM), WALZ Junior-PAM chlorophyll fluorometer
- Fluorescence Spectrometer, Agilent BioTek Synergy LX
- Freeze dryer, Buchi Lyovapor L-200

3.5.2 Method

Scenedesmus sp. cultures had an initial optical density of 0.333 (λ = 430 nm). 20 mL of *Scenedesmus* sp. culture was transferred into 50 mL Falcon tubes and centrifuged at 4000 rpm for 3 min at room temperature. The supernatant was removed, and cryoprotectant conditions were established by supplementing the cultures with either 10% (v/v) glycerol or 10% (v/v) demineralised water (control).

Samples were aliquoted into sterile containers and subjected to one of three preservation treatments:
(A-B) freezing at −20 °C for 120 h (n=3),
(C-D) freezing at −80 °C for 120 h (n=3),
(E-F) freezing at −80 °C for 24 h followed by freeze-drying at −60 °C (0.1 mbar) for 100 h (n=3) (Table 35).

Following preservation, frozen samples were thawed at room temperature. Freeze-dried samples were rehydrated with 25 mL BG11 medium, whereas frozen samples were supplemented with 5 mL BG11 medium to restore culture volume.

Samples were incubated under standard cultivation conditions (Appendix 1.1). Measurements were performed twice per week over a two-week period. Optical density (OD) was recorded to assess biomass growth, while pulse-amplitude modulation (PAM) fluorometry was used to evaluate photosynthetic activity (Appendix 1.4). Microscopic observations were conducted to assess cell morphology and distribution. In addition, visual documentation was recorded to monitor pigment intensity as an indicator of microalgal viability.

Table 35: Sample overview Protocol Cryoprocessing *Scenedesmus* sp. 1

Sample group	Preservation method	Additive
A (n=3)	*Scenedesmus* sp. frozen at -20°C	10% glycerol
B (n=3)	*Scenedesmus* sp. frozen at -20°C	10% demineralized water
C (n=3)	*Scenedesmus* sp. frozen at -80°C	10% glycerol
D (n=3)	*Scenedesmus* sp. frozen at -80°C	10% demineralized water
E (n=3)	Freeze-dried *Scenedesmus* sp.	10% glycerol
F (n=3)	Freeze-dried *Scenedesmus* sp.	10% demineralized water

3.6 Cryoprocessing *Scenedesmus* sp. 2 | Effect of Freezing-Thawing and Freeze-Drying on *Scenedesmus* sp. Viability

3.6.1 Materials

- *Scenedesmus* sp.
- Demineralise water
- BG11
- Filter 0.22 µm
- Monitoring Pulse-Amplitude-Modulation (PAM), WALZ Junior-PAM chlorophyll fluorometer
- Fluorescence Spectrometer, Agilent BioTek Synergy LX
- Freeze dryer, Buchi Lyovapor L-200

3.6.2 Method

10 mL of *Scenedesmus* sp. culture (OD = 0.413 at λ = 430 nm) was transferred into 50 mL Falcon tubes and centrifuged at 4000 rpm for 3 min at room temperature. The supernatant was removed, and the resulting algal pellets were resuspended in 10 mL BG11 medium supplemented with 10% (v/v) demineralised water.

Samples were divided into three experimental groups (Table 36):
(A) freezing at −20 °C for 120 h,
(B) freezing at −80 °C for 120 h,
(C) freezing at −80 °C for 24 h followed by freeze-drying at −60 °C (0.1 mbar) for 100 h.

Following preservation, frozen samples were thawed at room temperature for 24 h. Freeze-dried samples were rehydrated with 10 mL BG11 medium.

All samples were subsequently transferred to sterile cell culture flasks and maintained under standard cultivation conditions (Appendix 1.1) until analysis.

Microalgal viability and recovery were assessed over time using optical density measurements and pulse-amplitude modulation (PAM) fluorometry to evaluate biomass growth and photosynthetic activity (Appendix 1.4). Additional observations were conducted using light microscopy and visual assessment of pigment intensity. Measurements were performed approximately twice per week over the experimental period.

Table 36: Samples overview Protocol Cryoprocessing *Scenedesmus* sp. 2

Sample groups	Preservation method	Additive
A (n=3)	*Scenedesmus* sp. frozen at -20°C	10% demineralized water
B (n=3)	*Scenedesmus* sp. frozen at -80°C	10% demineralized water
C (n=3)	Freeze-dried *Scenedesmus* sp.	10% demineralized water

3.7 Thawing Duration | Effect of Thawing Duration Between Freeze-Thaw Cycles on *Scenedesmus* sp. Viability

3.7.1 Materials

- *Scenedesmus* sp.
- Multilayer woven textiles, consisting of outer layers of 60% cotton and 40% PVA in a plain weave, and an inner layer of 100% cotton, with compound twill edges (Appendix 4.1.1)
- Incubator Memmert, 25 °C

3.7.2 Method

Multilayer woven textile samples (80 × 20 mm) composed of outer layers (60% cotton, 40% PVA) and an inner layer (100% cotton), secured with a compound twill on all sides (Appendic 4.2, Figure XX), were used for all experiments. Prior to inoculation, the textile samples were sterilised using a UV-C sterilisation box (Appendix 1.2).

Each textile sample was fully immersed in 20 mL *Scenedesmus* sp. suspension culture (OD = 0.707 at λ = 430 nm).

Four experimental conditions were established to evaluate the effect of thaw duration and number of freeze-thaw cycles (Table 37).

Each freeze-thaw cycle consisted of freezing the samples at −80 °C for 24 hours, followed by thawing at room temperature for either 4 hours or 24 hours, depending on the assigned condition. This process was repeated for the specified number of cycles.

After completion of the freeze-thaw treatments, samples were placed in an incubator under standard cultivation conditions for a monitoring period of nine days.

Microalgal viability was assessed through daily visual documentation, with pigment intensity used as a qualitative indicator of growth and metabolic activity.

Table 37: Samples overview Protocol Thawing Duration

Sample group	Description
A (n=2)	Multilayer woven textile matrix immersed in *Scenedesmus* sp. suspension, subjected to 4 F-T cycles, 24 hours restoration in between F-T cyc les
B (n=2)	Multilayer woven textile matrix immersed in *Scenedesmus* sp. suspension, subjected to 4 F-T cycles, 4 hours restoration in between F-T cycles
C (n=2)	Multilayer woven textile matrix immersed in *Scenedesmus* sp. suspension, subjected to 5 F-T cycles, 24 hours restoration in between F-T cycles
D (n=2)	Multilayer woven textile matrix immersed in *Scenedesmus* sp. suspension, subjected to 5 F-T cycles, 4 hours restoration in between F-T cycles

3.8 Time of Inoculation | Effect of Pre- and Post-Cross-linking Inoculation on *Scenedesmus* sp. Attachment in a Cotton-Hydrogel Matrix

3.8.1 Materials

- *Scenedesmus* sp.
- Multilayer woven textiles, consisting of outer layers of 60% cotton and 40% PVA in a plain weave, and an inner layer of 100% cotton, with compound twill edges (Appendix 3)
- Incubator Memmert, 25 °C
- Vortex Genie 2, Scientific Industries
- Monitoring Pulse-Amplitude-Modulation (PAM), WALZ Junior-PAM chlorophyll fluorometer
- Fluorescence Spectrometer, Agilent BioTek Synergy LX
- Freeze dryer, Buchi Lyovapor L-200

3.8.2 Method

Multilayer woven textile samples (40 × 45 mm), consisting of a multilayer structure, secured with a compound twill on all sides, were used in this experiment (Appendix 4.2, Figure 82 D). Prior to inoculation, the textile samples were sterilised using a UV-C sterilisation box (Appendix 1.2).

Each textile sample was fully immersed in 20 mL *Scenedesmus* sp. suspension culture (OD = 0.873 at λ = 430 nm).

Seven experimental groups were prepared following two methodologies (Figure 42).

Freeze-thaw cross-linking (A-F) was performed at −80 °C. Each cycle consisted of freezing the samples for 24 hours, followed by thawing at room temperature for 24 hours. The number of cycles varied per group (Table 38). For freeze-drying (G), samples were first frozen at −80 °C for 24 h and subsequently freeze-dried at −60 °C under a pressure of 0.1 mbar for 24 h.

After cross-linking and/or inoculation, samples were incubated under standard cultivation conditions to allow microalgal attachment (Appendix 1.1).

To assess immobilisation, each sample was placed in a Falcon tube containing 40 mL demineralised water and vortexed (200 rpm, 2 minutes). The optical density of the surrounding liquid was then measured (λ = 430 nm) (Appendix 1.3) and compared to the initial optical density of the inoculated culture to quantify the amount of detached microalgal cells.

Table 38: Samples overview Protocol Time of Inoculation

Sample group	Description
A (n=2)	Multilayer woven textile matrix immersed in *Scenedesmus* sp., subsequently subjected to 3 F-T cycles
B (n=2)	Multilayer woven textile matrix immersed in *Scenedesmus* sp., subsequently subjected to 4 F-T cycles
C (n=2)	Multilayer woven textile matrix immersed in *Scenedesmus* sp., subsequently subjected to 5 F-T cycles
D (n=2)	Multilayer woven textile matrix subjected to 3 F-T cycles, subsequently immersed in *Scenedesmus* sp.
E (n=2)	Multilayer woven textile matrix subjected to 4 F-T cycles, subsequently immersed in *Scenedesmus* sp.
F (n=2)	Multilayer woven textile matrix subjected to 5 F-T cycles, subsequently immersed in *Scenedesmus* sp.
G (n=2)	Multilayer woven textile matrix subjected to 1 F-D cycle, subsequently immersed in *Scenedesmus* sp.

3.9 Yarn Attachment | Attachment of *Scenedesmus* sp. to Cotton and PVA Yarn Structures

3.9.1 Materials

- Cotton yarn
- PVA yarn, Solvron SF.330 (Dissolvable 55c+ Yarn) 330×3 d tex - Count: 1/10 Nm
- *Scenedesmus* sp.

3.9.2 Method

Cotton and PVA yarns were prepared to investigate microalgal attachment and growth in different material and structural configurations. Two bundling configurations were applied: tightly bundled yarns and circularly arranged bundles.

Four samples were prepared (Table 39).

Yarns were manually assembled according to the assigned configuration and placed in sterile *Petri* dishes. *Scenedesmus* sp. culture in BG11 medium was added until all yarn samples were fully immersed.

Samples were incubated under orbital shaking at 120 rpm for 3 days to promote microalgal attachment and growth. Following incubation, samples A and C were gently rinsed with demineralised water to assess the stability of microalgal attachment, while samples B and D remained untreated.

All samples were maintained under standard cultivation conditions (Appendix 1.1) and monitored over a period of 16 days. Microalgal presence, attachment, and viability were assessed through visual documentation, with pigment intensity used as a proxy for growth and retention on the yarn surfaces.

Table 39: Samples overview Protocol Yarn Attachment

Sample group	Description
A (n=1)	Cotton yarn in a tight bundle, washed with water
B (n=1)	Cotton yarn in a circular bundle, not washed
C (n=1)	PVA yarn in a tight bundle, washed with water
D (n=1)	PVA yarn in a circular bundle, not washed

3.10 Cotton-Hydrogel Ratio | Effect of Different Ratios of Cotton-Hydrogel on the Viability and CO_2 Fixation of *Scenedesmus* sp. in a Multilayer Textile Matrix

3.10.1 Materials

- *Scenedesmus* sp.
- Multilayer woven textiles, consisting of outer layers of 60% cotton and 40% PVA in a plain weave, and an inner layer of 100% cotton, with compound twill edges (Appendix 4.1.1)
- Multilayer woven textiles, consisting of outer layers of 69.2% cotton and 30.8% PVA in a plain weave, and an inner layer of 100% cotton, with compound twill edges (Appendix 4.1.2)
- Multilayer woven textiles, consisting of outer layers of 84.6% cotton and 15.4% PVA in a plain weave, and an inner layer of 100% cotton, with compound twill edges (Appendix 4.1.3)
- Multilayer woven textiles, consisting of outer layers of 53.8% cotton and 46.2% PVA in a plain weave, and an inner layer of 100% cotton, with compound twill edges (Appendix 4.1.4)
- Incubator Memmert, 25 °C
- Monitoring Pulse-Amplitude-Modulation (PAM), WALZ Junior-PAM chlorophyll fluorometer
- Fluorescence Spectrometer, Agilent BioTek Synergy LX
- CO_2 measurement setup

3.10.2 Method

Four cotton-PVA textile compositions were prepared: 60% cotton / 40% PVA, 69.2% cotton / 30.8% PVA, 84.6% cotton / 15.4% PVA, and 53.8% cotton / 46.2% PVA. Prior to inoculation, the textile samples were sterilised using a UV-C sterilisation box (Appendix 1.2).

Textile samples (40 × 45 mm) were first cross-linked using five freeze-thaw cycles at −80 °C. After cross-linking, each textile was immersed in *Scenedesmus* sp. culture until fully saturated (OD = 0.656 at λ = 430 nm). Samples were incubated on a rotational platform for two days at 100 rpm to promote uniform algal distribution.

Four experimental groups were prepared (Table 40).

Over a two-week period, microalgal growth and viability were monitored via visual documentation of pigment intensity. Photosynthetic activity was further evaluated using CO_2 measurements and pulse-amplitude modulation (PAM) fluorometry (Appendix 1.4). Additional observations were conducted using light microscopy to examine the density and distribution of *Scenedesmus* sp. within the textile matrix. Measurements were performed up to three times per week over the experimental period.

Table 40: Samples overview Protocol Cotton-Hydrogel Ratio

Sample group	Description
A (n=4)	Multilayer textile containing 60% cotton, 40% PVA, subjected to 5 F-T cycles, immobilised in *Scenedesmus* sp.
B (n=4)	Multilayer textile containing 69.2% cotton, 30.8% PVA, subjected to 5 F-T cycles, immobilised in *Scenedesmus* sp.
C (n=4)	Multilayer textile containing 84.6% cotton, 15.4% PVA, subjected to 5 F-T cycles, immobilised in *Scenedesmus* sp.
D (n=4)	Multilayer textile containing 53.8% cotton, 46.2% PVA, subjected to 5 F-T cycles, immobilised in *Scenedesmus* sp.

3.11 Optimised System Integration | Evaluation of an Optimised Cotton-Hydrogel Matrix Following Freeze-Thaw Cross-linking and Post-Inoculation with Scenedesmus sp. and Scenedesmus bacillaris

3.11.1 Materials

- *Scenedesmus* sp.
- *Scenedesmus bacillaris*
- Multilayer woven textiles, consisting of outer layers of 69.2% cotton and 30.8% PVA in a plain weave, and an inner layer of 100% cotton, with compound twill edges (Appendix 4.1.2)
- Incubator Memmert, 25 °C
- Monitoring Pulse-Amplitude-Modulation (PAM), WALZ Junior-PAM chlorophyll fluorometer
- Fluorescence Spectrometer, Agilent BioTek Synergy LX
- CO_2 measurement setup

3.11.2 Method

Multilayer woven textile samples (69.2% cotton / 30.8% PVA) were prepared and sterilised under UV-C light according to Appendix 1.2.

Textile samples (180 × 50 mm) were first cross-linked using five freeze-thaw cycles at −80 °C. After cross-linking, each textile was immersed in either 20 mL *Scenedesmus* sp. or *Scenedesmus bacillaris* cultures (OD = ~0.400 at λ = 430 nm) and incubated on a rotational platform at 100 rpm for two days to promote uniform cell distribution and attachment.

Four experimental groups were prepared, each consisting of five biological replicates (Table XX).

Over a 1.5-week period, samples were monitored via visual documentation of pigment intensity to assess microalgal growth and viability. Photosynthetic activity was additionally assessed using CO_2 measurements and pulse-amplitude modulation (PAM) fluorometry (Appendix 1.4). Light microscopy was used to examine microalgal density and distribution within the textile matrix. Measurements were conducted up to three times a week throughout the experimental period.

Table 41: Samples overview Protocol Optimised System Integration

Sample group	Description
A (n=5)	Multilayer textile containing 60% cotton, 40% PVA, subjected to 5 F-T cycles, subsequently inoculated with *Scenedesmus* sp.
B (n=4)	*Scenedesmus* sp. suspension culture
C (n=5)	Multilayer textile containing 60% cotton, 40% PVA, subjected to 5 F-T cycles, subsequently inoculated with *Scenedesmus bacillaris*
D (n=4)	*Scenedesmus bacillaris* suspension culture

3.12 Weaving Structure Variations | Effect of Weaving Architecture and Material Composition on Microalgal Viability and CO_2 Fixation

3.12.1 Materials

- *Scenedesmus* sp.
- Three-layer woven textiles, consisting of outer layers of 69.2% cotton and 30.8% PVA in a plain weave, and an inner layer of 100% cotton, with compound twill edges (Appendix 4.1.2)
- Two-layer textile matrix, containing cotton and PVA, with compound twill edges (Appendix 4.1.5)
- Six-layer textile matrix, containing cotton and PVA, with compound twill edges (Appendix 4.1.6)
- Waffle weave textile matrix, containing cotton and PVA, with compound twill edges (Appendix 4.1.7)
- Three-layer woven textiles, containing recycled denim, cotton and PVA, with compound twill edges (Appendix 4.1.2)
- Two-layer textile matrix, containing recycled denim, cotton and PVA, with compound twill edges (Appendix 4.1.5)
- Six-layer textile matrix, containing recycled denim, cotton and PVA, with compound twill edges (Appendix 4.1.6)
- Waffle weave textile matrix, containing recycled denim, cotton and PVA, with compound twill edges (Appendix 4.1.7)
- Incubator Memmert, 25 °C
- Monitoring Pulse-Amplitude-Modulation (PAM), WALZ Junior-PAM chlorophyll fluorometer
- Fluorescence Spectrometer, Agilent BioTek Synergy LX
- CO_2 measurement setup

3.12.2 Method

Textile samples with varying weaving structures and material compositions (cotton-PVA and recycled denim-cotton-PVA) were prepared. Detailed weaving patterns are provided in Appendix 4.1. All textile samples were sterilised under UV-C light prior to inoculation (Appendix 1.2).

The textile matrices were subjected to five freeze-thaw cycles at −80 °C to achieve hydrogel cross-linking. Following cross-linking, samples were inoculated with *Scenedesmus* sp. cultures (OD = 0.876 at λ = 430 nm) and incubated on a rotational platform at 100 rpm for two days to promote uniform cell distribution and attachment.

Nine experimental groups were prepared, representing different textile architectures (two-layer, three-layer, six-layer, and waffle weave) and material compositions (cotton or recycled denim), as well as a suspension culture for CO_2 measurements (Table 42). Each group consisted of two biological replicates.

Samples were monitored over a one-week period through visual documentation, with pigment intensity used as a proxy for microalgal growth and viability. Due to the inherent colour of recycled denim, direct visual comparison with cotton samples was limited. Photosynthetic activity was assessed using pulse-amplitude modulation (PAM) fluorometry (Appendix 1.4), while CO_2 measurements were conducted for selected groups (A and I) due to time constraints.

Table 42: Samples overview Protocol Optimised System Integration

Sample group	Description
A (n=2)	Three-layer textile matrix, 60% cotton, 40% PVA (Appendix 4.1.2). Subjected to 5 F-T cycles, subsequently inoculated with *Scenedesmus* sp.
B (n=2)	Two-layer textile matrix, containing cotton and PVA (Appendix 4.1.5), subjected to 5 F-T cycles, subsequently inoculated with *Scenedesmus* sp.
C (n=2)	Six-layer textile matrix, containing cotton and PVA (Appendix 4.1.6), subjected to 5 F-T cycles, subsequently inoculated with *Scenedesmus* sp.
D (n=2)	Waffle weave textile matrix, containing cotton and PVA (Appendix 4.1.7), subjected to 5 F-T cycles, subsequently inoculated with *Scenedesmus* sp.
E (n=2)	Three-layer textile matrix, containing recycled denim, cotton and PVA (Appendix 4.1.2). Subjected to 5 F-T cycles, subsequently inoculated with *Scenedesmus* sp.
F (n=2)	Two-layer textile matrix, containing recycled denim, cotton and PVA (Appendix 4.1.5), subjected to 5 F-T cycles, subsequently inoculated with *Scenedesmus* sp.
G (n=2)	Six-layer textile matrix, containing recycled denim, cotton and PVA (Appendix 4.1.6), subjected to 5 F-T cycles, subsequently inoculated with *Scenedesmus* sp.
H (n=2)	Waffle weave textile matrix, containing recycled denim, cotton and PVA (Appendix 4.1.7), subjected to 5 F-T cycles, subsequently inoculated with *Scenedesmus* sp.
I (n=2)	*Scenedesmus* sp. suspension culture

Appendix 4 | Multilayer Woven Textile

4.1 Weaving structures

The textile used in this study is mainly a three-layer woven architecture adapted from the design by Mancini [49]. The central structure is composed of three woven layers, with cotton-PVA ratios varying across different protocols. The layers are mechanically integrated along the edges using a compound twill, providing structural stability and maintaining the integrity of the textile matrix (Figure 77). Within the Weaving Structure Variations protocol, the textile matrix is modified to include alternative weaving structures beyond the three-layer woven architecture. These variations are described in Appendix 4.1.5-4.1.7.

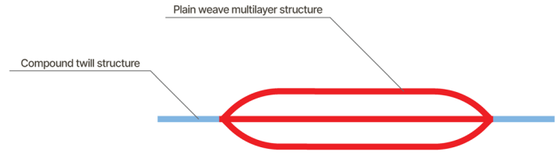

Figure 76: Cross section weaving strusture

4.1.1 Weaving Structure 60% cotton, 40% PVA

In Chapters 3.2, 3.3, 4.1, 4.4, 4.5 and 4.7, the original weaving matrix designed by Mancini was used to immobilise the microalgae. The matrix features a three-layered central structure, secured on two sides with a compound twill (Figure XX). The central structure is composed of 60% cotton and 40% PVA, the outer layers containing PVA wefts and cotton warps, while the middle layer consists of 100% cotton (Figure XX). The detailed construction and layering of the woven textile are illustrated in the AdaCAD file (Figure XX).

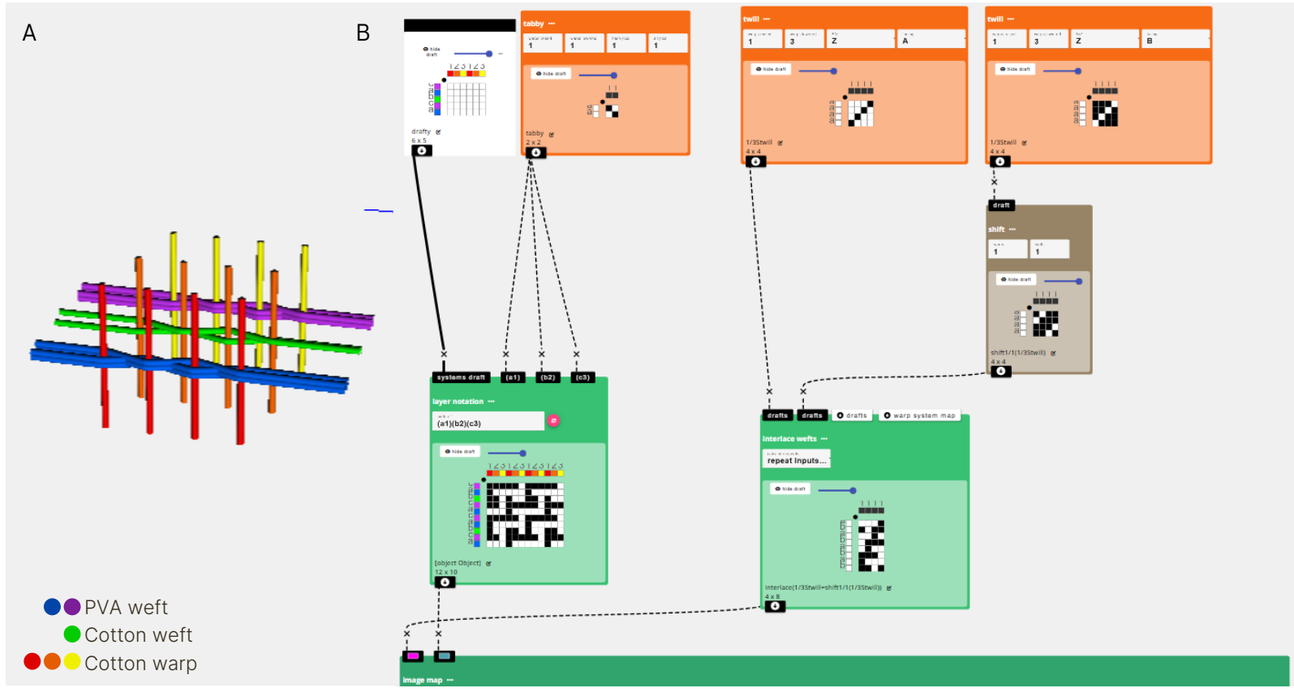

Figure 77: (A) Weaving Structure 60% cotton, 40% PVA 4.1.1 (B) AdaCAD file workspace

4.1.2 Weaving Structure 69.2% cotton, 30.8% PVA

In Chapters 4.7, 4.8 and 4.9, the original weaving matrix designed by Mancini was altered to contain a higher ratio of cotton. The matrix still features a three-layered central structure, secured on four sides with a compound twill (Figure 23). The central structure is composed of 69.2% cotton and 30.8% PVA, the outer layers containing PVA wefts and cotton warps, while the middle layer consists of 100% cotton, where the number of wefts was increased (Figure 78 A). The detailed construction and layering of the woven textile are illustrated in the AdaCAD file (Figure 78 B).

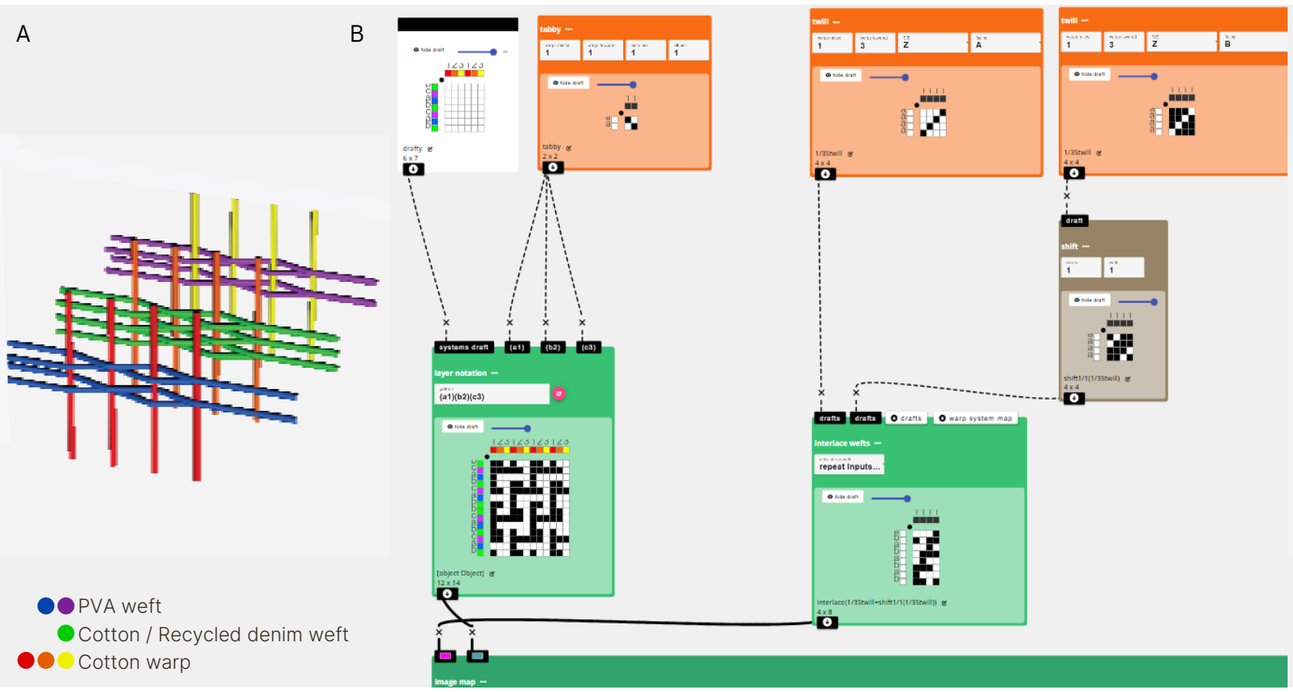

Figure 78: (A) Weaving Structure 69.2% cotton, 30.8% PVA 4.1.2 (B) AdaCAD file workspace. Green reprisents cotton for section 4.7 and 4.8, for section 4.9 it is either cotton (sample Group A) or recycled denim (sample Group E)

4.1.3 Weaving Structure 84.6% cotton, 15.4% PVA

In Chapter 4.8, the original weaving matrix designed by Mancini was altered to contain an even higher ratio of cotton than in 3.2. The matrix still features a three-layered central structure, secured on four sides with a compound twill (Figure 23). The central structure is composed of 84.6% cotton and 15.4% PVA, the outer layers containing PVA and cotton wefts and cotton warps, while the middle layer consists of 100% cotton, where the amount of wefts was also increased (Figure 79 A). The detailed construction and layering of the woven textile are illustrated in the AdaCAD file (Figure 79 B).

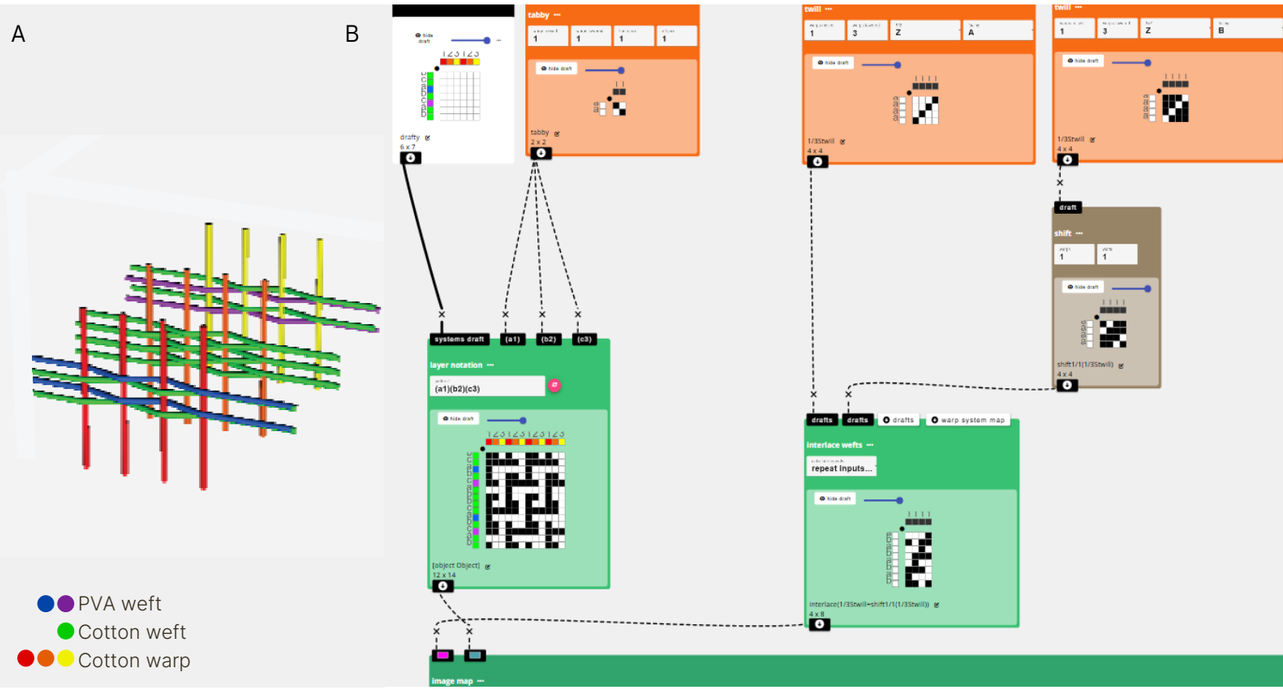

Figure 79: (A) Weaving Structure 84.6% cotton, 15.4% PVA 4.1.3 (B) AdaCAD file workspace

4.1.4 Weaving Structure 53.8% cotton, 46.2% PVA

In Chapter 4.8, the original weaving matrix designed by Mancini was altered to contain a higher ratio of PVA. The matrix still features a three-layered central structure, secured on four sides with a compound twill (Figure 23). The central structure is composed of 53.8% cotton and 46.2% PVA, the outer layers containing PVA wefts (where the amount of wefts was increased) and cotton warps, while the middle layer consists of 100% cotton (Figure 80 A). The detailed construction and layering of the woven textile are illustrated in the AdaCAD file (Figure 80 B).

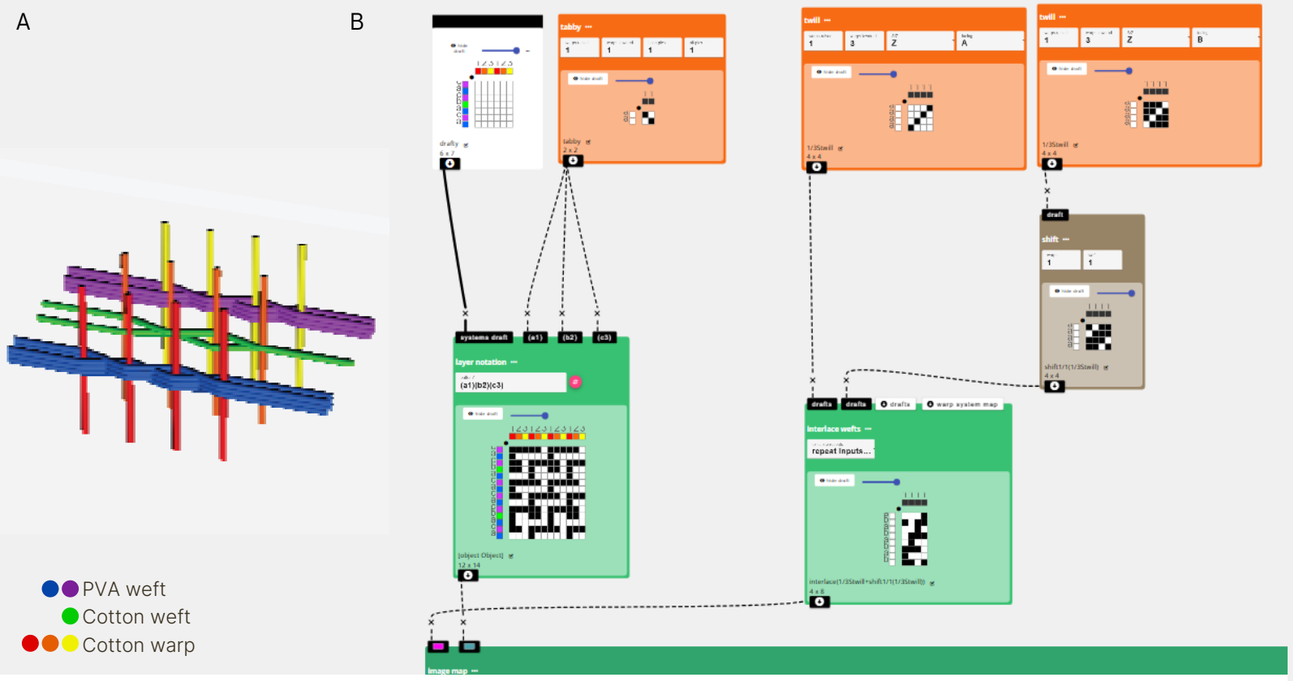

Figure 80: (A) Weaving Structure 53.8% cotton, 46.2% PVA 4.1.4 (B) AdaCAD file workspace

4.1.5 Weaving Structure Two-layer Woven Architecture

In Chapter 4.9, different weaving structures are evaluated, including a two-layer woven architecture. The core structure consists of two distinct woven layers: the first is a plain weave made from PVA wefts and cotton warps, while the second is a compound plain weave incorporating cotton/ recycled denim and PVA wefts with cotton warps. These layers are mechanically connected along the edges using a compound twill structure (Figure 23).

4.1.6 Weaving structure Six-layer Woven Architecture

In Chapter 4.9, an additional weaving structure is evaluated: a six-layer woven architecture. The core structure comprises six distinct woven layers, four of which consist of PVA wefts and cotton warps, while the remaining two are constructed from cotton/recycled denim wefts with cotton warps. These layers are mechanically connected along the edges using a compound twill structure (Figure 23).

4.1.7 Weaving Structure Waffle Architecture

In Chapter 4.9, an additional weaving structure is evaluated: a six-layer woven architecture. The core structure comprises a waffle weave either constructed of 66.7% cotton and 33.3% PVA or 16.7% recycled denim, 50% cotton and 33.3% PVA. These layers are surrounded along the edges using a compound twill structure (Figure 23).

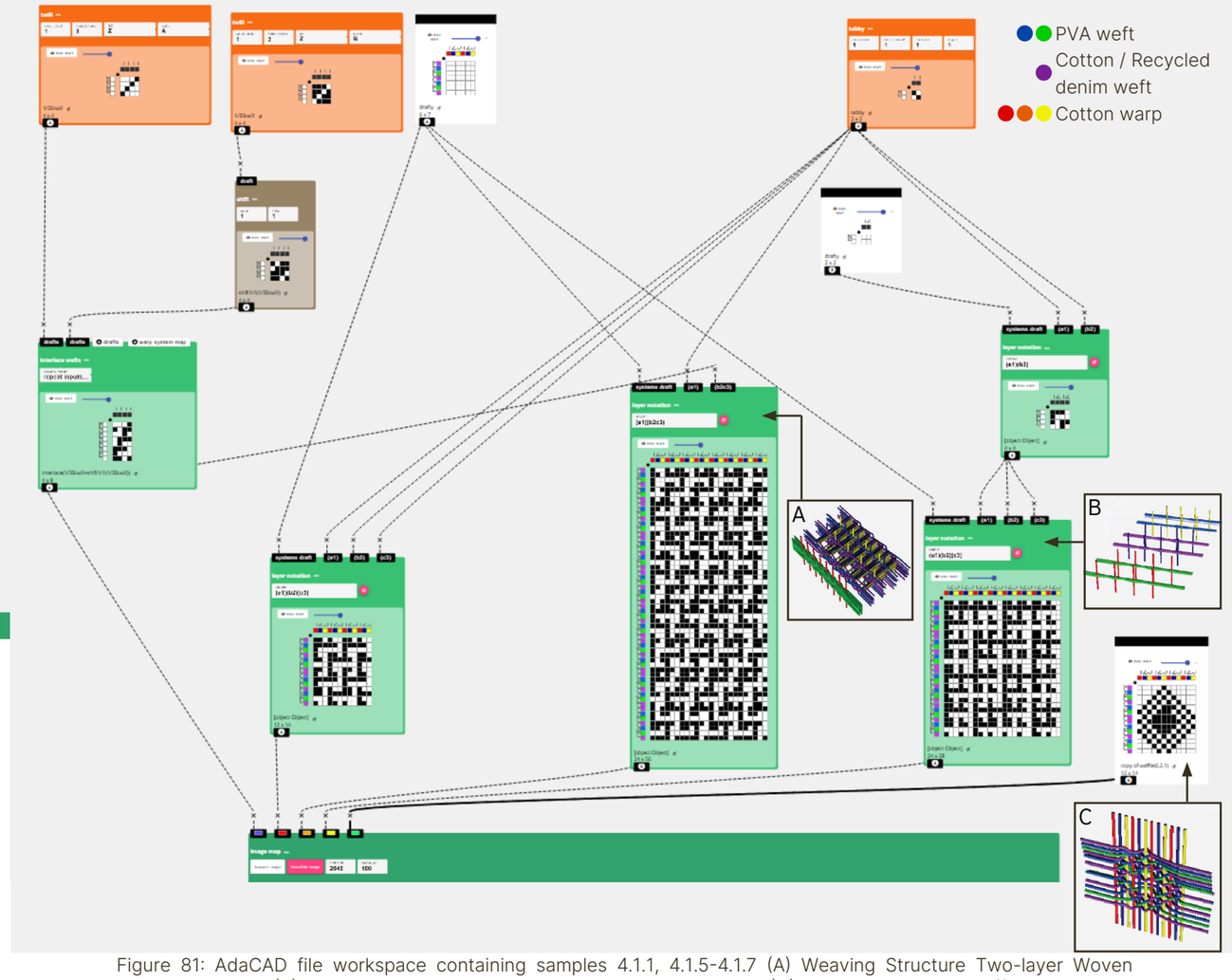

Figure 81: AdaCAD file workspace containing samples 4.1.1, 4.1.5-4.1.7 (A) Weaving Structure Two-layer Woven Architecture 4.1.5 (B) Weaving structure Six-layer Woven Architecture 4.1.6 (C) Weaving Structure Waffle Architecture 4.1.7. The material is dependent on the sample group (section 4.9)

4.2 Weaving patterns

Throughout the study, textile samples of various sizes were used. Initially, samples featured a compound twill on only two sides, which later evolved into designs with a compound twill along all edges of the textile. Figure 82 shows the patterns of all the weaving samples used in this study.

A: Weaving pattern 50 × 70 mm, used in Section 3.2 in combination with Appendix 4.1.1

B: Weaving pattern 40 × 360 mm, used in Section 3.3 in combination with Appendix 4.1.1

C: Weaving pattern 80 × 20 mm, used in Section 4.1, 4.5 in combination with Appendix 4.1.1

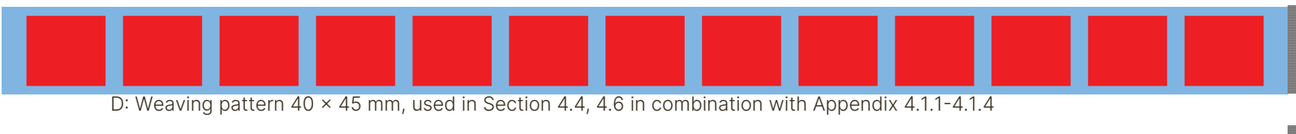

D: Weaving pattern 40 × 45 mm, used in Section 4.4, 4.6 in combination with Appendix 4.1.1-4.1.4

E: Weaving pattern 50 × 180 mm, used in Section 4.8 in combination with Appendix 4.1.2

F: Weaving pattern for multiple samples, used in Section 4.9 in combination with Appendix 4.1.1 and 4.15-4.1.7

Figure 82: Weaving patterns

4.3 Bitmaps

A: Bitmap Section 3.2

B: Bitmap Section 3.3

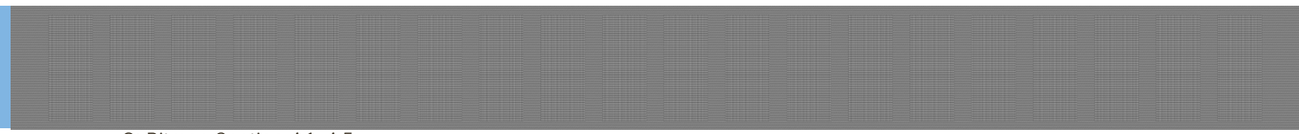

C: Bitmap Section 4.1, 4.5

D: Bitmap Section 4.4, 4.6 sample Group A

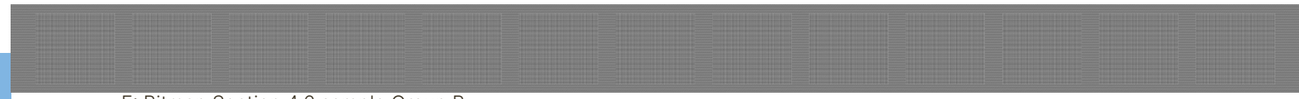

E: Bitmap Section 4.6 sample Group B

F: Bitmap Section 4.6 sample Group C

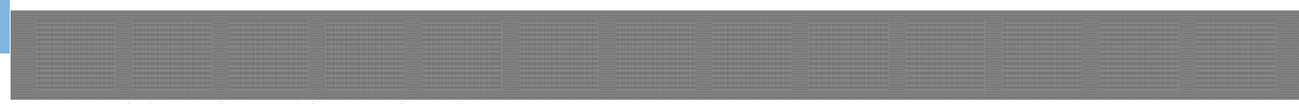

G: Bitmap Section 4.6 sample Group D

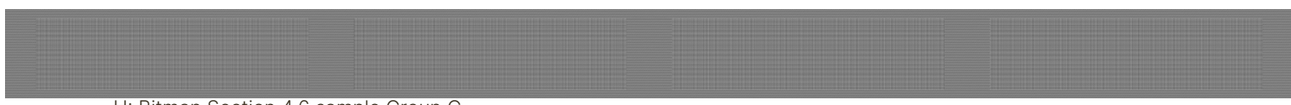

H: Bitmap Section 4.6 sample Group C

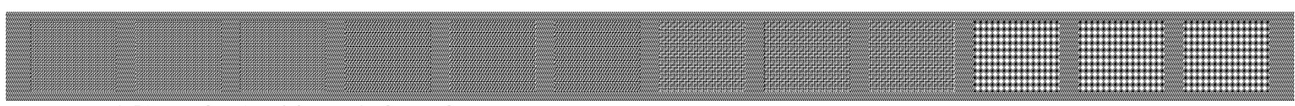

I: Bitmap Section 4.6 sample Group C

Figure 83: Bitmaps

Appendix 5 | Project Brief

DESIGN FOR our future

TU Delft

Personal Project Brief – IDE Master Graduation Project

Name student Renske van der Peet **Student number** 5897394

PROJECT TITLE, INTRODUCTION, PROBLEM DEFINITION and ASSIGNMENT
Complete all fields, keep information clear, specific and concise

Project title Engineered Living Textiles: Integrating Microalgae into Multilayer Woven Textiles

Please state the title of your graduation project (above). Keep the title compact and simple. Do not use abbreviations. The remainder of this document allows you to define and clarify your graduation project.

Introduction

Describe the context of your project here; What is the domain in which your project takes place? Who are the main stakeholders and what interests are at stake? Describe the opportunities (and limitations) in this domain to better serve the stakeholder interests. (max 250 words)

This research builds on Martina Mancini's Living Textiles: Exploring Microalgae Growth on 3D Woven Structures in Design (2025), continuing the exploration of textiles as living systems. The project explores woven textiles as a novel cultivation method that balances the advantages of two existing methods for microalgae cultivation: open ponds and photobioreactors (PBRs). While open ponds are affordable and low energy, they lack environmental control, and PBRs, though more efficient, require substantial infrastructure and energy. A textile-based approach could combine the accessibility of open ponds with the control of PBRs, offering a more sustainable middle ground.
The need for such innovation is rooted in escalating environmental challenges. Accelerating production and consumption patterns are driving up energy demand, resource extraction, and carbon emissions, resulting in widespread ecological degradation. Nature itself offers solutions: through photosynthesis, microalgae and cyanobacteria can capture significant amounts of CO_2, contributing to the removal of large amounts of greenhouse gas emissions.
The project sits within the biodesign and textile design domains. Core stakeholders include TU Delft, which provides the research environment, but also extends to the scientific community (seeking novel cultivation strategies), the textile and materials sector (with an interest in developing sustainable and functional fabrics), and environmental organisations and policymakers (who require innovative approaches to carbon mitigation and climate resilience).

→ *space available for images / figures on next page*

introduction (continued): space for images

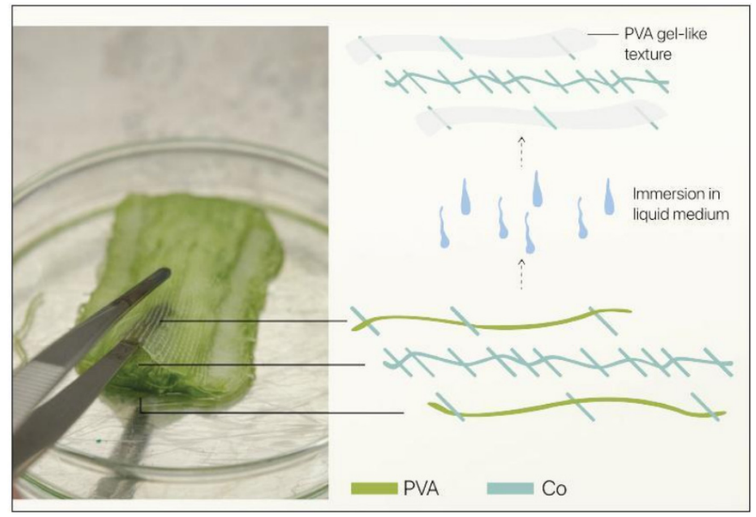

image / figure 1 Final protocol Martina Mancini

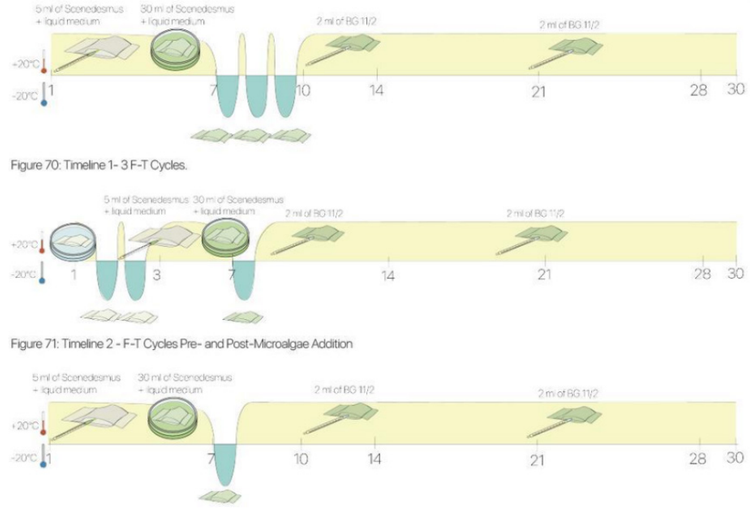

image / figure 2 Final method Martina Mancini

Problem Definition

What problem do you want to solve in the context described in the introduction, and within the available time frame of 100 working days? (= Master Graduation Project of 30 EC). What opportunities do you see to create added value for the described stakeholders? Substantiate your choice.
(max 200 words)

In this project, the primary challenge lies in optimising living textile materials to create a stable and supportive environment for microalgae, thereby enhancing their viability and overall functionality. By improving the structure and conditions of woven hydrogel textile samples—originally developed in Martina Mancini's earlier research—the aim is to increase the performance and durability of these living systems.

Once an optimised material system has been established, the next step is to quantify its effectiveness by measuring CO_2 uptake. At present, there is limited data on how much CO_2 living textiles can capture, making it difficult to evaluate their potential as a strategy for reducing greenhouse gases. Establishing reliable measurement methods and baseline data is therefore essential in order to assess their impact.

This dual approach provides value for multiple stakeholders. TU Delft benefits from advancing research in biodesign and sustainable textile innovation. The scientific community gains insights into improved methods for cultivating and integrating microalgae into materials, while environmental organisations and policymakers gain access to a potentially scalable solution for carbon capture.

Assignment

This is the most important part of the project brief because it will give a clear direction of what you are heading for. Formulate an assignment to yourself regarding what you expect to deliver as result at the end of your project. (1 sentence) As you graduate as an industrial design engineer, your assignment will start with a verb (Design/Investigate/Validate/Create), and you may use the green text format:

Design and Asses a 3D woven microalgae living textile to evaluate its CO_2 capture capacity and explore design improvements that enhance microalgal stability, and potentialy increase CO_2 uptake

Then explain your project approach to carrying out your graduation project and what research and design methods you plan to use to generate your design solution (max 150 words)

In this project, I will use a material-driven design (MDD) approach to improve the living textile, while evaluating its CO_2 capture capacity in the technical characterisation of the MDD method.

The first step of this project is to recreate the previously developed woven hydrogel textile samples from Martina Mancini's earlier research, assess the microalgae growth within them, and evaluate their CO_2 capture potential. Once this baseline has been established, the research will focus on systematically adjusting key variables, such as textile structure and material composition, to determine whether these modifications can enhance microalgae growth and increase overall CO_2 sequestration.

This page is intentionally left blank